Charles University

Faculty of Science

Study programme: Parasitology

Mgr. Barbora Šmídová

The role of myeloid cells in mice infected with the neuropathogenic schistosome *Trichobilharzia regenti*

Úloha myeloidních buněk během infekce myší neuropatogenní motolicí *Trichobilharzia regenti*

Doctoral thesis

Supervisor: RNDr. Tomáš Macháček, Ph.D.

Prague, 2024

Author’s declaration/Prohlášení autorky

I declare that I wrote this doctoral thesis and cited all references properly. Neither the thesis nor its substantial part has been used to obtain the same or any other academic degree.

Prohlašuji, že jsem tuto dizertační práci sepsala samostatně a všechny literární zdroje jsem řádně uvedla. Tato práce ani její podstatná část nebyla předložena k získání stejného či jiného akademického titulu.

Prague, 5. 8. 2024
Praha, 5. 8. 2024

Mgr. Barbora Šmídová

Supervisor’s declaration/Prohlášení školitele

I declare that Barbora Šmídová substantially contributed to the scientific work presented in this doctoral thesis and she is the author or co-author of the enclosed publications and manuscript. Her contributions are clearly stated in chapter 3.

Prohlašuji, že se Barbora Šmídová významně podílela na vědecké práci předložené v této dizertační práci a je autorkou či spoluautorkou uvedených publikací či rukopisů. Její podíl a zapojení jsou jasně uvedeny v kapitole 3.

Prague, 5. 8. 2024
Praha, 5. 8. 2024

RNDr. Tomáš Macháček, Ph.D.

Abstract

Trichobilharzia regenti is an avian schistosome extraordinary for its neurotropism. Besides infecting its final hosts, waterfowl, it can also infect mammals where the immune response quickly kills the parasite. Yet, the mechanisms are still unclear. Therefore, the main objective of this thesis was to describe the dynamics of the myeloid part of the immune system in the central nervous system (CNS) part of the infection. Our results showed that the main cells responding to the presence of *T. regenti* in the CNS of mice were eosinophils. Their numbers peaked at 14 days post infection when many of the migrating schistosomula are damaged or destroyed suggesting that eosinophils might play a role in parasite clearance. At the same time point the markers of M2 polarization of microglia/macrophages culminated. The most upregulated molecules were those inducing oligodendrogenesis and neuron regeneration. Based on the polarization of microglia/macrophages and their close proximity to schistosomula, they seem to be important for tissue repair after the infection.

Eosinophils, like neutrophils, can produce extracellular traps formed from DNA and contents of granules. These traps can capture and damage various nematodes and they might be effective against other parasites too. Therefore, we aimed to test whether these traps might be effective against *T. regenti*. Indeed, we observed increased *in vitro* trap formation after stimulating eosinophils with *T. regenti* schistosomula homogenate together with higher eosinophil apoptosis rate. However, whether the traps are effective against live schistosomula, especially in *in vivo* setting, remains to be tested.

Finally, we tested whether the M2 polarization, which is present in the whole CNS regardless of presence of the parasite in the CNS segment, is strong enough to counteract the inflammation induced by experimental autoimmune encephalomyelitis, a model of multiple sclerosis. Unfortunately, that is not the case as the *T. regenti* infection did not alleviate the clinical symptoms. However, we were able to uncover a novel interaction between IFN-γ and eosinophils which could diminish the M2 healing properties.

Taken together, this thesis presents a complex insight into the myeloid cell response during the *T. regenti* infection of CNS of mice, supports the importance of M2-polarized cells during and after neuroinfection or neuroinflammation, widens the range of parasites which can be fought using eosinophil extracellular traps and finally adds to the pool of immunomodulatory helminths unsuitable for treatment of autoimmune disease but helpful in understanding the immune pathways of some pathologies.

Key words

Trichobilharzia regenti; myeloid cells; microglia; macrophages; eosinophils; eosinophil extracellular traps; multiple sclerosis; experimental autoimmune encephalomyelitis

Abstrakt

Trichobilharzia regenti je ptačí motolice, která je výjimečná svým neurotropismem. Kromě definitivních hostitelů, vodního ptactva, dokáže nakazit i savce, ve kterých ji imunitní odpověď brzy zničí. Přesné mechanismy této odpovědi jsou však stále neznámé. Proto bylo hlavním cílem této práce popsat dynamiku myeloidní části imunitní odpovědi během infekce probíhající v centrální nervové soustavě (CNS). Naše výsledky ukázaly, že eosinofily byly hlavními buňkami infiltrující CNS, ve které se nacházela schistosomula *T. regenti*. Nejvíce eosinofilů se v CNS nacházelo 14 dpí po infekci, kdy je většina schistosomul částečně nebo úplně zničená. To ukazuje na možnou roli eosinofilů při boji s *T. regenti*. Ve stejnou dobu byla i transkripce markerů M2-polarizovaných mikroglií/makrofágů nejvyšší. Nejvíce byly upregulované molekuly, které podporují oligodendrogenezi a regeneraci neuronů. Díky tomu a blízkosti mikroglií/makrofágů ke schistosomulům se zdá, že M2 mikroglie/makrofágy jsou důležité pro opravu tkáně poškozené infekcí.

Eosinofily, stejně jako neutrofily, umí produkovat extracelulární pasti z DNA a obsahu granul. Tyto pasti mohou uvěznit a poškodit různá nematoda a je možné, že jsou účinné i proti jiným parazitům. Otestovali jsme tedy, jestli mohou být pasti účinné i proti *T. regenti*. Eosinofily skutečně produkovaly extracelulární pasti po stimulaci *T. regenti* antigenem v *in vitro* a míra apoptózy byla u těchto eosinofilů vyšší. Efektivitu těchto pastí proti živým schistosomulům je nicméně potřeba dále prozkoumat.

Na závěr jsme otestovali, jestli M2 polarizace přítomná ve všech částech CNS bez ohledu na to, jestli v segmentu byla schistosomula nebo ne, může soupeřit se zánětem vyvolaným experimentální autoimunitní encefalomyelitidou (model roztroušené sklerózy). Zdá se, že to tak bohužel není, protože jsme nepozorovali změnu v klinických symptomech po nákaze myší *T. regenti*. Popsali jsme nicméně novou interakci mezi IFN-γ a eosinofily, která mohla omezit ozdravné efekty M2 molekul.

Tato práce poskytuje komplexní vhled do odpovědi myeloidních buněk na nákazu CNS myší *T. regenti*, podporuje význam M2-polarizovaných buněk během infekce nebo zánětu CNS a po nich, zvyšuje množství parazitů, proti kterým mohou být účinné extracelulární pasti eosinofilů a na závěr rozšiřuje množinu parazitů nevhodných pro léčbu zánětlivé autoimunitní choroby CNS, kteří ale pomohli porozumět imunologii způsobující některé patologie.

Klíčová slova

Trichobilharzia regenti; myeloidní buňky; mikroglie; makrofágy; eosinofily; eosinofilické extracelulární pasti; roztroušená skleróza; experimentální autoimmunitní encefalomyelitida

Acknowledgements

The biggest thanks and gratitude undoubtedly belong to Tomáš for being a super-helpful and ultra-patient supervisor. We hit some rough patches but overall, I can't imagine doing this under anyone else's supervision. Thanks to him and Petr I could do what I loved while having a lot of freedom. Big thank you goes to Martin who helped me with so many experiments and trouble-shootings I can't even count it. Without Verča, I would probably make many more calculating errors and have so much less fun. Thanks to Lenka K. for the help with the overwhelming bureaucracy and for always cheering me up. Finally, thank you to the whole lab for creating such a pleasant work environment.

Next thanks go to AG Hübner in Bonn, to Marc, Jesuthas, Christina, Celia and others for taking me under their wings both in and out of the lab. From the Bonn group, I am most grateful to Alex for all the help, fun, wine, flammkuchen, painting and support.

I would also like to thank my sister, Alča, Magda and Nessie for picking me up and keeping me sane. Without Helča and Krtek, it would probably take me much longer to write this thesis. Thanks, Adél, for the huge support in the finish line. And finally, I would like to thank everyone in my family and my friends, especially those who I met at Zeptej se vědce, for their support and understanding.

Table of contents

Abbreviations

Arg-1	arginase 1
CCR3	C-C chemokine receptor type 3
CD	cercarial dermatitis
CNS	central nervous system
CSF	cerebrospinal fluid
dpi	days post infection
EAE	experimental autoimmune encephalomyelitis
EETosis	eosinophil ETosis
FhESP	*Fasciola hepatica* excretory-secretory products
FhHDM	*Fasciola hepatica* helminth defence molecule
FhTLM	*Fasciola hepatica* TGF-like molecule
HpARI	*Heligmosomoides polygyrus* alarmin release inhibitor
HpBARI	*Heligmosomoides polygyrus* binds alarmin receptor and inhibits
HpTGM	*Heligmosomoides polygyrus* TGF-β mimic
Chil3l3	chitinase-like 3
IFN	interferon
IL	interleukin
IL-4R	interleukin 4 receptor
MOG	myelin oligodendrocyte glycoprotein
MS	multiple sclerosis
NK cells	natural killer cells
NO	nitric oxide
PLP	proteolipid protein
SEA	soluble egg antigen
TGF-β	transforming growth factor beta
Th	T helper
TNF-α	tumor necrosis factor alpha
TrAg	*Trichobilharzia regenti* antigen
Treg	regulatory T (cell)
Ym1	chitinase-like 3

1. Introduction

Although avian schistosomes are globally distributed, their biology is still not well described. However, the little we know shows they deserve more attention. Besides infecting their final avian hosts, they can also infect mammals. In humans, it leads to cercarial dermatitis, a very unpleasant allergic skin reaction. In mice, they can serve as a safe laboratory models for studying the immune response to not only avian, but also human schistosomes as they have very similar migratory routes (Horák et al., 2024). Furthermore, *Trichobilharzia regenti*, an avian schistosome unique for its neurotropism, can be used to study the immune response to other, less available, neuropathogens and uncover mechanisms which could be used in treatment of both neuroinfections and chronic inflammatory diseases of the central nervous system (CNS).

Therefore, in the theoretical part of this thesis, I shortly introduce avian schistosomes and cercarial dermatitis to give way to thorough description of the immune response in the CNS of mice infected with *T. regenti*. The topic of nervous tissue then carries through the rest of the introduction as the myeloid part of the immune response to other neurotropic helminths, then multiple sclerosis and the possibility of treatment using parasitic helminths are described.

1.1. Avian schistosomes and cercarial dermatitis

Besides the infamous human schistosomes, the family Schistosomatidae (Digenea) includes 13 genera of flukes using waterbirds as their final hosts (Horák et al., 2024). Although they do not cause such severe disease as human schistosomes, they should still be of concern to the researchers due to their worldwide distribution (Lashaki et al., 2020; Loker et al., 2022; Valero and Bargues, 2008) and their ability of at least five of them to cause cercarial dermatitis (CD) in humans (Horák et al., 2024).

CD or “swimmer’s itch” is an allergic reaction to the cercariae of (mostly) avian schistosomes penetrating the human skin (Kolářová et al., 2013; Kouřilová et al., 2004a; Macháček et al., 2018). Although the disease is not life threatening as the mammalian immune system is effective against the parasite (Kouřilová et al., 2004b; Lichtenbergová and Horák, 2012; Lichtenbergová et al., 2011), it can cause significant economic losses to the owners of or the vendors near the affected waterbodies as the areas need to be closed until the causative agents are gone. Due to the recent increase in CD outbreaks in various parts of the world (Al-Jubury et al., 2021; Bispo et al., 2024; Gohardehi et al., 2013; Horák et al., 2015; Kerr et al., 2024; Skirnisson et al., 2009; Soldánová et al., 2013), it becomes more and more important to understand the biology of avian schistosomes to adjust the preventive

and protective measures in the critical areas. So far, the measures have been rather ineffective, difficult or with high ecological impact (Soldánová et al., 2013)

In most outbreaks, trematodes of the genus *Trichobilharzia* are responsible for CD (Bispo et al., 2024; Horák et al., 2015; Kolářová, 2007). In the Czech Republic, three species stand out: *T. regenti*, *T. franki* and *T. szidati* (Pokrupová, 2021). While *T. szidati* and *T. franki* adults are found in the blood vessels of peritoneal organs, namely intestine (*T. szidati*, Neuhaus, 1952) and liver (*T. franki*, Müller and Kimmig, 1994), *T. regenti* is extraordinal for its neurotropism (Horák et al., 1999). The facts that *T. regenti* is safe to work with, its life cycle can be maintained in the laboratory, and it prefers nervous tissue, make it an interesting and useful laboratory model for studying neuroimmunology or neuropathology, and the main star of this thesis.

1.2.Immunity against *Trichobilharzia regenti* in the CNS of mice

Trichobilharzia regenti was first described in both its intermediate host, water snail *Radix peregra*, and the nasal cavity of the final host, duck *Anas platyrhynchos*, in 1998 (Horák et al., 1998). Since then, it has been a subject of many experiments in respect to both final and accidental mammalian hosts (Bulantová et al., 2016; Horák et al., 1999; Hrádková and Horák, 2002; Kolářová et al., 2001; Leontovyč et al., 2016; Lichtenbergová and Horák, 2012; Lichtenbergová et al., 2011; Macháček et al., 2016, 2020; Turjanicova et al., 2015). Already in 1999, it was shown that in the accidental host, such as mice, *T. regenti* is unable to finish the cycle as it is eliminated in the spinal cord at the latest (Horák et al., 1999). Yet, the exact reason for *T. regenti* being eliminated in mice remains unknown.

When *T. regenti* penetrates the skin of mice, it prompts skin inflammation (Kouřilová et al., 2004a). The skin response is so strong that only 3-10% of the penetrating cercariae manage to transform into schistosomula and find the nervous tissue (Hrádková and Horák, 2002; Kouřilová et al., 2004b). The successful schistosomula are very quick to find the peripheral nerves and get to the spinal cord as they were found there as soon as 2-3 days post infection (dpi) regardless of the mouse strain used (Horák et al., 1999; Hrádková and Horák, 2002; Kouřilová et al., 2004b; Lichtenbergová et al., 2011).

However, soon afterwards the results begin to depend on the mouse strain. In BALB/c mice, the highest number of schistosomula in the CNS was recorded at 6 dpi and a few schistosomula managed to reach cerebellum, even hemispheres (Horák et al., 1999; Kouřilová et al., 2004b; Lichtenbergová et al., 2011). On the other hand, in hr/hr strains the peak of infection occurred at 3 dpi already and no schistosomula reached the brain (Kouřilová et al., 2004b). Furthermore, the course of infection in immunodeficient mice is different from both mentioned immunocompetent mouse strains. In immunodeficient mice, more schistosomula escape the skin and migrate further in the CNS than in immunocompetent mice

(Hrádková and Horák, 2002; Kouřilová et al., 2004b; Lichtenbergová et al., 2011). The end of the infection brings all the strains together as the spinal cord is basically parasite free by day 24 post infection (Kouřilová et al., 2004b).

The different course of infection between the mouse strains suggests the involvement of the immune system in the parasite elimination. Given the generally insufficient immune responses in immunodeficient mice, only immunocompetent mice will be discussed further. Although the CNS of both mouse strains (BALB/c and hr/hr) was infiltrated by immune cells, the composition of the infiltrate was different (Kolářová et al., 2001; Kouřilová et al., 2004b; Lichtenbergová et al., 2011). Kouřilová et al. (2004b) described massive clusters of granulocytes, mainly neutrophils, around schistosomula in hr/hr mice. The white matter was also infiltrated by eosinophils, lymphocytes and plasma cells. Sometimes, even hemorrhages occurred (Kouřilová et al., 2004b). Kolářová et al. (2001) detected similar immune response in BALB/c mice, furthermore observing macrophages, plasma cells and so-called "giant cells". The immune reaction was accompanied by dystrophy of surrounding neurons (Kolářová et al., 2001) which supported previously described neuromotor damage (Horák et al., 1999). However, when similar experiments were performed with BALB/c mice later, the results were very different. Suddenly, microglia, not granulocytes, were the predominant cells in the infiltrate around *T. regenti* schistosomula. They were accompanied by macrophages and $CD3^+$ lymphocytes and small amount of granulocytes. As for the neurodamage, mild demyelinization and glial scars were observed (Lichtenbergová et al., 2011) but not neuronal damage or hemorrhages. The discrepancy between the BALB/c results can be, to some extent, explained by different staining techniques – Kouřilová et al. (2004b) and Kolářová et al. (2001) used non-specific histological staining whereas Lichtenbergová et al. (2011) used also more specific immunohistochemistry. However, to ultimately decipher the composition of observed clusters more experiments need to be conducted.

Looking closer at microglia, the resident macrophages in the CNS, which are accumulating around the schistosomula (Lichtenbergová et al., 2011), they provenly play a big role in regulating the neuroinflammation. In simple terms, microglia can protect the nervous tissue in two ways depending on their polarization which leads to different cytokine production. Either they fight the pathogen (M1 polarization, production of nitric oxide (NO) and cytokines IL-1β, TNF-α or IL-6) or repair the damaged tissue (M2 polarization, production of tissue repairing factors such as arginase 1, Ym1 and others) (Kwon and Koh, 2020). Due to their ability to fight pathogens (Rock et al., 2004) and their amount around the damaged *T. regenti* schistosomula, they were suggested as the cells responsible for *T. regenti* clearance (Lichtenbergová et al., 2011). Therefore, their response to various *T. regenti* antigens was tested. In *in vitro* settings, microglia produced NO and cytokines IL-6 and TNF-α after stimulation

with schistosomula homogenate (Macháček et al., 2016), all of which are connected with M1 polarization. Together these results support the hypothesis of microglia being the anti-*T. regenti* cells.

Given the antiparasitic potential of NO (Alonso-Trujillo et al., 2007; Bogdan, 2001) even in infection with closely related *Schistosoma japonicum* (Shen et al., 2017), the *in vitro* effect was tested *in vivo* as well. In the early phase of *T. regenti* infection (3 dpi), inducible NO synthase, enzyme producing NO during infections, was detected in the tissue surrounding the schistosomula. However, later (7 and 14 dpi) only 3-nitrotyrosine, the result of NO presence, was detected in the CNS (Macháček et al., 2020). Therefore, the hypothesis of the importance of microglial NO production in fighting *T. regenti* infection was supported only for the early phase. The question of the immune response later in the infection is yet to be answered.

Together the data show that *T. regenti* attracts eosinophils, microglia, macrophages, lymphocytes, plasma cells and others to its location in the CNS. However, there is not a consensus on the composition of the immune cell infiltrate and the role of the attracted cells in parasite clearance. Although a hypothesis suggesting that microglia are the main cells fighting the infection, further experiments supported this only for the early phase of the infection. Therefore, to unravel which parts of the immune system damage T. regenti in the CNS, more experiments need to be performed.

1.3.Immune response to other neurotropic helminths

The affinity to nervous tissue is far from unique amongst helminths. Just in humans, there have been documented *Schistosoma* spp. eggs, *Paragonimus* spp. juveniles, *Echinococcus* spp. or *Taenia solium* hexacanths, or *Angiostrongylus* spp., *Baylisascaris* spp., *Gnathostoma* spp., *Spirometra mansoni*, *Toxocara* spp. and *Trichinella* spp. larvae in the CNS (Finsterer and Auer, 2013; Katchanov and Nawa, 2010; Lv et al., 2010). However, only few of them have been further studied and can provide insight into the involvement of myeloid cells in response to helminths in the CNS. Therefore, this chapter includes only *Angiostrongylus cantonensis*, *Taenia solium* and *Toxocara* spp. Lastly, *Schistosoma* spp. is included as it is a close relative of *T. regenti* and probably induces similar immune response. The helminths are organized alphabetically in this chapter.

Angiostrongylus cantonensis

Angiostrongylus cantonensis is mostly known as the causative agent of eosinophilic meningitis in humans, a disease endemic to Southeast Asia and the Pacific Basin (Alicata, 1991; Gosnell and Kramer, 2013; Wang et al., 2012). As the larvae migrate through the CNS, they induce an inflammatory response, which can then lead to neuron damage, in some cases even to death. As the range of intermediate hosts widens because of introduction of new species, and the incidence is rising (Cowie,

2017; Eamsobhana, 2014; Lv et al., 2010), the understanding of the immune response in the CNS of infected individuals is essential.

As the name of the disease indicates, eosinophils are the main cells attracted to the *A. cantonensis* larvae in the CNS (Gosnell and Kramer, 2013; Martins et al., 2015). Research on mice has shown than upon larvae entering the CNS, inflammasome is formed (Lam et al., 2020) and eosinophil-attracting cytokines and chemokines, such as IL-5, IL-13, IL-33, Ym1 or eotaxin, are produced (Li et al., 2012; Peng et al., 2013; Sugaya et al., 1997; Wei et al., 2015; Zhao et al., 2013) leading to eosinophilia in the CNS. For a strong eosinophilic response, IL-5 and CCR3 receptor on the surface of eosinophils are indispensable (Chuang et al., 2010, 2014; Sugaya et al., 1997).

The role of eosinophils in the infected CNS is still discussed. Although Sugaya et al. (1997) suggested that eosinophils are directly responsible for killing the parasite, their proposition was based on *in vitro* data and has never been confirmed *in vivo*. Results from both human and rodent samples show eosinophils as a main part of granulomas around damaged or dead larvae, leaving the live larvae free (Li et al., 2012; Martins et al., 2015). However, eosinophils can also participate in tissue remodelling and repair by releasing neurotrophins or immune regulation by producing IL-12 and IFN-γ, which muffle the Th2 response happening in *A. cantonensis*-infected CNS (Gosnell and Kramer, 2013). This hypothesis, nevertheless, remains unchallenged.

Other cells responding to *A. cantonensis* infection are microglia, monocytes, plasma cells and T lymphocytes (Chuang et al., 2014; Gosnell and Kramer, 2013; Martins et al., 2015; Wei et al., 2015; Zhao et al., 2013). Of those, only microglia have been further studied. Comparing the cell infiltrate in mice, permissive hosts, and rats, less susceptible hosts, revealed the importance of microglial activation for starting the eosinophil infiltration during the infection (Wei et al., 2015). In mice, it was described that microglia produce Ym1, an eosinophilic chemoattractant. Blocking the activation of microglia limited the eosinophil infiltration and subsequently the symptoms of meningitis (Zhao et al., 2013). Furthermore, microglia produce pro-inflammatory cytokines which loosen the blood-brain barrier and promote general inflammation of the CNS (Wei et al., 2015).

Summarizing the aforementioned studies, it seems that the presence of *A. cantonensis* larvae in the CNS activates microglia which in turn produce Ym1 and pro-inflammatory cytokines. Ym1 then attracts large number of eosinophils which accumulate around damaged or dead larvae, probably to repair the tissue and modulate the ongoing inflammation of the CNS. Even if the repairing hypothesis is confirmed, the inflammation is still so strong that no number of eosinophils can control it and patients develop eosinophilic meningitis.

Schistosoma spp.

Schistosoma spp. is widely known as the causative agent of human schistosomosis. According to WHO, more than 200 million people are at risk and the majority of them are infected (WHO, 2024 [online]). In the endemic areas, autopsy revealed schistosome eggs in up to 28% of examined brains (Vale et al., 2012). However, the number of diagnosed cases is usually around 5% (Berkowitz et al., 2015; Ferrari and Moreira, 2011). Be it as it may, the fact is that the disease is still underrecognized (Dastoli et al., 2023; Ferrari et al., 2008) and the underlying immunopathology is not well studied.

While *S. japonicum* is usually found the brain, *S. haematobium* and *S. mansoni* are more common in other parts of the CNS (Pittella, 1997). Based on the location of the schistosome eggs, the symptoms range from no symptoms to encephalitis or stroke-like symptoms to motor impairment, which is caused by hemorrhage and necrosis of the spinal cord (Ferrari and Moreira, 2011; Ferrari et al., 2008; Vale et al., 2012). The infection can also manifest as slow-expanding lesions imitating tumor growth (Ferrari and Moreira, 2011).

As there is not a good laboratory model for studying neuroschistosomosis, it is difficult to study the immune response to the infection in the CNS. However, it seems to be similar to the immune reaction in the peripheral organs where schistosome eggs are mostly found. In particular, schistosome eggs stimulate granuloma formation by $CD4^+$ cells regardless of the tissue (Ferrari et al., 2008). The granulomas are also populated by eosinophils, microglia/macrophages, lymphocytes and plasma cells (Pittella, 1997). Immune cells are also present in the cerebrospinal fluid (CSF) of patients with eosinophils and lymphocytes forming most of the infiltrate (Dastoli et al., 2023; Ferrari et al., 2008).

Furthermore, the CSF is used for confirming the infection (Dastoli et al., 2023; Ferrari and Moreira, 2011; Vale et al., 2012) and for measuring cytokines. If schistosome eggs are present in the CNS, IL-4, IL-6, IL-10 and IL-13 are elevated while TNF-α and IFN-γ are detected in much lower levels (Ferrari et al., 2006; Sousa-Pereira et al., 2006). The situation was similar in the sera suggesting that the infection influences the whole immune system. Moreover, eotaxins were detectable in the sera (Ferrari et al., 2006; Sousa-Pereira et al., 2006) explaining the influx of eosinophils into the CNS.

Taken together, *Schistosoma* spp. is another helminth capable of infecting the CNS causing eosinophilia in the brain and the CSF. Furthermore, it decreases the levels of inflammatory cytokines TNF-α and IFN-γ. However, without a suitable model, the immune response and more targeted therapy cannot be described.

Taenia solium

From all helminths found in the CNS, *Taenia solium* is the most common one (Coyle and Tanowitz, 2009; Qi et al., 2011). Its hexacanths are often disseminated into the CNS where they develop into

cysts and cause neurocysticercosis. The symptoms can include seizures and epilepsy. In the endemic areas, neurocysticercosis is the leading cause of epilepsy being responsible for over 30% of cases, in high-risk communities the number can go as high as 70% (WHO, 2024 [online]).

Given the incidence of neurocysticercosis, it is understandable it is widely studied and well described (reviewed p.e. in Coyle and Tanowitz, 2009; Fleury et al., 2016; Garcia et al., 2020; Prabhakaran et al., 2010; Qi et al., 2011). Looking at the overall picture, the immune response to viable cysts consists mainly of macrophages and microglia, neutrophils, eosinophils, lymphocytes, plasma cells and the quickly changes from mixed Th1/Th2 to Th2 (Chavarría et al., 2003; Fleury et al., 2016; Toenjes and Kuhn, 2003). Once the cysts start to degenerate, a strong Th1 immune response is induced with involvement of NK cells, macrophages and T cells. The dead cysts are then surrounded by plasma cells, B and T lymphocytes, macrophages and mast cells. At this point, the immune response is mixed Th1/Th2 (Fleury et al., 2016; Garcia et al., 2014).

The interesting things about the course of the immune reaction are the changes in the polarization of the immune response. The correlation between the presence of viable cysts and generally less devastating Th2 response, which was also experimentally confirmed (Tharmalingam et al., 2016), points to an involvement of immunoregulatory molecules produced by the parasite.

In neurocysticercosis, M2 microglia are essential for the immune switch and maintaining the Th2 response (Chauhan et al., 2015; Rodríguez-Sosa et al., 2002; Sun et al., 2014). To this end, the parasites produces molecules that limit release of Ca^{2+} stored in microglia, thus indirectly downregulating the pathways leading to production of inflammatory cytokines (Sun et al., 2014). At the same time, parasitic glycans induce the M2 polarization of microglia and macrophages, which then in turn clear the CNS of neutrophils and limit the overall inflammatory response (Quenum Zangbede et al., 2018). M2 polarized cells can also limit the neuropathology and disease severity (Gundra et al., 2011; Mishra et al., 2009; Quenum Zangbede et al., 2018).

Taken together, parasitic stimulation of M2 response in microglia and macrophages is important for the survival of the parasite and the host. If the parasite discontinues the immunomodulation, the immune response returns to the inflammatory response which then can manifest as neurodegenerative symptoms or epilepsy.

Toxocara spp.

Larvae of *Toxocara canis* and *T. cati*, which normally infect cats and dogs, respectively, can use humans as paratenic hosts (Strube et al., 2013). When that happens, the larvae migrate to organs like liver, lungs or eyes. They can also pass through the blood brain barrier to the brain where they cause neurotoxocarosis (Finsterer and Auer, 2013). As the infections are usually asymptomatic, the

epidemiological data are not very precise (Nicoletti, 2016; Rostami et al., 2019). Supposedly, there were only 47 reported cases of neurotoxocarosis in 50 years (Eberhardt et al., 2005), which is a very low number given the widespread occurrence of *Toxocara* spp. Nevertheless, when the symptoms appear, they vary from headaches or encephalitis to vision impairment, epilepsy or dementia depending on the site affected by the migrating larvae (Fan et al., 2015; Finsterer and Auer, 2013; Nicoletti, 2016; Rostami et al., 2019). With the low reported number of cases and variability of symptoms, *Toxocara* spp. is often omitted as a source of the symptoms, therefore, compared to *Taenia solium*, human data on *Toxocara* spp. are rare.

In rodents, the CNS infection with *Toxocara* spp. is better understood. Similarly to *T. regenti*, larvae of *Toxocara* spp. migrate to the CNS within days (Janecek et al., 2014; Resende et al., 2015). Larvae of *T. cati* accumulate mostly in the cerebellum, while *T. canis* larvae prefer the hemispheres (Waindok and Strube, 2019). The immune response itself then depends on the mouse strain (Cox and Holland, 2001). In humans, the parasite often causes eosinophilia (Mohammad et al., 2019). However, the only strain where mild influx of eosinophils in form of perivascular cuffs was observed is C57BL6/J (Springer et al., 2019).

Directly in the brain, *Toxocara* spp. infection inhibits expression of pro-inflammatory cytokines such as IFN-γ, TNF-α, IL-17 or IL-6 (Waindok and Strube, 2019). Especially TNF-α and IL-6 are necessary for inducing inflammatory and demyelinating processes via microglia (Tian et al., 2012). The immune milieu is further shifted by overexpression of Th2-related cytokines IL-4 and IL-5 (Waindok and Strube, 2019). In such environment microglia take on a scavenging role and slowly change into phagocytic gitter cells (Janecek et al., 2014; Springer et al., 2019).

The cytokine situation is mirrored in the periphery as well (Resende et al., 2015). Together these results support the hypothesis of immunomodulatory, even immune evading *Toxocara* spp (Maizels, 2013). Indeed, Toxocara excretory-secretory products contain molecules affecting both innate and adaptive immure response on many levels and are promising candidates for allergy or rheumatoid arthritis treatment (Abou-El-Naga and Mogahed, 2023).

Taken together, *Toxocara* spp. is an underrecognized causative agent of many neurological problems. However, studying the immune response is complicated as the mouse models mostly do not develop eosinophilia which is very common in human neurotoxocarosis. Nevertheless, the results highlight microglia as scavengers and *Toxocara* spp. as an immunomodulator.

To summarize, this subchapter provides an insight into the many roles of eosinophils and microglia during the helminth infection of the CNS. Where during angiostrongylosis microglia are essential for

attracting eosinophils and driving the inflammation to counteract the parasite-killing Th2 response, in neurocysticercosis and neurotoxocarosis the M2 polarization of microglia/macrophages is necessary. While in angiostrongylosis eosinophils might have tissue-repairing qualities, in neurotoxocarosis microglial scavenging is more important. However, in all presented diseases the parasite can modulate the immune response to its advantage and limit the neuropathology.

1.4.Multiple sclerosis

Helminths are well known for their immunomodulatory properties and the previous subchapter shows that neurotropic helminths are no exception. However, parasites dwelling in other organs are more studied and in some cases, researchers managed to characterize and test molecules with immunomodulatory potential (Maizels et al., 2018). Some of these molecules were even tested as a treatment of various chronic inflammatory diseases (Arai and Lopes, 2022; Helmby, 2015; Khan and Fallon, 2013; Trujillo-Vargas et al., 2007).

This area is widely studied and reviewed (e.g. in Dixit et al. (2017), Finlay et al. (2016) or Khan and Fallon (2013). Therefore, given the neurotropism of my model organism, only multiple sclerosis and most researched helminths changing the course of the disease are further described in this chapter.

Multiple sclerosis and its laboratory model

Multiple sclerosis (MS) is an autoimmune neuroinflammatory disease with rising incidence worldwide. Its onset usually appears in 30-40 years old patients, mostly women (Walton et al., 2020). The symptoms are variable – it can manifest as sensory or motor impairment, dysfunction of digestive or secretory system, psychological disorders or cognitive deficits and other neurological problems (Compston and Coles, 2008). However, they are all the result of the ongoing inflammation in the CNS leading to demyelinated lesions, neuronal damage and gliosis (Frischer et al., 2009). The first immune cells in the lesions leading the inflammatory attack are autoreactive Th1 and Th17 lymphocytes (Liu et al., 2022). The latter, together with M1 macrophages, can damage the oligodendrocytes revealing the otherwise hidden antigens to which the Th1 lymphocytes respond (Dendrou et al., 2015; Larochelle et al., 2021).

Other cells infiltrating the CNS during MS are $CD8^+$ T cells, B cells and plasma cells where B cells are other important cells driving the neurodamage (Lassmann, 2013). B cells have various ways of supporting the disease progression. Firstly and most importantly, they present the antigens and produce pro-inflammatory cytokines (Miyazaki and Niino, 2022). Next, they produce factors and autoantibodies supporting the damage of myelin sheath and neurons (Comi et al., 2021). Last, they

can serve as a reservoir for Epstein-Barr virus (Tracy et al., 2012) which in recent years becomes more evidently involved in the onset of MS (Bjornevik et al., 2022; Handel et al., 2010; Vietzen et al., 2023).

However, MS is a multifactorial disease. Other risk factors include (epi)genetics, vitamin D deficiency, gut microbiome composition, smoking and obesity (Liu et al., 2022). Given the variability of triggers and symptoms, MS is very difficult to treat. At this moment, most treatments are based on IFN-β or B cell depletion (Annibali et al., 2015; Greenfield and Hauser, 2018). Although B cell targeting therapy is in many cases more effective than IFN-β treatment (Hauser et al., 2017), both treatment regimes influence the whole immune system, which can increase the risk of infection (Luna et al., 2020) or even malignancies (Miyazaki and Niino, 2022). Therefore, the quest for finding more targeted treatment is still ongoing.

To research this topic, a laboratory model of MS called experimental autoimmune encephalomyelitis (EAE) is used. The model has many variations of used animals (e.g. mice, rats, guinea pigs or marmosets) and stimulus leading to the disease development. It can either be induced by injection of MOG (myelin oligodendrocyte glycoprotein) or PLP (proteolipid protein) peptide, the antigens to which the cells react in human MS, accompanied by a strong adjuvans like complete Freund's adjuvans and supported by pertussis toxin. Alternative option is transfer of autoreactive T cells sometimes coupled with autoantibodies transfer (Hart, 2019; Lassmann and Bradl, 2017). EAE most resembling MS is the one standing on MOG (Lassmann and Bradl, 2017), which is also the EAE induction mechanism used later in this thesis.

In MOG-induced EAE, the immunopathology happens due to autoreactive $CD4^+$ T cells and autoantibodies (Linington et al., 1988) similarly to human MS. The resulting lesions mimic the humans' in the demyelination with neurodamage and infiltration by Th17 cells (Aranami and Yamamura, 2008; Lassmann and Bradl, 2017). However, in many animals the lesions start with axonal damage and follow with demyelination, whereas in MS it is the opposite (Lassmann and Bradl, 2017). Furthermore, in EAE the signature cytokine is IFN- γ while IL-17A reigns in MS (Becher et al., 2003; Hart, 2019). Nevertheless, regardless of the differences between MS and EAE (summarized in Table 1), the main immune mechanisms work in both models: Th1 and Th17 cells drive the neuropathology with support from B cells, while Treg proliferation and activation ameliorates the symptoms (Hart, 2019; Lassmann and Bradl, 2017). When keeping in mind the differences, EAE is nowadays still the best model for studying MS.

Table 1: Comparison of multiple sclerosis and experimental autoimmune encephalomyelitis, its laboratory model. Adapted from Hart (2019) and Lassmann (2013).

	MULTIPLE SCLEROSIS	EXPERIMENTAL AUTOIMMUNE ENCEPHALOMYELITIS
	DIFFERENCES	
TRIGGER	Unknown (EBV infection, genetic predisposition)	Injection of MOG peptide
DEVELOPMENT	Spontaneous	Induced
SIGNATURE CYTOKINE	IFN-γ	IL-17A
LESIONS	Primary demyelination	Primary axonal loss
	SIMILARITIES	
	Th1, Th17 → pathology, symptoms Treg → milder inflammation	

Recently, the importance of myeloid cells in EAE onset and progression has come to light. In the presence of Th17 cells, macrophages support the inflammation, lesion formation and tissue damage (Larochelle et al., 2021). On the other hand, M2-polarized macrophages produce Th2-related cytokines (Shapouri-Moghaddam et al., 2018), therefore dampen the pathological Th1/Th17 response. Furthermore, they can produce molecules driving oligodendrogenesis and neuron growth supporting the tissue renewal (Miron and Franklin, 2014; Shapouri-Moghaddam et al., 2018).

The possibility of reducing the inflammation and pathology via induction of M2 polarization is already being tested. Che et al. (2022) found a molecule that stood out among many others for its ability to induce a strong M2 response *in vitro*. Administering this molecule to the EAE model *in vivo* led to milder symptoms and reduced demyelination. On the cellular level, the M2 polarization was adamant but Th1/17 response was diminished (Che et al., 2022).

The cababilities of M2 macrophages were also shown when their adoptive transfer alleviated the symptoms of EAE (Chu et al., 2021) or when mice with imbalanced M1/M2 polarization in favor of M1 showed more extensive demyelination, stronger inflammation and longer recovery time (Mazzon et al., 2016). Taken together, M2 stimulation seems to be a rising uportunity for new treatments of EAE and MS.

Helminth immunomodulation as a treatment

Given the complexity of the disease, various helminths have been tested, a few of them even got to clinical trials. However, as this topic is beyond the scope of this thesis and is nicely reviewed in Dixit et al. (2017), this subchapter includes only well studied *Fasciola hepatica*, *Heligmosomoides polygyrus* and *Schistosoma* spp., which is, moreover, related to *T. regenti*. They are, again, organized alphabetically.

Fasciola hepatica

In 2009, Walsh et al. began the story of treating EAE with *Fasciola hepatica*. They discovered that infecting mice with *F. hepatica* metacercariae stimulated macrophages to produce IL-10 and TGF-β which then induces the production of immunosuppressive Treg cells that in turn limit the production of IFN-γ in mice. This mechanism worked during EAE as well and it significantly decreased the symptoms of the disease. Looking for the part most efficient in the improvement of the symptoms, they discovered that TGF-β is the molecule driving the Treg production which then ameliorates the symptoms (Walsh et al., 2009).

In the next step, the group started looking for the immunomodulatory molecules and started with the excretory-secretory products (FhESP). Administering FhESP had similar effect as the infection itself – it promoted IL-10 and TGF-β production, diminished the production of IFN-γ and IL-17 and attenuated the symptoms. Furthermore, after FhESP administration, the CNS was heavily infiltrated by eosinophils and the production of IL-5 and IL-33 rocketed. While untangling the processes, they discovered that FhESP stimulate IL-33 production which then induces IL-5 resulting in eosinophilia and protection. In this study, IL-5 was the cytokine driving the protection by attracting eosinophils into the CNS (Finlay et al., 2016).

Diving further in, they tested whether *F. hepatica* total extract (FHTE) directly changes the ability of IL-17-producing cells (namely γδ T cells and CD4 cells) as they are crucial for EAE-related neuropathology (McGinley et al., 2018). They discovered that not only did FHTE diminish IL-17A and IFN-γ production *in vitro*, but also that injecting MOG-reactive T cells treated with FHTE into naïve mice induced milder EAE symptoms than injecting untreated MOG-reactive T cells. Moreover, injecting FHTE-treated MOG-reactive T cells mitigated the migration of IL-17 producing cells into the CNS further supporting the immunomodulatory potential of *F. hepatica* products (Quinn et al., 2019).

After the discovery of family of *F. hepatica* helminth defence molecules (FhHDM) and their ability to modulate innate cell responses (Robinson et al., 2011), one of them was tested as EAE treatment. Injecting mice with FhHDM-1 also led to milder symptoms but the underlying mechanism was very different. In this study, the CNS was less inflamed and demyelinated after FhHDM-1 treatment, but the

levels of IL-17, IFN-γ and IL-10 remained unchanged. Instead, FhHDM-1 inhibited M1 polarization of macrophages. The authors suggested that this inhibition limited the activation of Th1/Th17 response which damages the tissue the most (Lund et al., 2016). Their results clearly support the importance of macrophages in the disease outcome.

Taken together, these results show that although the treatment with the parasite, its excretory-secretory products or one molecule all lead to less severe symptoms of the disease, the underlying pathways may vary. Furthermore, the fact that the first 3 studies were performed on C57BL6/j mice while in the third study they used BALB/c mice, shows the importance of the genetic background in the immune reaction and the disease outcome.

Heligmosomoides polygyrus

One of the first studies testing the effect of *H. polygyrus* on the course of EAE (Donskow-Łysoniewska et al., 2012) brought two novelties. Not only did the researchers introduce the parasite after the symptoms appeared, they also looked on the other side and studied how the disease influences the number of parasites providing complex insight into the events in the hosts. Furthermore, they used not only classic EAE scoring system but also diarrhea score which develops in EAE mice days before the traditional neurologic symptoms. In both scoring systems, infecting the mice with *H. polygyrus* significantly decreased the score. On the other hand, the number of retrieved parasites after the experiment was much lower in mice suffering from EAE. Considering the immunomodulatory properties of the parasite, the infection reduced the concentration of inflammatory cytokines IL-2, IL-17, IL-12 and TNF-α but increased the levels of anti-inflammatory cytokines TGF-β, IL-10 and IL-6 suggesting the *H. polygyrus*-driven protection against severe symptoms lies in its ability to stimulate Treg response (Donskow-Łysoniewska et al., 2012).

Thanks to the role of TGF-β in EAE amelioration following *H. polygyrus* infection, the discovery of HpTGM, a TGF-β mimic from the excretory-secretory products of *H. polygyrus* (Johnston et al., 2017), offered a great opportunity to test whether one molecule can substitute an infection. In a study by White et al. (2020) they did just that. First, they confirmed that the infection reduces symptoms via Treg stimulation. Second, they tested the effect of HpTGM and of the excretory-secretory products as a whole. Unfortunately, in this case, the molecule itself was not able to reduce the symptoms of the disease and the excretory-secretory products only slightly delayed the onset without the subsequent decrease in clinical score. Taken together, these results show that in this case, the whole parasite stimulates the immunomodulation in a way that a set of molecules cannot (White et al., 2020).

Nevertheless, the team studied the immunomodulatory mechanisms of the disease further and discovered that *H. polygyrus* is most potent as the tissue-invading stages when they induce a spike in

IL-4 levels and increased Th2 polarization. It is therefore a parasite that in any case has to be used as a treatment, not as prevention. Furthermore, they uncover the importance of IL-4 signalling, especially on the side of IL-4R, in the *H. polygyrus*-stimulated EAE-healing mechanism (White et al., 2020).

Taken together, *H. polygyrus* is a strong immunomodulator that is most efficient in its active phase making it a great option for treating EAE. However, it is unclear how this infection could work in humans during MS as it is a specific parasite of mice. In this case, it would be even more helpful if the *H. polygyrus*-derived immunomodulatory molecules had the same effect on the disease symptoms. Unfortunately, the most promising molecule capable of mimicking TGF- β cannot do this. Fortunately, there are more *H. polygyrus*-derived molecules with proven effects in other diseases (Maizels et al., 2018); it is therefore just a question of testing them in EAE.

Schistosoma spp.

The story of *Schistosoma* spp. and EAE begins with a finding that a preexisting *S. mansoni* infection decreases incidence of EAE and delays the onset of symptoms. *S. mansoni* induces production of Th2-related IL-4 and IL-5 which stays high even after EAE induction. On the other hand, the levels of pro-inflammatory IFN γ, TNF-α and IL-12 were much lower in infected mice with EAE than in non-infected mice with EAE. Furthermore, the immune cell infiltrate in the CNS was smaller in infected EAE mice than in those with just EAE. This study, therefore, showed that *S. mansoni*-stimulated Th2 response was strong enough to alleviate the symptoms of EAE (La Flamme et al., 2003).

However, *S. mansoni* infection also brings many side effects to the "treatment". Therefore, looking for a safer life stage or, better yet, a molecule is much needed. Sewell et al. (2003) preconditioned mice with *S. mansoni* ova, induced EAE and later observed much lower clinical score in preconditioned mice compared to the only EAE group. Looking at the immune response, the situation was very similar to that described above. EAE mice preconditioned with ova showed reduced inflammatory cell recruitment to the CNS and the ratio of Th1:Th2 cells was shifted in favour of Th2 compared to non-treated EAE mice. Moreover, macrophages from preconditioned EAE mice produced less IL-12 than non-treated EAE mice (Sewell et al., 2003). IL-12 is a cytokine inducing IFN-γ production and is essential for differentiation of Th1 cells (Trinchieri, 2003). Therefore, reduction of its level confirms the strength of *S. mansoni*-induced Th2 response.

In 1999, a very potent set of immunomodulatory molecules capable of Th2 induction was discovered in the soluble egg antigen (SEA) (Okano et al., 1999). It was therefore only logical to test this set as the next step of researching schistosomes as a possible MS treatment. Zheng et al. (2008) took SEA from *S. japonicum,* tested its effect on the course of EAE in both pre- and post-induction phase of the disease and discovered that in both cases the treatment reduced the severity of the disease and delayed the

disease onset. Furthermore, they confirmed SEA also stimulated IL-4 but decreased the levels of IFN-γ. Finally, SEA preconditioning protected the nervous tissue from demyelination and nerve damage (Zheng et al., 2008). Therefore, it is safe to assume that *S. japonicum* SEA have similar immunomodulatory properties as *S. mansoni* infection or ova administration. However, given the complex composition of SEA, it is very difficult to isolate and test the unique molecules and it is likely one of the reasons why this research has not been extended.

Taken together, the schistosome story shows that although various life stages and parasite-derived molecules can present similarly in modulating the immune response during EAE, the severe side effects and complexity of the antigens might stop at showing the underlying mechanisms and the importance of Th2 in reducing the severity of the disease.

To summarize, this subchapter shows that the mechanisms in relieving the EAE symptoms are many and they depend not only on the parasite but also on the life stage or specific molecule. Furthermore, the genetic background of the mouse plays a part as well. On top of all that, most of research conducted on this topic uses parasites and their products as a prevention, before the disease onset. Given that MS symptoms often go unnoticed until they are severe, the understudied model of introducing parasites after the symptom onset is much more important. At this moment, the research brings much needed understanding of the immune pathways behind the symptom improvement. However, for translation into treatment, research using infections after the symptom onset is necessary.

2. Aims

This thesis aims at describing the immune response to the avian schistosome *Trichobilharzia regenti* in the central nervous system (CNS) of mice with focus on myeloid cells, uncovering the involvement of eosinophils in parasite clearance and testing whether *T. regenti*-induced immunomodulation could relieve mice suffering from experimental autoimmune encephalomyelitis (EAE), laboratory model of multiple sclerosis. Its benefits for the science community lie in taking a step towards recognizing mechanisms of eosinophil defence against neurotropic helminths and testing a schistosome with immunomodulatory properties residing in the CNS against EAE, where other researchers use helminths localized elsewhere.

The specific aims were to:

- Describe which myeloid cells infiltrate the CNS of *T. regenti* infected mice and what is the cell dynamics during the course of infection.
- Characterize the polarization of macrophages/microglia responding to *T. regenti* schistosomula in the CNS at different timepoints.
- Unravel whether and how *T. regenti* schistosomula stimulate extracellular trap formation in eosinophils.
- Test the efficacy of the immunomodulatory properties of *T. regenti* in the CNS of mice with induced EAE.

3. List of publications

The thesis contains two publications and one manuscript in a story order rather than a chronological one. My contributions to the publications are stated below in *italics*. The summarizing discussion of the three papers is in the following chapter.

PUBLICATION #1

Macháček, T., Leontovyč, R., **Šmídová, B**., Majer, M., Vondráček, O., Vojtěchová, I., Petrásek, T., and Horák, P. (2022). Mechanisms of the host immune response and helminth-induced pathology during *Trichobilharzia regenti* (Schistosomatidae) neuroinvasion in mice. PLoS Pathog. *18*, 1–34.

> *My contributions: Performing experiments (nervous tissue collection, flow cytometry analysis of the nervous tissue, immunohistochemical staining and consequent analysis of the spinal cord, identification of differentially expressed genes connected to macrophage/microglia polarization and blood-brain barrier tightness) with subsequent data analysis, writing of the corrseponsing parts in the original draft.*

MANUSCRIPT #1

Šmídová, B., Nieto Peréz, C., Ajendra, J., Macháček, T., Ehrens, A. (2024). Eosinophils and *Trichobilharzia regenti*, the neuropathogenic schistosome, in the roles of hunters and prey. (manuscript)

> *My contributions: Designing and performing the experiments (antigen preparation, cell cultivation, immunocytochemical staining, flow cytometry, DNA quantification), analyzing and visualizing the data, writing the manuscript.*

PUBLICATION #2

Šmídová, B., Majer, M., Novák, J., Revalová, A., Horák, P., and Macháček, T. (2024). The neurotropic schistosome vs experimental autoimmune encephalomyelitis: are there any winners? Parasitology *151*, 412–420.

> *My contributions: Designing the experiments, EAE inductions, scoring mice symptoms, flow cytometry analysis of the nervous tissue, histology of the spinal cord, cytokine ELISA, data analysis and visualisation, writing the manuscript, being the corresponding author.*

Publication #1

Macháček, T., Leontovyč, R., **Šmídová, B**., Majer, M.,
Vondráček, O., Vojtěchová, I., Petrásek, T., and Horák, P.

Mechanisms of the host immune response and helminth-induced pathology during *Trichobilharzia regenti* (Schistosomatidae) neuroinvasion in mice.

PLoS Pathogens, 2022
DOI: 10.1371/journal.ppat.1010302

PLOS PATHOGENS

RESEARCH ARTICLE

Mechanisms of the host immune response and helminth-induced pathology during *Trichobilharzia regenti* (Schistosomatidae) neuroinvasion in mice

Tomáš Macháček[1]*, Roman Leontovyč[1], Barbora Šmídová[1], Martin Majer[1], Oldřich Vondráček[1], Iveta Vojtěchová[2,3], Tomáš Petrásek[2,3], Petr Horák[1]

1 Department of Parasitology, Faculty of Science, Charles University, Prague, Czechia, **2** National Institute of Mental Health, Klecany, Czechia, **3** Laboratory of Neurophysiology of Memory, Institute of Physiology of the Czech Academy of Sciences, Prague, Czechia

* tomas.machacek@natur.cuni.cz

Citation: Macháček T, Leontovyč R, Šmídová B, Majer M, Vondráček O, Vojtěchová I, et al. (2022) Mechanisms of the host immune response and helminth-induced pathology during *Trichobilharzia regenti* (Schistosomatidae) neuroinvasion in mice. PLoS Pathog 18(2): e1010302. https://doi.org/10.1371/journal.ppat.1010302

Editor: Elise O'Connell, National Institutes of Health Clinical Center, UNITED STATES

Received: August 24, 2021

Accepted: January 24, 2022

Published: February 4, 2022

Data Availability Statement: All relevant data are within the manuscript and its Supporting Information files. RNA-seq read data are available for download via the NCBI sequence read archive (BioProject ID: PRJNA716607).

Funding: TM, RL, BŠ, MM, OV, and PH were supported by the Czech Science Foundation (18-11140S; https://gacr.cz/en), European Regional Development Fund and Ministry of Education, Youth and Sports of the Czech Republic

Abstract

Helminth neuroinfections represent serious medical conditions, but the diversity of the host-parasite interplay within the nervous tissue often remains poorly understood, partially due to the lack of laboratory models. Here, we investigated the neuroinvasion of the mouse spinal cord by *Trichobilharzia regenti* (Schistosomatidae). Active migration of *T. regenti* schistosomula through the mouse spinal cord induced motor deficits in hindlimbs but did not affect the general locomotion or working memory. Histological examination of the infected spinal cord revealed eosinophilic meningomyelitis with eosinophil-rich infiltrates entrapping the schistosomula. Flow cytometry and transcriptomic analysis of the spinal cord confirmed massive activation of the host immune response. Of note, we recorded striking upregulation of the major histocompatibility complex II pathway and M2-associated markers, such as arginase or chitinase-like 3. Arginase also dominated the proteins found in the microdissected tissue from the close vicinity of the migrating schistosomula, which unselectively fed on the host nervous tissue. Next, we evaluated the pathological sequelae of *T. regenti* neuroinvasion. While no demyelination or blood-brain barrier alterations were noticed, our transcriptomic data revealed a remarkable disruption of neurophysiological functions not yet recorded in helminth neuroinfections. We also detected DNA fragmentation at the host-schistosomulum interface, but schistosomula antigens did not affect the viability of neurons and glial cells *in vitro*. Collectively, altered locomotion, significant disruption of neurophysiological functions, and strong M2 polarization were the most prominent features of *T. regenti* neuroinvasion, making it a promising candidate for further neuroinfection research. Indeed, understanding the diversity of pathogen-related neuroinflammatory processes is a prerequisite for developing better protective measures, treatment strategies, and diagnostic tools.

(CZ.02.1.01/0.0/0.0/16_019/0000759; https://ec.europa.eu/regional_policy/en/funding/erdf), and Charles University institutional funding (PROGRES Q43, Cooperatio Biology, UNCE/SCI/012-204072/2018, SVV 260432/2018; https://cuni.cz/UKEN-65.html). OV was supported by Charles University Grant Agency (1374119; https://cuni.cz/UKEN-753.html). Microscopy was performed in the Laboratory of Confocal and Fluorescence Microscopy co-financed by the European Regional Development Fund and the state budget of the Czech Republic (CZ.1.05/4.1.00/16.0347, CZ.2.16/3.1.00/21515; https://ec.europa.eu/regional_policy/en/funding/erdf) and supported by the Czech-BioImaging large RI project LM2018129. Computational resources were supplied by the project "e-Infrastruktura CZ" (e-INFRA LM2018140) provided within the program Projects of Large Research, Development and Innovations Infrastructures, and ELIXIR-CZ projects LM2015047 and LM2018131, part of the international ELIXIR infrastructure supported by Ministry of Education, Youth and Sports of the Czech Republic (https://www.msmt.cz/?lang=2). The funders had no role in study design, data collection and analysis, decision to publish, or preparation of the manuscript.

Competing interests: The authors have declared that no competing interests exist.

Author summary

Infections of the human central nervous system by parasitic worms, such as pork tapeworm or rat lungworm, are a health threat, especially in communities with poor hygiene and sanitation. Understanding the diversity of host-parasite interactions, possibly leading to development of effective treatment or vaccine, requires suitable animal models. Our study deeply characterized the neuroinvasion of the mouse spinal cord by the neuropathogenic flatworm *Trichobilharzia regenti*. Its behavior within the nervous tissue (active migration, eager feeding) and clinical outcome of the infection (weight loss, motor dysfunctions, strong neuroinflammation) resemble those observed in human diseases. Using an integrative approach, we elucidated how the mice fight against the parasites and which mechanisms could be responsible for the pathological sequelae. Moreover, we identified pathways potentially involved in the reparation of the injured nervous tissue. All these features make *T. regenti* in mice a promising candidate for further research in parasitology, and neuroimmunology.

Introduction

Parasitic helminths often invade the central nervous system (CNS) of mammals, including humans. Invasion of the CNS is either a natural part of their somatic migration or represents an unwanted, ectopic localization [1]. The clinical manifestation of helminth neuroinfections ranges from mostly asymptomatic to very severe, leading to sensory or cognitive deficits and seizures or epilepsy [2–4]. Many factors, such as parasite burden or localization within the CNS, influence the course and outcome of the neuroinfection [5]. Moreover, the host immune response affects helminth growth and survival but might also participate in the pathogenesis or behavioral alterations [6,7]. Therefore, a deep understanding of host-parasite immune interactions is required to develop better protective measures, treatment strategies, and diagnostic tools.

The availability of suitable laboratory models dictates the primary orientation of the helminth neuroinfection research. Neurocysticercosis, cerebral angiostrongylosis, and neurotoxocarosis are hence in focus as their models have been established [8–13]. On the contrary, a valid model representing, e.g., the neurological form of schistosomosis or echinococcosis is lacking [14–16]. Novel model species for studying helminth neuroinfections are thus needed to reveal the diversity of host-parasite interactions and (immuno-)pathological sequelae. Even if they do not fully mirror any specific human disease, investigating their interactions with the host could bring valuable insights. This is also the case of some filarial or intestinal model helminths that only partially reflect the human diseases but are useful after integrating the experimental findings [17,18]. Regarding the neurotropic helminths, the species naturally invading the CNS should be considered as no artificial manipulations, such as injections of parasites into the CNS [12,16], are required.

Trichobilharzia regenti is a schistosome that naturally migrates through the CNS of birds and mammals (birds are the definitive hosts, whereas mammals represent the accidental hosts). After penetration of the host skin, the newly transformed schistosomula find the peripheral nerves *via* which they enter the spinal cord [19,20]. Here they eagerly feed on the nervous tissue, but no significant demyelination is observed [21–23]. However, leg paralysis is often reported in ducks and immunocompromised mice due to a higher schistosomula burden and/or their prolonged persistence within the CNS [21,22]. On the contrary, immunocompetent mice effectively control *T. regenti* neuroinvasion. Indeed, recruited peripheral leukocytes entrap and destroy the schistosomula in the spinal cord 7–14 days post infection (dpi) [22,24].

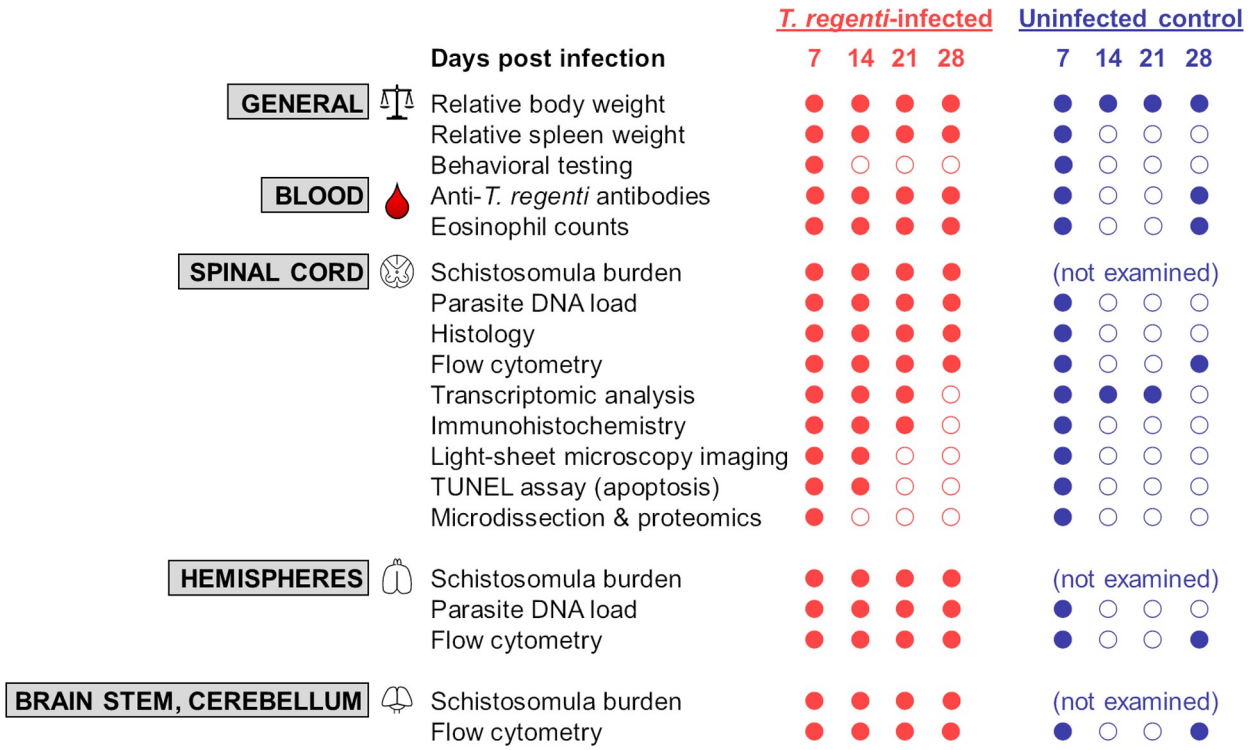

Fig 1. Summary of experimental procedures. C57BL/6J female mice were infected with *T. regenti* cercariae and examined at desired time points (indicated by filled red dots). Uninfected mice were used as controls; particular age-matching is shown for each analysis (filled blue dots). Empty dot means that the analysis was not performed at the respective time point.

https://doi.org/10.1371/journal.ppat.1010302.g001

The CNS-resident microglia are also activated [22] but do not seem to harm the living schistosomula, e.g., by the production of nitric oxide [25,26]. Even though living schistosomula are rarely found after 21 dpi [22,24], the host effector immune mechanisms remain unclear.

Here we employed a complex approach, ranging from behavioral testing to 'omics' analyses (Fig 1), to explore mechanisms of the host immune response and helminth-induced pathology in the CNS of mice infected with *T. regenti*. Our comprehensive insight allows us to compare *T. regenti*- neuroinvasion with other medically important helminth neuroinfections and uncover the diversity of host-parasite interactions within the nervous tissue. In this regard, the remarkable disruption of neurophysiological functions (not observed in other helminths yet) and a strong M2 polarization in *T. regenti*-infected spinal cords should be of particular interest.

Results

T. regenti triggered peripheral immunity and invaded the CNS, especially the spinal cord

First, we briefly characterized general features of *T. regenti* infection to establish the model and validate its reproducibility in C57BL/6J mice 7, 14, 21, and 28 dpi. The infection did not alter mouse survival, but the infected individuals exhibited a decreased gain in body weight (Fig 2A; $p(7\ dpi) = 0.0022$; $p(14\ dpi) = 0.0024$; $p(28\ dpi) = 0.0009$) despite having the same feed consumption rate as the uninfected group. The infected mice produced both parasite-specific IgG1 and IgG2a as soon as 7 dpi. Levels of Th2-associated IgG1 rose continuously and prevailed over Th1-associated IgG2a (Fig 2B), especially 28 dpi ($p < 0.0001$). These observations of antibody response corroborate with the previous studies [27–29], which demonstrates

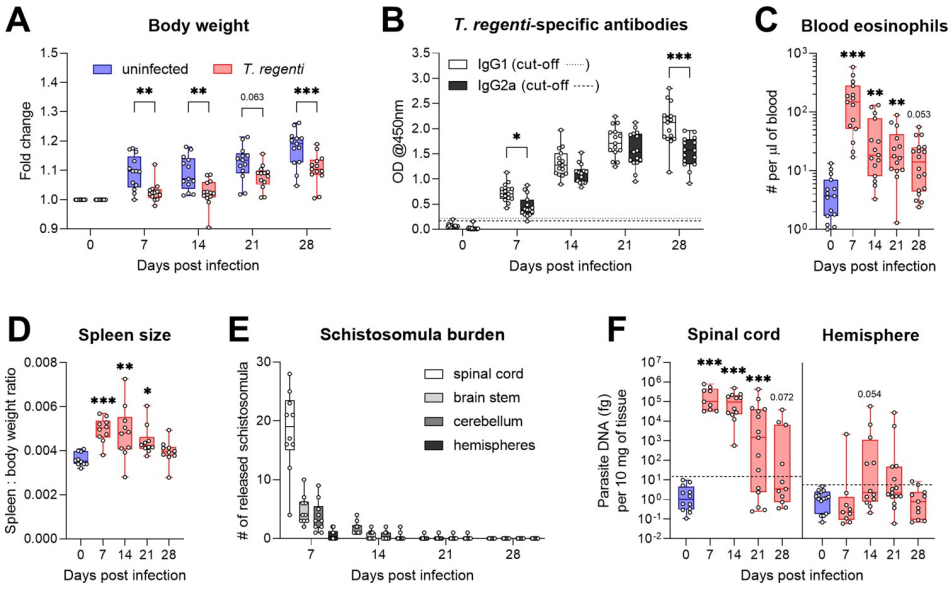

Fig 2. General features of *T. regenti* infection in C57BL/6J mice. (A) Infected mice exhibited a lower gain in body weight than age-matched uninfected controls. **(B)** The levels of *T. regenti*-specific IgG1 and IgG2a detected in mouse sera rose steadily throughout the infection. Th2-associated IgG1 dominated over Th1-associated IgG2a, especially 28 dpi. **(C)** Blood eosinophil counts have increased in infected mice 7–21 dpi. **(D)** Spleen enlargement was observed in infected mice 7–21 dpi. **(E)** Within the CNS, most viable schistosomula were found 7 dpi being localized predominantly in the spinal cord. The amount of released schistosomula remarkably decreased at later time points. **(F)** Contrary to those from hemispheres, *T. regenti* DNA was detected in most of the spinal cord tissue samples 7–21 dpi. In each graph, points show data from individual mice. Pooled data from 2–3 independent experiments are shown. Data were evaluated by 2-way ANOVA for repeated measures and Šidák's test (A), ordinary 2-way ANOVA and Šidák's test (B, F), Kruskal-Wallis and Dunn's test (C), or ordinary 1-way ANOVA and Dunnett's test (D); $^{*}p<0.05$, $^{**}p<0.01$, $^{***}p<0.001$.

https://doi.org/10.1371/journal.ppat.1010302.g002

reproducibility of the host immune reaction. The number of blood eosinophils peaked 7 dpi and remained elevated 14 and 21 dpi (Fig 2C; p(7 dpi) < 0.0001; p(14 dpi) = 0.0017; p(21 dpi) = 0.0053). A similar trend was observed in the case of spleen enlargement (Fig 2D; p(7 dpi) = 0.0007; p(14 dpi) = 0.0019; p(21 dpi) = 0.0456), which correlates with already reported increased numbers of splenic CD4+ and CD8+ T cells 7 and 14 dpi [29].

Due to *T. regenti* neurotropism, we further examined the distribution of schistosomula within the CNS, which has not been thoroughly done in C57BL/6J mice. The highest number of viable schistosomula was extracted 7 dpi (27.3 ± 9.8 per mouse, n = 10). They predominantly invaded the spinal cord (Fig 2E) but were also localized in the brain stem or the cerebellum. However, only 3 out of 10 mice harbored 1–2 schistosomula in the hemispheres. Markedly fewer schistosomula were released from the entire CNS 14 dpi (3.0 ± 2.1 per mouse, n = 10) and 21 dpi (4 schistosomula isolated from 2 mice out of 10); no schistosomula were recorded 28 dpi. Such migration pattern agrees with the historical records (obtained from other mouse strains) showing accumulation of schistosomula in the spinal cord and the highest burden within the CNS around 7 dpi [20,21]. To complement the data on schistosomula distribution, we also analyzed *T. regenti* DNA content in the spinal cord and hemisphere tissue samples. The parasite DNA was present in the spinal cords of all mice 7 and 14 dpi, and most of the mice 21 dpi (Fig 2F; p(7, 14, and 21 dpi) < 0.0001). On the contrary, the hemispheres seldom contained the parasite DNA; less than half of the samples were positive 14 and 21 dpi.

Collectively, our data demonstrated early activation of the peripheral immune response against *T. regenti*, which successfully invaded the CNS, especially the spinal cord, by 7 dpi.

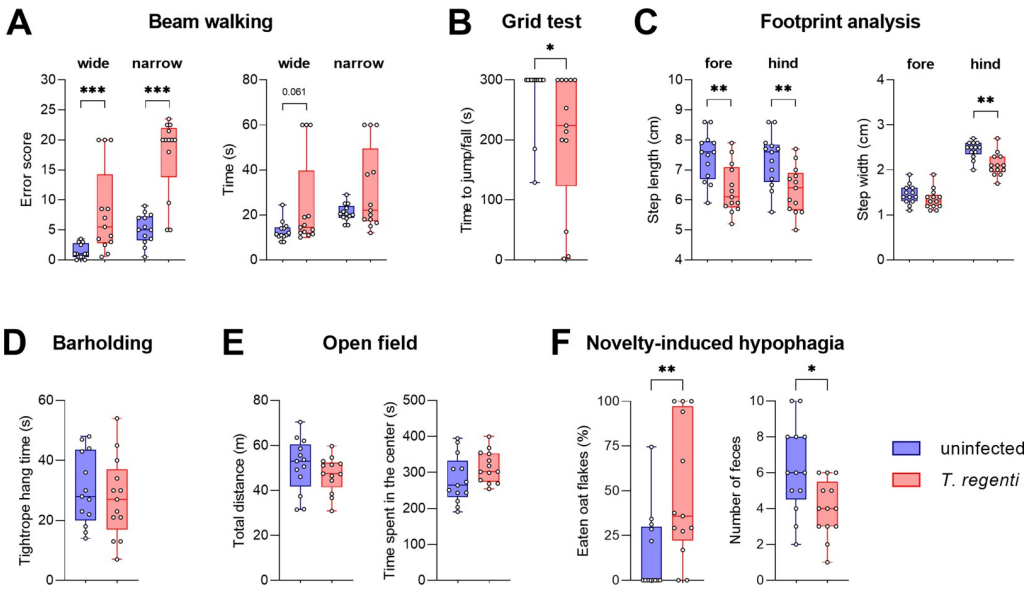

Fig 3. Effects of *T. regenti* infection on mouse behavior 7 dpi. **(A)** Beam walking on wide and narrow beams, impaired motor coordination in infected mice. **(B)** Grid test, worse endurance, and strength of the forelimbs and hindlimbs of infected mice. **(C)** Footprint analysis of forelimbs and hindlimbs, altered posture and gait in infected mice. **(D)** Bar holding, normal endurance, and strength of the forelimbs in both groups. **(E)** Open field, unaffected locomotor activity, and anxiety in both groups. **(F)** Novelty-induced hypophagia, higher amount of eaten oat flakes caused by stronger appetitive motivation, rather than increased anxiety of infected mice. In each graph, points show data from individual mice. Pooled data from 3 independent experiments are presented. Data were evaluated by Mann-Whitney test (A, B, F—eating) or unpaired t-test (C, D, E, F—feces); $^{*}p<0.05$, $^{**}p<0.01$, $^{***}p<0.001$.

https://doi.org/10.1371/journal.ppat.1010302.g003

Motor function deficits affected the lower body of *T. regenti*-infected mice

The highest schistosomula burden was detected in the spinal cord 7 dpi. At this moment, we assessed the impact of neuroinvasion on various aspects of mouse behavior. Most importantly, the infected mice showed a deficit in motor functions. They made more errors when traversing a wide ($p = 0.0006$) or narrow ($p < 0.0001$) beam (Fig 3A and S1 Video), exhibited lower endurance when hanging upside-down on a grid (Fig 3B; $p = 0.0313$), and made shorter steps (Fig 3C; p(forelimbs) = 0.0027; p(hindlimbs) = 0.0059). Visual observations also showed altered tail posture in the infected mice (tail dragging, reduced tail motility). We suggest that motor functions of the lower body were affected as the performance in the bar holding task, depending predominantly on forelimb strength, was unaltered (Fig 3D), and step width was decreased in hindlimbs only (Fig 3C; p(forelimbs) = 0.2545; p(hindlimbs) = 0.001). However, general locomotor activity in the open field (Fig 3E), plus maze or Y-maze was normal, as well as spatial working memory in the Y-maze (S1 Fig). In the test of novelty-induced hypophagia, the infected mice ate more ($p = 0.0094$) and defecated less ($p = 0.0117$) than controls (Fig 3F). This behavior is more likely related to a stronger appetitive motivation than altered emotionality as we detected no signs of elevated anxiety (Fig 3E) or depression-like behavior in several other tests (S1 Fig). Collectively, our experiments showed that deficits in motor functions were the most evident behavioral sequelae of *T. regenti* neuroinvasion.

Eosinophil-rich infiltrates entrapped and eliminated schistosomula in the spinal cord

After assessing the general impact of *T. regenti* infection on mice, we performed a histological examination of the spinal cord to elucidate the course of the infection in the most affected

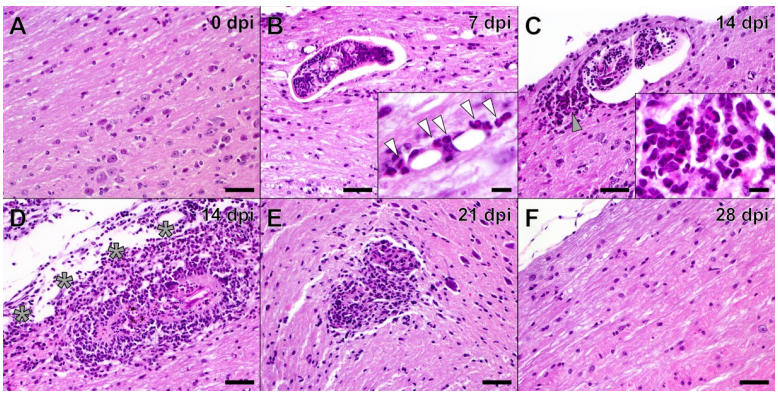

Fig 4. Histological examination of the *T. regenti*-infected spinal cord. (A) In the uninfected spinal cord, no leukocyte infiltration was apparent. **(B)** The intact schistosomulum in the white matter 7 dpi. No inflammatory cells surrounded the schistosomulum, but eosinophil extravasation was recorded in the adjacent areas (inset, eosinophils marked by white arrowheads). **(C)** The "rocket-tail" leukocyte cluster behind the schistosomulum 14 dpi. Eosinophils and mononuclear cells prevailed in the cluster (gray arrowhead and inset). **(D)** The inflammatory lesion around the destroyed schistosomulum 14 dpi. The adjoining leptomeningeal spaces (gray asterisks) were thickened and heavily inflamed. **(E)** The schistosomulum remnants within the fading inflammatory lesion 21 dpi. **(F)** The spinal cord tissue 28 dpi, no schistosomula residues or inflammatory foci were evident. Representative images from 2 independent experiments (each with 2–3 mice) per time point are shown. Scale bar (large image) = 50 μm, scale bar (inset) = 10 μm.

https://doi.org/10.1371/journal.ppat.1010302.g004

segment of the CNS. Only intact schistosomula were observed 7 dpi being localized predominantly in the white matter (Fig 4B). Flattened cells with squeezed nuclei surrounded some of the schistosomula, while some were followed by "rocket-tail" leukocyte clusters (see below). Extravasation of leukocytes, mainly eosinophils (Fig 4B, inset), was recorded in the areas close to migrating schistosomula. The neuroinflammation culminated 14 dpi when no schistosomula were left unnoticed by the host immune cells. Of note, striking "rocket-tail" leukocyte clusters, consisting mainly of eosinophils and mononuclear cells (Fig 4C, inset), formed behind schistosomula (Fig 4C). Some parasites were still compact but had a thinner body wall and vacuolized internal tissues with condensed nuclei. However, some schistosomula were already damaged, and eosinophils, neutrophils, monocytes, and lymphocytes extensively infiltrated the lesions (Fig 4D). The adjacent leptomeningeal spaces were also thickened and heavily inflamed. The inflammatory foci around hardly distinguishable schistosomula or their remnants were still apparent 21 dpi (Fig 4E), but the leukocyte infiltration was fading away. Neither schistosomula residues nor inflammatory foci were detected 28 dpi (Fig 4F). Taken together, *T. regenti* neuroinvasion caused eosinophilic meningomyelitis with a peak 14 dpi. The cellular infiltrate was presumably essential for parasite elimination.

Eosinophils were the most numerous cells infiltrating the entire CNS during *T. regenti* infection

Based on histological findings, we employed flow cytometry to quantify the immune cells infiltrating the infected nervous tissue to see the dynamics of the cellular immune response. Apart from the spinal cord, we also examined the brain stem, the cerebellum, and the hemispheres, which can also be invaded by schistosomula, however, to a much lesser extent (Fig 2E). The spinal cord and hemispheres were infiltrated mainly by eosinophils, lymphoid cells, and macrophages/monocytes with a peak 14 dpi (Fig 5A and 5D). A similar situation was observed in the brain stem (Fig 5B), where a significant increase was also noticed in microglia and neutrophil counts 7 dpi. In the cerebellum, eosinophil counts spiked 14 dpi (Fig 5C), but neutrophil,

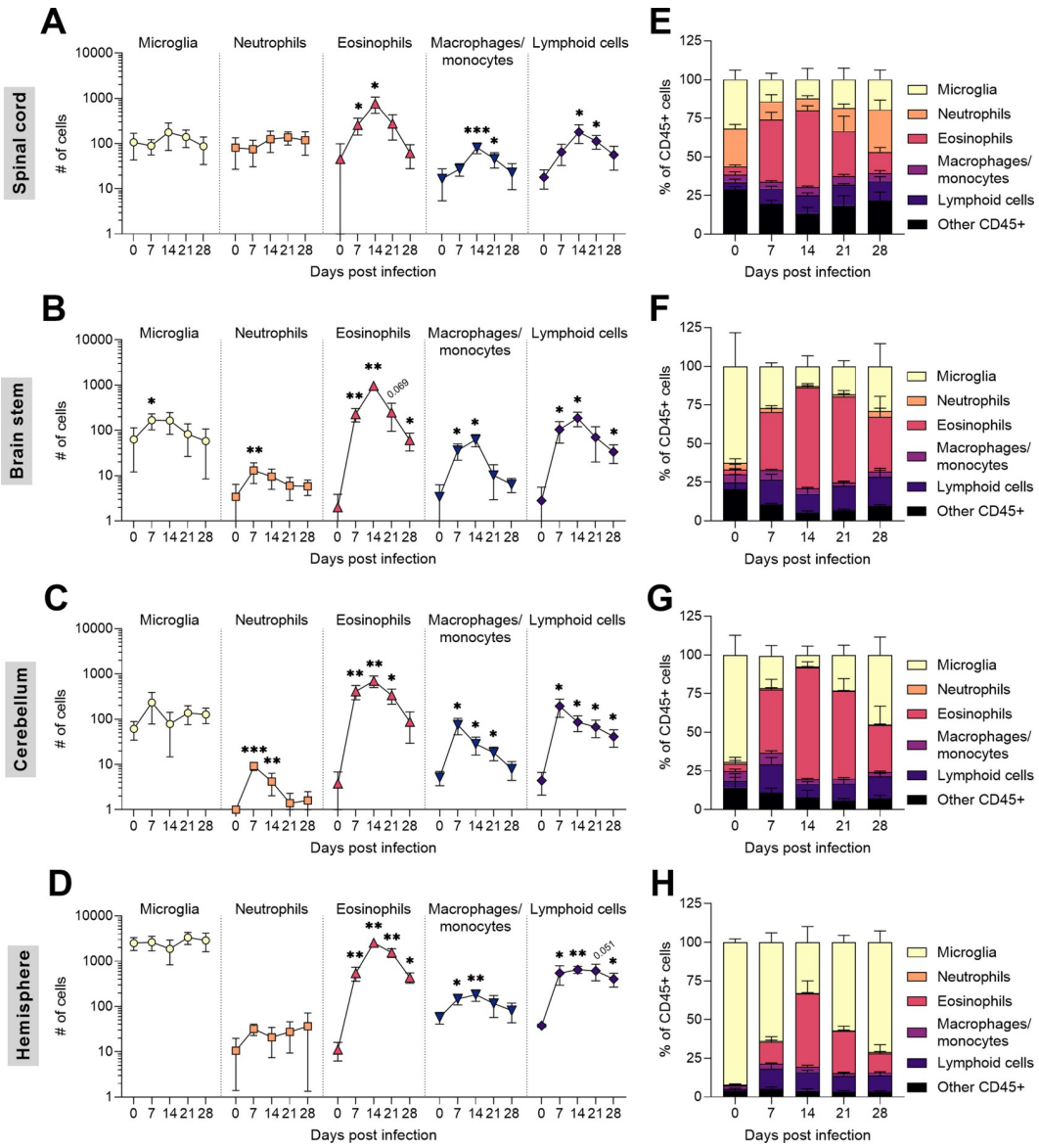

Fig 5. Dynamics of major immune cell populations in the mouse CNS during *T. regenti* infection. (A–D) Microglia, neutrophils, eosinophils, macrophages/monocyte, and lymphoid cells were analyzed by flow cytometry in the spinal cord (A), the brain stem (B), the cerebellum (C), and the hemisphere (D). In all examined segments, the most prominent increase was observed in eosinophil counts 14 dpi. Gating strategies are shown in S2 Text. Data (n = 5 per each time point) were evaluated by ordinary 1-way or Welch's ANOVA followed by Dunnett's test; $^{*}p<0.05$, $^{**}p<0.01$, $^{***}p<0.001$. **(E–H)** The relative proportion of the examined immune cell populations in the spinal cord (E), the brain stem (F), the cerebellum (G), and the hemisphere (H). Massive infiltration of peripheral leukocytes caused an apparent decrease in the proportion of microglia. Representative data from 1 out of 2 independent experiments are shown.

https://doi.org/10.1371/journal.ppat.1010302.g005

macrophage/monocyte, and lymphoid cell counts reached climax already 7 dpi. The microglia counts remained unchanged in all segments, except for the brain stem 7 dpi (see above). However, their relative representation stooped in favor of infiltrating leukocytes, especially eosinophils (Fig 5E–5H). Taken together, *T. regenti* neuroinvasion led to striking infiltration of the CNS with peripheral leukocytes. Eosinophils undoubtedly prevailed in all examined segments having a peak 14 dpi.

Infected spinal cords displayed transcriptional upregulation of immune system pathways and disruption of neurophysiological functions

To get a complex insight into the processes ongoing in the infected spinal cords, transcriptomic analysis of the whole tissue was performed 7, 14, and 21 dpi using respective age-matched uninfected controls. In total, 24 transcriptomes were sequenced with an average number of 43,115 ± 2,276 transcripts (Fig 6A). RNA-seq read data are available for download *via* the NCBI sequence read archive (BioProject ID: PRJNA716607). Differential expression analysis showed the highest number of differentially expressed transcripts (DETs) 7 dpi when more transcripts were downregulated (6,943) than upregulated (4,128). The number of DETs decreased 14 and 21 dpi, and upregulated transcripts prevailed over downregulated ones (Fig 6B and S1 Table).

Kyoto Encyclopedia of Genes and Genomes (KEGG) database was used to annotate DETs to get a general overview of the up-/downregulated processes. In total 2,225, 1,536, and 1,248 upregulated KEGG-IDs were identified 7, 14, and 21 dpi, respectively (Fig 6C), and represented 27 (7 dpi), 47 (14 dpi), and 27 (21 dpi) significantly enriched biological pathways (S1 Table). The most enriched pathways were linked to the immune system at all time points (Fig 6D). For example, chemokine signaling and leukocyte transendothelial migration pathways were significantly enriched 7 and 14 dpi when the spinal cord infiltration by peripheral leukocytes was on the rise (Fig 5A). A detailed analysis revealed the upregulation of several chemokines (*Ccl2*, *Ccl5*, *Ccl7*, *Ccl8*, *Ccl24*, *Cxcl9*, *Cxcl16*) and their receptors (Fig 7A and 7B) which facilitate the recruitment of leukocytes into the CNS. Throughout the infection, remarkable enrichment was also noticed in the Toll-like receptor signaling pathway, which participates in recognizing pathogen-associated molecular patterns. Namely, *Tlr8*, *Tlr11*, and *Tlr12* exhibited the highest upregulation (Fig 7C). Pathways associated with antigen processing were also enriched, especially 7 dpi. Indeed, cathepsin S (*Ctss*), a lysosomal enzyme critical for antigen presentation, was found among the top 20 upregulated DETs 7 dpi (Fig 6F) and retained the markedly elevated expression also 14 and 21 dpi (log_2fold change = 15 and 11, respectively). Accordingly, Th1/Th2/Th17 cell differentiation and B cell receptor signaling pathways were upregulated as soon as 7 dpi, suggesting early adaptive response activation. These transcriptomic data correspond to our experimental results demonstrating the production of parasite-specific antibodies (Fig 2B) or mixed Th1/Th2/Th17 splenic phenotype [29] 7 dpi. Interestingly, complement and coagulation cascades and the C-type lectin receptor pathway were mostly enriched 14 dpi when the highest eosinophil infiltration and first injured schistosomula were found in the spinal cord (Fig 4C and 4D).

The infection of the mouse spinal cord was also linked with significant downregulation of transcription. Overall, 2,492, 827, and 857 downregulated KEGG-IDs were identified 7, 14, and 21 dpi, respectively (Fig 6C), and represented 33 (7 dpi), 18 (14 dpi), and 9 (21 dpi) enriched pathways (S1 Table). They were mostly associated with signal transduction, synaptic transmission, and axonal development (Fig 6E). Accordingly, we observed enormous downregulation of kinesin family members *Kif1a* and *Kif1b*, essential players in the axonal transport of synaptic vesicles and mitochondria [30,31], and cytosolic carboxypeptidase 1 (*Agtpbp1*, also known as *Ccp*) deficiency of which causes coordination deficits [32]. They all were even among the top 20 downregulated DETs at all time points (Fig 6F). On the contrary, the expression of structural neurofilaments remained almost unchanged except for nestin (*Nes*, Fig 7D) required for glial scar formation [33,34]. Of myelin-associated transcripts, only proteolipid protein 1 (*Plp1*) was strikingly upregulated 7 dpi (Fig 7E), which might boost the activation of microglia [35]. Importantly, no transcriptional evidence was found for demyelinating processes (Fig 7E), which accords with previous histopathological studies [22,26]. However,

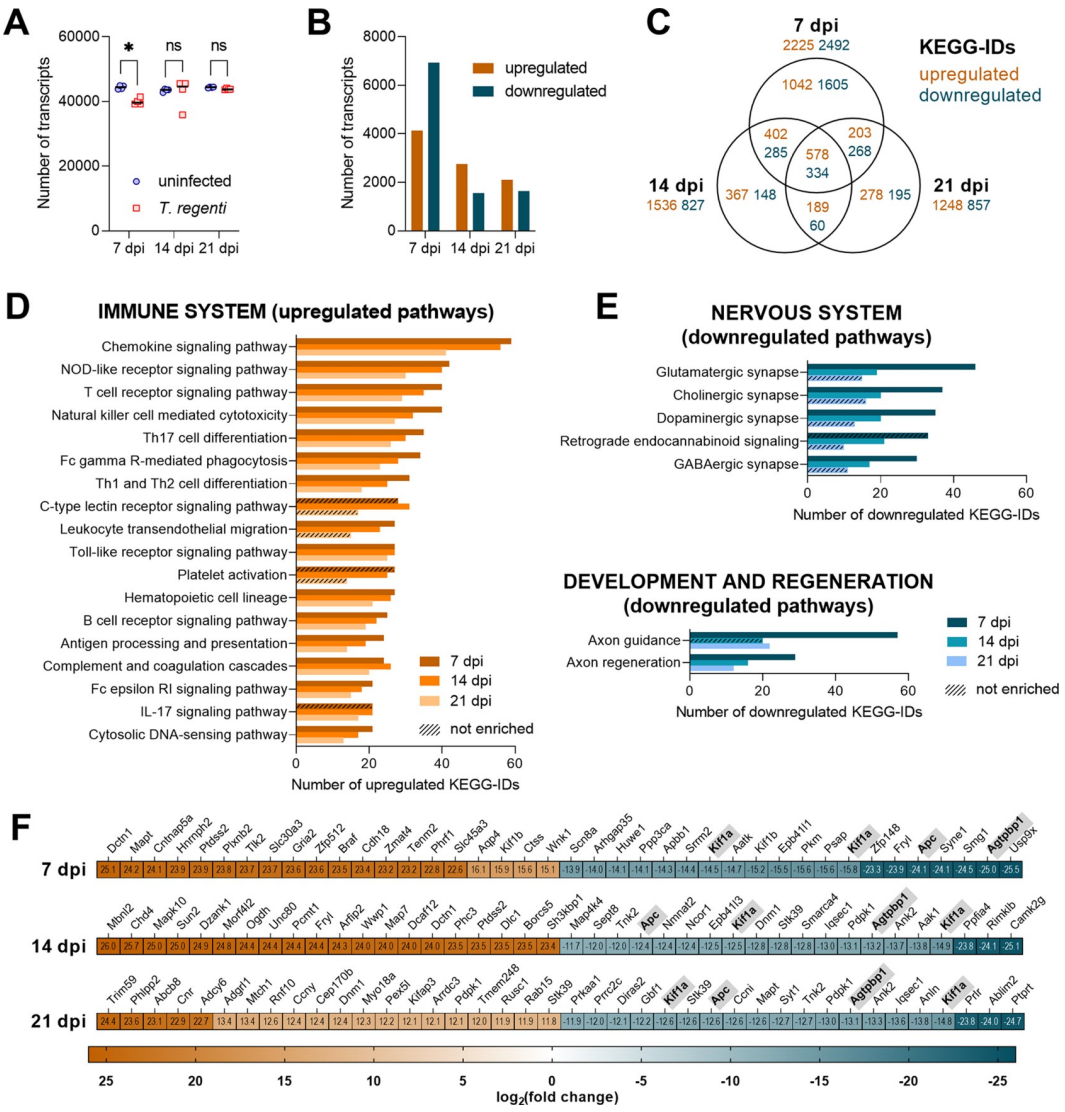

Fig 6. Transcriptomic analysis of the spinal cord of *T. regenti*-infected mice. (A) The number of transcripts identified in the spinal cords of infected or age-matched uninfected (control) mice 7, 14, and 21 dpi. The transcriptomic analysis was performed with a group of mice (n = 4 per each time point) infected independently from other experiments presented herein. Data were evaluated by ordinary 2-way ANOVA and Šidák's test; $^{*}p<0.05$. **(B)** The number of differentially expressed transcripts 7, 14, and 21 dpi based on $\log_2$fold change (FC; upregulated >2, downregulated <-2). **(C)** Differentially expressed transcripts with Kyoto Encyclopedia of Genes and Genomes (KEGG) annotation and their exclusive/shared occurrence in the infected spinal cord 7, 14, and 21 dpi. **(D)** Enriched immune system pathways of upregulated transcripts according to KEGG annotation. **(E)** Enriched pathways of downregulated transcripts linked with the nervous system and development and regeneration according to KEGG annotation. **(F)** Top 20 up-/downregulated transcripts (based on $\log_2$FC) 7, 14, and 21 dpi. Abbreviated gene names are shown, gray background marks genes found among the "top 20" at all time points.

https://doi.org/10.1371/journal.ppat.1010302.g006

massive upregulation was observed in the case of the amyloid precursor protein (*App*, Fig 7F) at all time points, which is likely linked to axonal injury caused by migrating schistosomula [22].

Altogether, the transcriptional analysis of *T. regenti*-infected spinal cords substantially elucidated general features of the host-parasite relationship. Most importantly, we demonstrated upregulation of immune processes and downregulation of neurophysiological pathways. Based on the transcriptomic data, we further examined several aspects of *T. regenti* neuroinvasion.

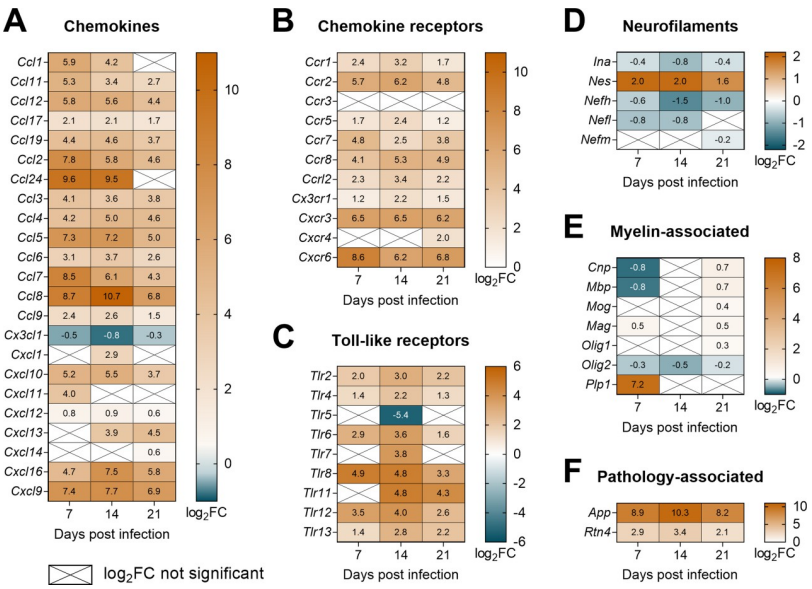

Fig 7. Expression of immune and neural markers in the spinal cord of *T. regenti*-infected mice. (A–F) The heatmaps show $\log_2$fold change (FC) in the expression of chemokines (A), chemokine receptors (B), Toll-like receptors (C), neurofilaments (D), myelin-associated markers (E), and pathology-associated markers (F). Genes/transcripts with $\log_2$FC >2 or <−2 were considered as upregulated or downregulated, respectively. Only genes with a significant $\log_2$FC are shown unless indicated otherwise (crossed cells). Spinal cords of 4 infected and 4 uninfected age-matched mice were analyzed at each time point.

https://doi.org/10.1371/journal.ppat.1010302.g007

Arginase-1 dominated among the proteins found exclusively around the migrating schistosomula, which unselectively fed on the nervous tissue

To better understand the biological processes in the close vicinity of the migrating schistosomula, we microdissected the surrounding tissue within 100 μm from the schistosomula (Fig 8A) and subjected it to the mass spectrometry (MS) analysis. Infected spinal cords were analyzed only 7 dpi as the highest number of schistosomula can be found at this time point and it is possible to properly distinguish the schistosomula-host tissue interface (Figs 6B and 8B). Also, most DETs were found at this time point. Initially, microdissects from three spinal cord segments (sacral, lumbar, thoracic) were analyzed separately. As no significant differences were found in the protein composition of microdissects from different segments (S2 Table, sheets F–H), the subsequent data analysis was performed on merged datasets from all three segments.

Altogether, 1,690 proteins were identified in infected and uninfected (control) spinal cords. In total, 752 proteins were recorded in at least 3 out of 4 replicates and therefore were considered reliably identified. The vast majority (705) of proteins were common to microdissects from infected and control spinal cords, but 15 of them were differentially abundant in infected (8) or control (7) ones (Fig 8C, dashed line outline and S2 Table, sheet C). Fifteen proteins were exclusively found in the microdissects from infected spinal cords (Fig 8C, thick red outline and S2 Table, sheet A), including those presumably involved in the host immune response: arginase (a marker of alternatively activated M2 microglia/macrophages), integrin beta 1 (leukocyte adhesion molecule), or interferon-induced guanylate-binding protein 2 (enigmatic protein with antiparasitic activity; [36]). On the contrary, 35 proteins were exclusively found in uninfected mice (Fig 8C, thick blue lines and S2 Table, sheet B). They were linked mainly with the cytoskeleton and cell signaling, but no specific pathway/pattern was recognized. Corroborating with the proteomic data, most exclusive and differentially abundant proteins were

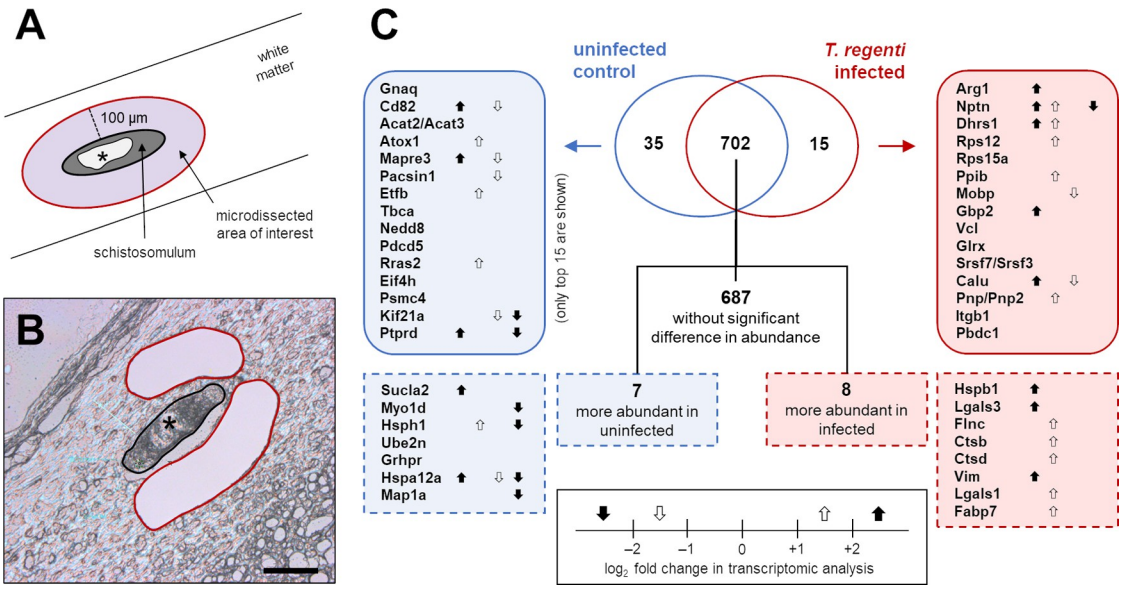

Fig 8. Proteomic analysis of the spinal cord tissue around *T. regenti* schistosomula. (A) A schematic representation of the region of interest. The area within 100 μm from the schistosomulum was microdissected as well as the schistosomulum digestive tract (marked by an asterisk; for intestinal results see the main text). **(B)** A real image from the microscope, labeling is consistent with (A)–i.e., the already microdissected area is outlined in red. Scale bar = 100 μm. **(C)** A summary of the proteomic analysis of the microdissected nervous tissue. Proteins exclusively found (thick line) or more abundant (dashed line) in uninfected (blue) or *T. regenti*-infected (red) spinal cords are shown. The up/down arrows indicate a $\log_2$fold change (FC) in the expression of the protein mRNA as revealed by the transcriptomic analysis (see Fig 6). More arrows per one protein mean that more isoforms were detected in the transcriptome. If no arrow is shown, the $\log_2$FC was negligible (−1; +1) or not significant. The proteomic analysis was performed with samples obtained from a group of mice (n = 3–4, see Materials and Methods for details) infected independently from other experiments presented herein.

https://doi.org/10.1371/journal.ppat.1010302.g008

identified as differentially expressed (either up- or downregulated) in the "7 dpi" transcriptome. Some of them were represented by multiple transcription variants differing in the level of expression (Fig 8C, up/down arrows and S2 Table, sheet E).

Additionally, the protein composition of the schistosomula digestive tract was analyzed by MS to reveal the parasite diet. A better understanding of *T. regenti* eating habits might help to unveil the host-parasite interactions. Out of 237 reliably identified proteins, 179 were annotated as mouse proteins, 39 as *T. regenti*, and 19 shared homology with both organisms (S2 Table, sheet I). The most abundant among mouse proteins were those associated with myelin, such as myelin basic protein, myelin proteolipid protein, 2,3-cyclic-nucleotide 3-phosphodiesterase, and myelin-oligodendrocyte glycoprotein. Furthermore, neuronal and astrocytic intermediate filaments were present (neurofilament light and medium polypeptides, glial fibrillary acidic protein, vimentin) as well as the CNS extracellular matrix glycoprotein periostin. Interestingly, the schistosomula digestive tract also contained proteins related to the host immune system like lysozyme C-1, arginase, or eosinophil cationic protein 1. Endogenous *T. regenti* proteins were represented mainly by digestive peptidases (cathepsins B1.6, B1.3, B1.4, C, and leucine aminopeptidase), detoxification enzymes (thioredoxin, peroxiredoxin, and glutathione S-transferase), and metabolic enzymes (lactate dehydrogenase A and glyceraldehyde 3-phosphate dehydrogenase). Proteins homologous to both mouse and *T. regenti* included highly conserved proteins such as actin, tubulin, calmodulin, and histones.

Collectively, the proteomic analysis of tissue microdissects demonstrated that markers suggesting activation of the host immune response were present around the schistosomula already 7 dpi. Arginase was the most abundant exclusive protein indicating the presence of microglia/

macrophages with the M2 phenotype. We also found that migrating schistosomula are not selective in the diet as a mixture of proteins associated with the nervous tissue and the host immune system was detected in their digestive tract.

T. regenti infection induced M2 polarization of microglia/macrophages which accumulated around the migrating schistosomula

Polarization of activated microglia/macrophages, either pro-inflammatory M1 or anti-inflammatory M2, largely determines their role in the host immune response. Marked upregulation of *Aif1* (also known as *Iba1*), the marker of microglia/macrophages [37,38], indicated activation of the cells in response to the spinal cord invasion by *T. regenti* (Fig 9A). Initially, Iba-1 was mostly detected in the schistosomula migratory tracks (7 dpi), but later, it accumulated around schistosomula (14 dpi) or even within their damaged bodies (Fig 9D). As this observation suggested the active participation of microglia/macrophages in the schistosomula elimination, we further examined the expression of markers related to M1/M2 polarization. Despite upregulation of M1-promoting cytokines (*Ifng*, *Il1b*) throughout the infection, inducible NO synthase (*Nos2*), the effector molecule of M1 polarization, exhibited none or negligible changes in expression (Fig 9B). It corroborates our previous immunohistochemical data demonstrating the lack of inducible NO synthase in the infected spinal cord [26].

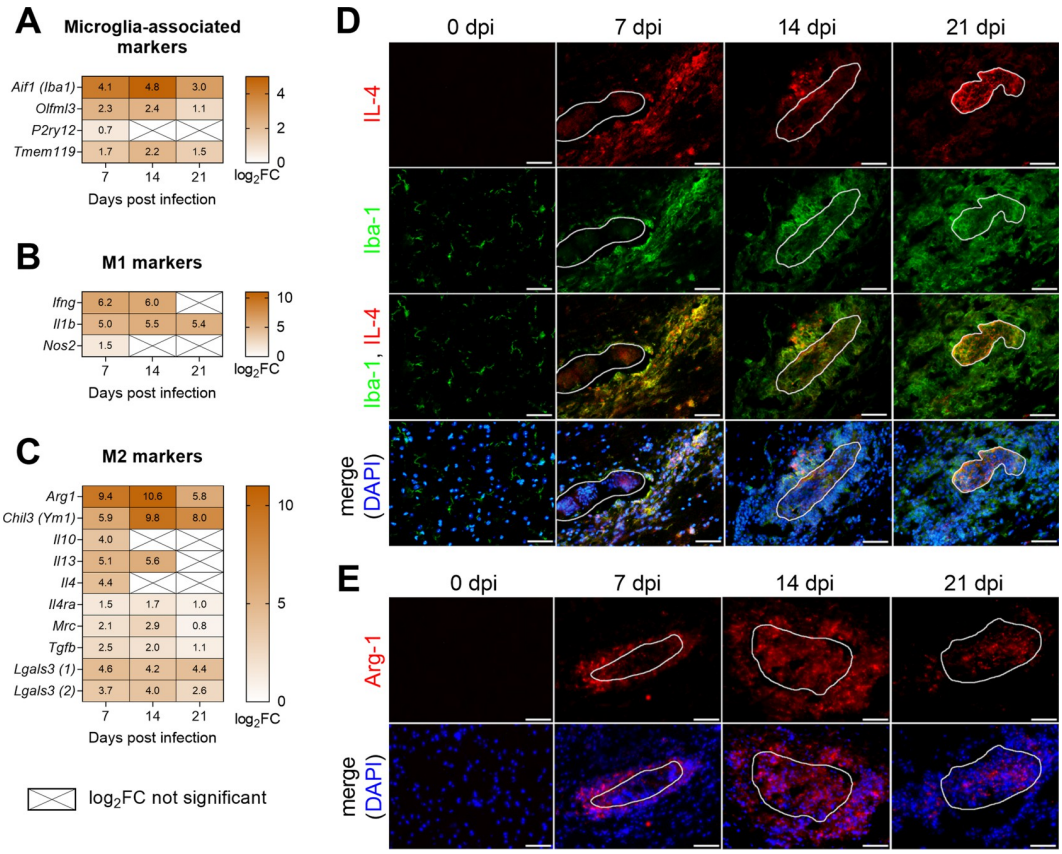

Fig 9. M1/M2 polarization in the spinal cord of *T. regenti*-infected mice. (A–C) The heatmaps show $\log_2$fold change (FC) in the expression of markers associated with microglia (A), M1 (B), and M2 (C) polarization. Genes/transcripts with $\log_2$FC >2 were considered upregulated, and only genes with a significant $\log_2$FC are shown unless indicated otherwise (crossed cells). Spinal cords of 4 infected and 4 uninfected age-matched mice were analyzed at each time point. **(D–E)** Immunolocalization of IL-4+Iba-1 (D), and Arg-1 (E). Representative images are shown, the white line indicates the space occupied by the schistosomulum. Scale bar = 50 μm.

https://doi.org/10.1371/journal.ppat.1010302.g009

On the other hand, we recorded striking upregulation of M2-associated markers, such as arginase (*Arg1*) and chitinase-like 3 (*Chil3*, also known as *Ym1*). Accordingly, M2-triggering cytokines (*Il4*, *Il10*, *Il13*, *Tgfb*) were upregulated 7 and/or 14 dpi along with M2-promoting galectin-3 (*Lgals3*) [39] (Fig 9C). To validate the transcriptomic data, we proceeded with the immunohistochemical detection of IL-4, which drives M2 polarization and the production of arginase [40]. IL-4 colocalized with Iba-1 in the schistosomula migratory tracks 7 dpi but diminished 14 dpi (Fig 9D). However, a strong IL-4 signal was detected in the area of the destroyed schistosomula 21 dpi. On the contrary, arginase (Arg-1) closely surrounded the schistosomula 7 dpi (Fig 9E), which agreed with the previously shown microdissection data (Fig 8C). At 14 dpi, the Arg-1 signal spread further into the tissue but accumulated mostly within the damaged schistosomula 21 dpi.

Collectively, transcriptomic and immunohistochemical data confirmed a strong M2 polarization of microglia/macrophages in the infected spinal cord, especially in the close vicinity of the schistosomula.

3D-imaging revealed the expansion of MHC II+ cells during *T. regenti* neuroinvasion

Expression of major histocompatibility complex (MHC) II, either by professional antigen presenting or other cells, mirrors the activation status of the host immune response. In *T. regenti*-infected spinal cords, we recorded striking upregulation of *Cd74*, *H2-Aa*, *H2-Ab1*, and other members of the MHC II pathway throughout the infection (Fig 10A). Immunohistochemistry revealed accumulation of MHC II+ cells around the schistosomula and partial colocalization of MHC II with Iba-1, the marker of microglia/macrophages (Fig 10B). Thanks to the availability of a suitable model (MHC II-EGFP mice), we employed light-sheet fluorescence microscopy (LSFM), which allowed us to display a 3D tissue context and visualize MHC II distribution *in toto* 7 and 14 dpi. High levels of background autofluorescence impeded analysis of the gray matter, so we examined white matter regions of the thoracic spinal cord, which is preferred by the schistosomula anyway [41].

Seven dpi, the MHC II+ cells were scattered in the parenchyma, but some of them already contacted the schistosomula (Fig 10C and S2 and S3 Videos). Massive MHC II+ clusters formed around the schistosomula 14 dpi when the MHC II signal often copied the shape of parenchymal blood vessels and anterior or posterior median sulci (Fig 10C and S4 Video). These observations correlated with data from the volumetric analysis of the MHC II signal, which rocketed 14 dpi ($p < 0.0001$). Indeed, a 1000-fold increase was recorded in comparison to uninfected mice (Fig 10D). We also attempted to count the exact amount of MHC II+ cells, but the clusters were so dense that single nuclei were hardly recognizable, which hampered the analysis. Nevertheless, the large-scale optical sectioning provided us with a robust insight into the intensity of the immune reaction (seen as MHC II accumulation) around individual schistosomula. We established three categories of the immune reaction (Fig 10E): "mild" (+) with very few MHC II + cells around/behind ("rocket tail") the intact schistosomula; "moderate" (++) with noticeable infiltration of MHC II+ cells enclosing the intact schistosomula (but no MHC II signal within the schistosomula); "severe" (+++) with massive clusters enclosing the damaged schistosomula (MHC II signal present also inside the schistosomula). While mild and moderate reactions prevailed 7 dpi, severe reactions dominated 14 dpi (Fig 10F; $p = 0.0009$).

Altogether, transcriptomic analysis and 2D/3D imaging demonstrated a strong upregulation of the MHC II pathway in *T. regenti*-infected spinal cords. Interestingly, the MHC II occurred not only around the migrating schistosomula but also along the blood vessels and within the meningeal areas indicating extensive neuroinflammation.

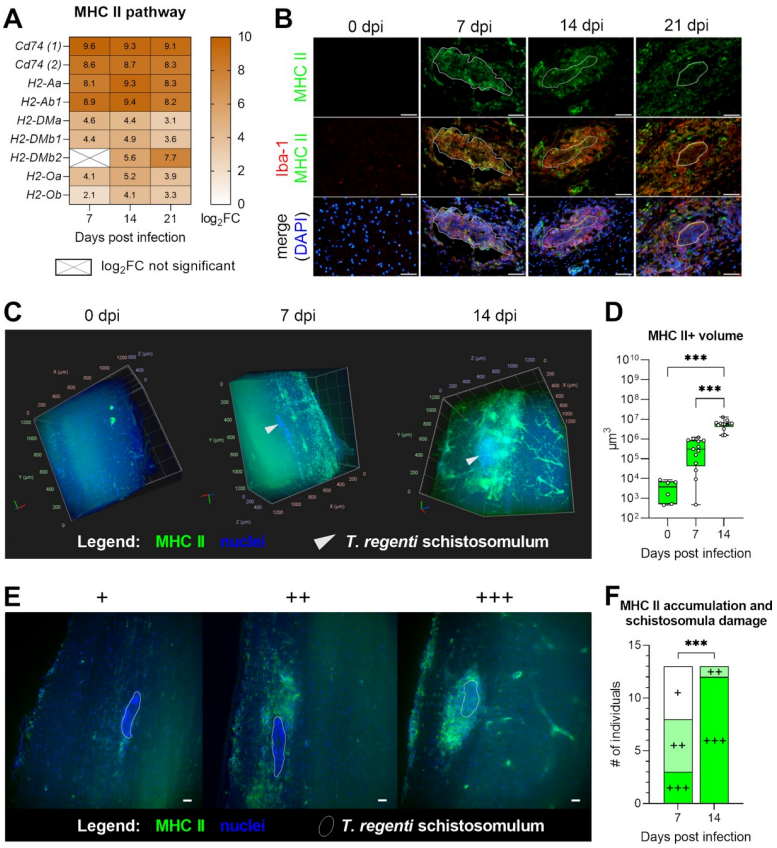

Fig 10. Major histocompatibility complex (MHC) II in the spinal cord of *T. regenti*-infected mice. (A) The heatmaps show log_2fold change (FC) in the expression of markers associated with the MHC II pathway. Genes/transcripts with $log_2FC > 2$ were considered upregulated, and only genes with a significant log_2FC are shown unless indicated otherwise (crossed cells). Spinal cords of 4 infected and 4 uninfected age-matched mice were analyzed at each time point. **(B)** Immunolocalization of MHC II and Iba-1. Representative images are shown, the white line indicates the space occupied by the schistosomulum. Scale bar = 50 μm. **(C)** 3D images obtained by light-sheet fluorescence microscopy (LSFM) showing MHC II+ cells in the spinal cord. Schistosomula are marked with grey arrowheads. **(D)** Quantification of MHC II+ volume around schistosomula. It was computed in the virtual box around the schistosomula (400×800×110 μm, S5 Video) or six randomly chosen areas in healthy mice. **(E)** Patterns of MHC II accumulation and its relation to schistosomula damage. Three categories were recognized: (+) very few MHC II+ cells around/behind intact schistosomula, (++) noticeable infiltration of MHC II+ cells enclosing intact schistosomula (but no MHC II signal within the schistosomula), (+++) massive clusters enclosing damaged schistosomula (MHC II signal present also inside the schistosomula). 2D images were obtained by LSFM and created from five stitched planes in the z-axis (1.4 μm each). Scale bar = 50 μm. **(F)** Quantification of MHC II accumulation and schistosomula damage using the categories from (E). Thirteen schistosomula out of two mice were examined at each time point. Data were evaluated by Kruskal-Wallis and Dunn's test (D) and Fisher's exact test (F); $^{***}p<0.001$.

https://doi.org/10.1371/journal.ppat.1010302.g010

T. regenti infection affected vascular permeability, blood-brain barrier integrity and triggered reactive astrogliosis

Schistosomula migration within the CNS might cause severe pathology. First, we focused on changes in vascular permeability and integrity of the blood-brain barrier, which are critical for maintaining CNS homeostasis. Among markers of vascular permeability, aquaporin-4 (*Aqp4*), the water channel localized to astrocyte endfeet, was strikingly upregulated 7 dpi (Fig 11A). Expression of E-cadherin (*Cdh1*) and occludin (*Ocln*), proteins responsible for tightness of the blood-brain barrier [42], was also increased, especially 7 dpi (Fig 11B). On the contrary, remarkable downregulation was noticed in tight junction protein 1 (*Tjp1*, also known as *Zo1*),

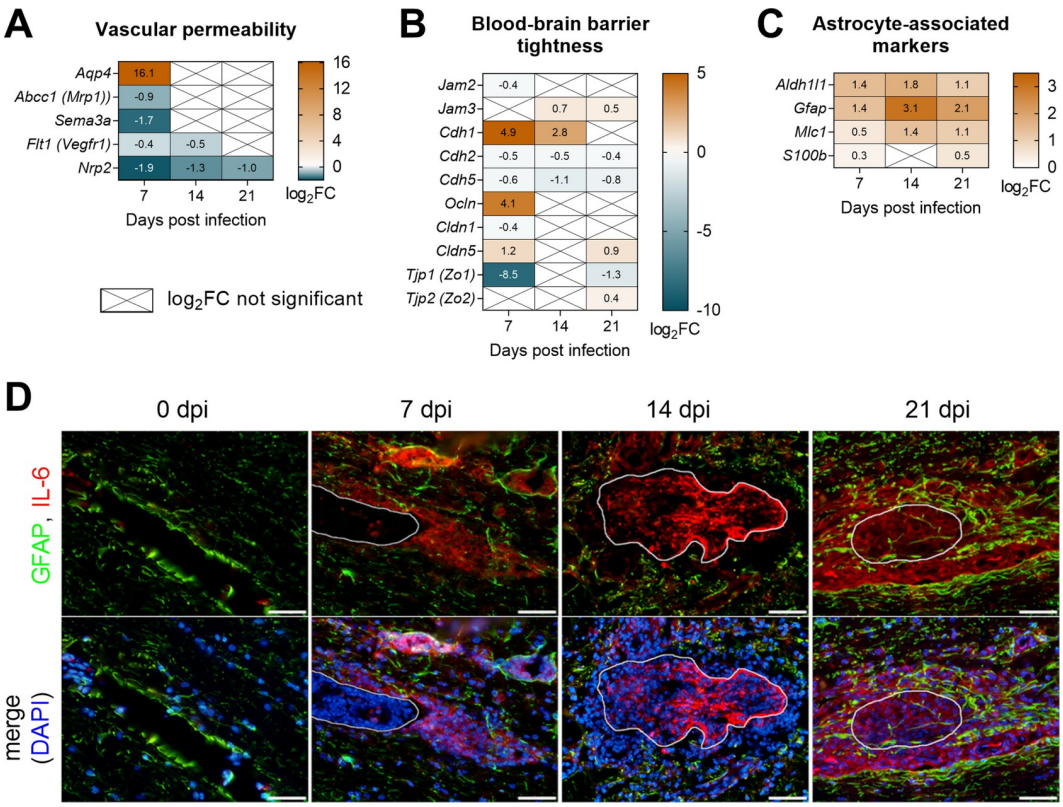

Fig 11. Pathology associated with *T. regenti* migration within the mouse spinal cord. (A–C) The heatmaps show $\log_2$fold change (FC) in the expression of markers associated with vascular permeability (A), blood-brain barrier tightness (B), and astrocytes (C). Genes/transcripts with $\log_2$FC >2 or <-2 were considered upregulated or downregulated, respectively. Only genes with a significant $\log_2$FC are shown unless indicated otherwise (crossed cells). Spinal cords of 4 infected and 4 uninfected age-matched mice were analyzed at each time point. **(D)** Immunolocalization of astrocytic glial fibrillary acidic protein (GFAP) and astrogliosis-promoting IL-6 demonstrated the most prominent astrocyte hypertrophy 21 dpi. Representative images are shown, the white line indicates the space occupied by the schistosomulum. Scale bar = 50 μm.

https://doi.org/10.1371/journal.ppat.1010302.g011

a scaffold protein anchoring tight junctions to the actin fibers [42]. Although our transcriptomic data suggested that vascular permeability and blood-brain barrier integrity were mildly altered 7 dpi, we did not observe any significant increase in extravasation of Evans blue into the nervous tissue (S2 Fig).

Second, we examined the tissue injury associated with schistosomula migration. Astrocytic glial acidic fibrillary protein (*Gfap*) was upregulated 14 and 21 dpi (Fig 11C), which pointed to the initiation of reactive astrogliosis and formation of glial scar [43]. While GFAP showed normal distribution within the nervous tissue 7 dpi, it accumulated around schistosomula lesions and in their migratory tracks at later time points (Fig 11D). Astrocyte hypertrophy was most prominent 21 dpi when astrocyte processes enclosed the schistosomula or even grew through the space occupied by them. To support the observation of astrocyte activation, we also immunolocalized IL-6, which promotes astrogliosis and glial scar formation [44]. IL-6 was detected in the schistosomula migratory tracks 7 dpi and in the area of the damaged schistosomula and their surroundings 14 and 21 dpi (Fig 11D). These data indicated that reactive astrogliosis and glial scar, presumably driven by IL-6, developed to repair the tissue injured by schistosomula migration.

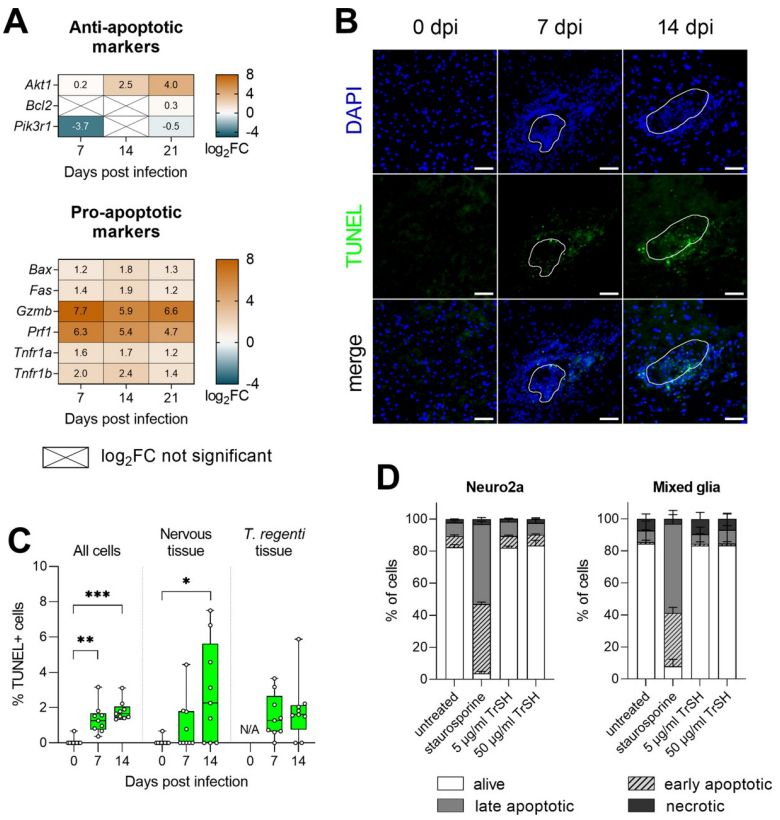

Fig 12. Apoptosis in the spinal cord of *T. regenti*-infected mice. (A) The heatmaps show log_2fold change (FC) in the expression of pro- and anti-apoptotic markers. Genes/transcripts with $log_2FC > 2$ or < -2 were considered as upregulated or downregulated, respectively. Only genes with a significant log_2FC are shown if not indicated otherwise (crossed cells). Spinal cords of 4 infected and 4 uninfected age-matched mice were analyzed at each time point. **(B)** Detection of DNA fragmentation (TUNEL+ cells) in the spinal cord cryosections. Representative images are shown, the white line indicates the space occupied by the schistosomulum. Scale bar = 50 μm. **(C)** Quantification of TUNEL+ cells in the spinal cord cryosections shown in (B). The frequency of TUNEL+ cells is shown among all cells or separately for the host nervous tissue and *T. regenti* tissue. **(D)** Detection of apoptotic populations in Neuro2a and mixed glial cultures treated by *T. regenti* schistosomula homogenate (TrSH) for 48 hours; staurosporine was used as a positive control. Pooled data from 4 experiments are shown. Data (C, D) were evaluated by Kruskal-Wallis and Dunn's test; $^{*}p<0.05$, $^{**}p<0.01$, $^{***}p<0.001$.

https://doi.org/10.1371/journal.ppat.1010302.g012

DNA fragmentation occurred at the host-schistosomulum interface, but schistosomula antigens did not trigger apoptosis in neurons or glial cells

Apoptosis plays an important role in host-parasite interactions as it can be responsible for tissue pathology or help parasites evade the host immune system. In *T. regenti*-infected spinal cords, we observed upregulation of pro-apoptotic genes *Gzmb* and *Prf* coding for granzyme B and perforin-1, respectively (Fig 12A). They are expressed by cytotoxic T lymphocytes and natural killer cells which employ them to induce apoptosis in target cells [45]. Therefore, we stained fragmented DNA, a hallmark of apoptosis, by the TUNEL assay to localize the apoptotic cells within the infected spinal cord. While no TUNEL+ cells were found in the uninfected spinal cord, their frequency increased 7 and 14 dpi, both in host and schistosomula tissues (Fig 12B and 12C). The TUNEL+ cells were localized especially at the host-parasite interface, but some were also recorded in the schistosomula migratory tracks. To assess the possibility that schistosomula-derived molecules directly induce apoptosis of the host neural cells, we stimulated mouse Neuro2a and primary mixed glial cultures with a soluble fraction of schistosomula

homogenate. However, the treatment did not alter the frequency of apoptotic populations (Fig 12D). These data suggested that apoptosis was not a major feature of *T. regenti* neuroinvasion and was not responsible for tissue pathogenesis.

Discussion

Apart from being a causative agent of human cercarial dermatitis [46,47], *T. regenti* invades the CNS of experimentally infected mice [19,20]. However, neuroinvasion by this species has not been reported from humans. Here we thoroughly investigated the invasion of the mouse CNS by *T. regenti* to better understand the diversity of host-parasite interactions during neuroinfections. Although *T. regenti* does not fully recapitulate any human neuroinfection, it represents a well-characterized and easily trackable system, providing novel insights into the diversity of pathogen-related neuroinflammation.

Of the mouse CNS, *T. regenti* predominantly affects the spinal cord to where it migrates from the skin *via* peripheral nerves [19–22,41]. Such a route is extraordinary among neurotropic helminths, which mostly rely on hematogenous spread into the CNS [48]. Indeed, *T. regenti* intraneural pathway rather resembles that of the neuropathogenic amoeba *Naegleria fowleri* [49]. Corroborating with the previous studies [19–22], we observed the highest schistosomula burden in the spinal cord 7 dpi. In addition, we detected *T. regenti* DNA in some of the hemisphere samples 14–21 dpi, but we assume that it originated from a few and most likely already damaged schistosomula since viable parasites were only rarely isolated even 7 dpi. Largely restricted access of schistosomula to the brain could explain the lack of working memory deficit, anxiety, or depression-like behavior, which stem from dysfunction of hemisphere centers [50–52].

By affecting mostly the spinal cord, *T. regenti* differs from other neurotropic helminths, such as *Angiostrongylus cantonensis*, *Toxocara* spp., or *Taenia solium*, which primarily invade the brain and impair cognitive functions or cause seizures [9,53–56]. Nevertheless, *T. regenti* resembles the neurotropic larvae of *A. cantonensis* and *Toxocara* spp. regarding size and active migration within the nervous tissue [9,54]. On the contrary, passive dissemination of schistosome eggs into the spinal cord induces human neuroschistosomosis, which often manifests as myelitis [57]. Despite sharing some histopathological or clinical features, such as myelitis and motor dysfunction of lower/hind limbs [58], *T. regenti* neuroinvasion cannot be directly compared to neuroschistosomosis, mainly due to the different nature of the causative agents (migrating schistosomula vs. disseminated eggs). As a whole, *T. regenti* neuroinvasion represents a unique biological phenomenon, but in particular regards, it can be compared to other neurotropic helminths. Regarding the general features, such as size and behavior, *T. regenti* represents a relevant comparative model especially for studying the pathology related to the migration of neurotropic helminths such as *A. cantonensis* or *Toxocara* spp.

Our complex approach revealed a serious impact of *T. regenti* neuroinvasion on the well-being of mice. They manifested with the reduced gain in body weight despite unchanged feed consumption or locomotion. We speculate that this could be explained by increased energy demands related to fighting the infection [59–61]. Of note, a decreased body weight was observed at all time points. It indicates that the peripheral immune response, with a peak 7 dpi [29], and the later neuroinflammation could have affected the weight gain. Reduction of body weight accompanies mouse infections with *A. cantonensis* and *Toxocara* spp. as well and often correlates with impaired neurological scores [55,62,63]. These observations highlight the systemic impacts of helminth neuroinfections, however, direct evidence linking the weight loss with presumably increased energy consumption related to the host immune reaction is missing.

Extensive behavioral testing revealed deficits in lower body motor functions in *T. regenti*-infected mice. Up to now, mainly ducks (definitive hosts) and immunocompromised mice were reported to suffer from neuromotor disorders related to *T. regenti* neuroinvasion [19]. This fact was explained by the higher schistosomula burden in such hosts and hence more frequent axonal injury [21,22]. Similar neuromotor abnormalities are also often present in mice infected with *A. cantonensis* and *Toxocara* spp. [53,62,64,65]. Dysregulated expression of myelin-associated genes, extensive tissue demyelination, and neuronal apoptosis are believed to be the pathological basis of such behavioral changes [63,65–68]. However, we detected no remarkable apoptosis or downregulation of myelin-associated genes in *T. regenti*-infected spinal cords. Also, no loss of myelin was seen in previous histological studies [22,26]. On the contrary, our transcriptomic data unveiled a massive downregulation of neuronal signal transduction, synaptic transmission, and axonal development. For example, we noticed striking downregulation of kinesin superfamily motor proteins *Kif1a* and *Kif1b*, which are essential for anterograde axonal transport [30,31]. Their effect is evident in *Kif1a*- and *Kif1b*-knockout mice, which exhibit reduced motor activity, abnormal limb movements, and impaired balance [69,70]. Therefore, we suggest that the disruption of neurophysiological functions in the spinal cord was responsible for the observed motor deficits. Such wide-range downregulation of neuronal functions has so far not been noticed in other transcriptomic studies focusing on helminth neuroinfection [65,66] but was recently reported from mouse brains infected with *Toxoplasma gondii* [7]. Specifically, Boillat *et al.* propose that behavioral alterations caused by *T. gondii* reflect side effects of neuroinflammation, i.e., the neuro-immune response plays a major role in modulating host behavior [7]. Therefore, we suggest that impairment of neurophysiological functions, potentially triggered by neuroinflammation, might be a novel pathological mechanism also in helminth neuroinfections.

Contrary to ducks, mice as accidental (dead-end) hosts efficiently control *T. regenti* neuroinvasion. This makes them apt species for studying the protective immune response. Moreover, the lack of well-defined duck strains and a suitable toolbox (mainly antibodies) markedly limits the immunological studies on *T. regenti* in ducks anyway. Our complex data strongly support the view that rapid activation of the mouse immune response leads to the elimination of schistosomula within 2–3 weeks post infection. It agrees with historical records of schistosomula suspended growth and reduced survival in immunocompetent mice [21,22,71]. Such immune-mediated host incompatibility is also observed in the case of *A. cantonensis*–it flourishes in rats but is retarded in mice. The latter develop much stronger neuroinflammation than rats, which is pronounced after the death of migrating larvae [9,11,72,73]. On the contrary, mice are suitable paratenic hosts for *Toxocara* spp., which are well adapted to survival in their tissues, including the CNS [74]. Similarly, viable cysticerci of *T. solium* actively evade the human immune response and cause no or mild inflammation [56]. Hence, *T. regenti* in mice is a perfect model enabling us to study natural mechanisms leading to helminth elimination within the CNS.

A strong eosinophilic meningomyelitis was the most prominent histopathological hallmark of *T. regenti* neuroinvasion. Comparison of peaks in eosinophil counts in the peripheral blood (7 dpi) and the spinal cord (14 dpi) demonstrated spatiotemporal separation of the eosinophil-based immune response in the periphery and within the CNS. A similar distinction was also observed in mice infected with *A. cantonensis* [73]. Recruitment of eosinophils into the *T. regenti*-infected spinal cords, found in our study, was presumably mediated mainly by eotaxin-2 coded by *Ccl24* [75], which displayed 180- and 700-fold increased expression 7 and 14 dpi, respectively. However, participation of other eosinophil-attracting chemokines upregulated at these time points (*Ccl5*, *Ccl7*, *Ccl8*) cannot be excluded and is even likely. Moreover, elevated expression of *Chil3* could have boosted maintenance of the tissue eosinophilia [76], especially

14 dpi. It was suggested for *A*. *cantonensis*-infected mice that Chil3 aggravates eosinophilic meningitis *via* a positive feedback loop mediated by IL-13 [73] which was also markedly upregulated in our samples. Our data collectively demonstrate a significant infiltration of eosinophils into the *T*. *regenti*-infected spinal cords, suggesting their prospective role in eliminating schistosomula.

Eosinophils harm helminths by antibody- and/or complement-induced secretion of toxic granule proteins and reactive oxygen species [77]. The role of eosinophils in limiting the parasite burden was demonstrated in murine neurocysticercosis [78], but specific effector mechanisms employed to combat helminths have not been defined. As our dissection and histological data indicated elimination of schistosomula around 14 dpi, we searched the transcriptomic datasets for pathways related to eosinophil effector functions upregulated/enriched mostly at this time point. Interestingly, we found that the complement and coagulation cascades were enriched. Specifically, components of C1 complex and C2, C3, C4, and C5 complement components were significantly upregulated ($\log_2$fold change >2), suggesting activation of the classical complement pathway initiated by antigen-antibody complexes. This mechanism is known to trigger eosinophil degranulation leading to killing schistosomula of *S*. *mansoni* [79] and we propose that it harms *T*. *regenti* schistosomula within the CNS in the same manner.

Eosinophil extracellular DNA traps (EETs) represent another component of the antimicrobial arsenal. Being released in the C-lectin-dependent manner, the EETs can immobilize helminths and facilitate their further clearance, as recently demonstrated in the case of nematode microfilariae [80]. In *T*. *regenti*-infected spinal cords, the C-lectin receptor signaling pathway was mostly enriched 14 dpi and, e.g., dectin-1 was upregulated ($\log_2$fold change >5) even at all time points. Of note, dectin-1 is a C-type lectin functioning as a transmembrane pattern-recognition receptor [81] mediating the release of eosinophil extracellular DNA traps [80]. Our observation raises an exciting question to be further tested of whether EETs are released in *T*. *regenti*-infected spinal cords and if they can halt the actively moving helminths in the CNS.

Microglia, the CNS-resident macrophage-like cells, are vital players in the CNS innate immunity as they sense and eliminate invading pathogens [82]. Therefore, they were implicated as the cells initiating the neuroinflammation in *A*. *cantonensis*- or *T*. *regenti*-infected mice [25,83]. Our transcriptomic and 2D/3D imaging data confirmed upregulation of microglia/macrophage markers in the infected spinal cord and continuous accumulation, even very intimate, of Iba-1+ MHC II+ cells around the schistosomula as soon as 7 dpi. At this time point, we noticed upregulation of *Tlr2*, *Tlr6*, *Tlr8*, and *Tlr12*, which can be expressed by microglia [84]. Of them, the heterodimer of TLR2/TLR6 might participate in recognition of the *T*. *regenti* infection similarly to murine neurocysticercosis [85]. However, the role of TLR8 and TLR12 in the initial schistosomula recognition is expected to be relatively minor as they both are intracellular receptors, and mouse TLR8 is even nonfunctional in terms of immune recognition [86]. Moreover, a C-type lectin-dependent pathway, including dectin-1 as a receptor [87,88], might be involved in detecting glycans, which are abundant on the surface and in the excretory-secretory products of the parasites [89,90]. Phagocytosis by mononuclear cells of glycan-rich material was shown in murine neurocysticercosis and promoted the infiltration of immune cells into the CNS [8,91]. Thus, we conclude that microglia might serve as sensors for *T*. *regenti* in the spinal cord using diverse and complementary recognition pathways.

Beyond recognition, Lichtenbergová *et al*. proposed that activated microglia/macrophages play the main role in destroying *T*. *regenti* schistosomula in the nervous tissue [22]. However, our data show that a strong type 2 cytokine milieu, driven by upregulated *Il4* and *Il13*, was established in the infected spinal cords suggesting induction of the alternatively activated M2 microglia/macrophage [40,92–94]. The transcriptomic M2 signature was confirmed by the

detection of arginase, a hallmark of alternatively activated microglia/macrophages, on the protein level. Induction of such environment is typical also for other helminth neuroinfections [95–97] and can be interpreted as helminth-induced prevention of M1 polarization, which is associated with the production of detrimental nitric oxide. Corroborating with this assumption, *T. regenti* schistosomula were shown not to trigger nitric oxide production *in vitro* or the spinal cord [25,26]. The role of microglia/macrophages in killing *T. regenti* schistosomula thus needs to be significantly reconsidered. We propose that activated microglia/macrophages phagocytose the tissue debris in the schistosomula migratory tracks–similarly to the gitter cells in *Toxocara*-infected brains [54,68]. Later, they might also clean the opsonized remnants of the already damaged schistosomula. Localization of Iba-1+ and/or MHC II+ cells, revealed by 2D/3D imaging techniques, and enriched FcγR-mediated phagocytosis pathway underpins the novel hypothesis on microglia/macrophage functions in *T. regenti*-infected spinal cords.

Finally, we suggest that the M2 polarization promotes repair of the injured nervous tissue. Astrocyte-mediated IL-6-driven formation of the glial scar, which we observed 14–21 dpi, is commonly considered the primary mechanism of the nervous tissue repair, also known from other helminth neuroinfections [22,98,99]. However, M2 microglia/macrophages promote tissue regeneration and remyelination by driving differentiation of oligodendrocytes [100,101]. Chil3, expressed and secreted by M2 cells, promotes oligodendrogenesis [102] and arginase helps axon regeneration by synthesizing polyamines, such as spermidine [103,104]. Both *Chil3* and *Arg1* were massively upregulated in *T. regenti*-infected spinal cords, and arginase was even the most abundant protein found in the close proximity to the schistosomula. At the same time, no signs of demyelination or remarkable tissue pathology were noticed. Thus, we conclude that induction of M2 polarization within the infected spinal cord limits extensive pathology potentially associated with *T. regenti* neuroinvasion. Identification of the parasite molecules responsible for this effect is warranted as they might represent suitable, tissue-specific immunomodulators applicable against autoimmune or neurodegenerative diseases.

In summary, we present a comprehensive, transcriptome-driven study of the schistosome invasion into the mouse spinal cord. We revealed a remarkable downregulation of neurophysiological functions, which contribute to motor deficits observed in infected mice. The host immune response is dominated by eosinophilic inflammation, which eliminates the infection. A strong M2 polarization evidenced, i.a., by substantial production of arginase, presumably prevents extensive tissue damage. Due to parasitological, immunological, or pathological similarities with human neuropathogens, *T. regenti* represents a suitable model for further research of neuroinfections.

Materials and methods

Ethics statement

Animal experiments were conducted in compliance with the European and Czech legislation (EU Directive 2010/63/EU, Act No 246/1992). Animal welfare committees of the Faculty of Science, Charles University, and the Ministry of Education, Youth and Sports of the Czech Republic approved all experimental procedures (MSMT-33740/2017-2, MSMT-37946/2020-3). Isoflurane anesthesia followed by transcardial perfusion (exsanguination) were employed to sacrifice the mice as indicated below.

Animals

C57BL/6JOlaHsd mice (Envigo, Venray, Netherlands) were housed in the Centre for Experimental Biomodels (First Faculty of Medicine, Charles University) or the animal housing facility (Faculty of Science, Charles University). The mice were kept in groups of 4–10 individuals/

cage (if not stated otherwise) and provided with food and water *ad libitum*; food consumption was monitored on a weekly basis. Infection with *T*. *regenti* cercariae was performed at the age of 8 weeks. Mixed glial cultures were prepared from newborn pups of both sexes, no older than 48 hours. Light-sheet fluorescence microscopy imaging was performed on organ samples from MHC II-EGFP C57BL/6J knock-in mice provided by Prof. Jan Černý (Department of Cell Biology, Faculty of Science, Charles University).

Parasites and infection of mice

A complete life cycle of *T*. *regenti* is kept at the Department of Parasitology, Faculty of Science, Charles University. Freshwater snails (*Radix lagotis*) and domestic ducks (*Anas platyrhynchos* f. domestica) are used as intermediate and definitive hosts, respectively [19]. Percutaneous infection of female mice was done according to the well-established "water bath" protocol using the infection dose of 2000 freshly collected cercariae [22,26,29,41].

Experimental design

A comprehensive investigation was carried out to examine the effects of *T*. *regenti* infection on mice, emphasizing the host immune response and pathology in the CNS (Fig 1). To characterize the general/systemic impact of the infection, body and spleen weights were monitored as well as levels of *T*. *regenti*-specific serum antibodies, blood eosinophil counts, and behavioral alterations of infected mice. Host-parasite interactions in the CNS, especially in the spinal cord, were then broadly explored by several approaches summarized in Fig 1. Uninfected mice were always used as a control group, and specific age-matching is shown in Fig 1. The time points at which the analyses were performed represent distinct phases of the infection [22].

ELISA

T. *regenti*-specific IgG1 and IgG2a were analyzed in the serum samples (diluted 1:80) of mice according to [29]. The cut-off value was calculated according to [105] for a 99.9% confidence level.

Parasite burden in the CNS

Two complementary methods were used to assess *T*. *regenti* burden in the CNS. First, we directly quantified *T*. *regenti* schistosomula actively released from the spinal cord, brain stem, cerebellum, and hemispheres after the organs were torn into 1–2 mm pieces by sharp forceps in phosphate-buffered saline (pH 7.4; PBS) [26]. The organ suspensions were independently inspected by three people within 6 hours which is enough for viable schistosomula to leave the tissue.

Second, we detected schistosomula DNA by a quantitative real-time polymerase chain reaction (PCR) in the spinal cord and hemisphere samples intended for flow cytometry. Specifically, we used the material remaining in the cell strainers after filtration of the cell suspensions (~10 mg, see "Flow cytometry" for details). Total DNA was isolated by Exgene Tissue SV (plus!) (GeneAll; Lisbon, Portugal) using 100 μl of the elution buffer and stored at –20˚C. qPCR was then carried out in iQ5 Multicolor Real-Time PCR Detection System (Bio-Rad) employing iQ SYBR Green Supermix (Bio-Rad; Hercules, California, USA). *Trichobilharzia*-specific *Sau3A* repetitive sequence was selected as the molecular target, 5'-GTGACTTGCTA-CAGGTTGG-3' (forward) and 5'-GGCAAGCTCGTATACCATTC-3' (reverse) primers were used [106] to amplify the PCR product of the expected size of 200 bp. Five μl of eluted DNA were added into an individual reaction, and each sample was run in a triplicate. UltraPure

DNase/RNase-free dH_2O (Invitrogen; Waltham, Massachusetts, USA) was included as a negative control, while 10 ng of DNA isolated from *T. regenti* cercariae (corresponding to the highest standard, see below) served as a positive control in each run. qPCR amplification was performed as follows: 3 min at 95˚C, 40 cycles of 15 s at 95˚C, 15 s at 57˚C, 15 s at 72˚C, and 1 min at 72˚C. Quantitative cycle values were obtained, and the final parasite DNA calculation was done according to the standard curve ranging from 10 ng to 1 fg (a series of 10-fold dilution). Melting curves were always checked to ensure the specificity of the reaction. The cut-off value was calculated as the mean plus three standard deviations of samples from uninfected mice.

Behavioral tests

Several tests were performed and evaluated by blinded researchers to explore various aspects of mice behavior (see Table 1 for details). A detailed description of task procedures can be found in S1 Text. Mice intended for behavioral tests were housed individually. In all the tests, the apparatuses were cleaned with 70% ethanol and dried after each session.

Histology

Spinal cords were carefully extracted from isoflurane-anesthetized mice perfused by heparinized (10 IU/ml) PBS and 4% paraformaldehyde (PFA). The tissue was post-fixed in 4% PFA overnight at 4˚C, dehydrated, and embedded in paraffin blocks. Five μm thick sections were prepared and routinely stained with hematoxylin-eosin.

Flow cytometry

Flow cytometry was employed to characterize peripheral and CNS-infiltrating leukocytes in infected mice. Uninfected mice age-matched to 7 and 28 dpi were used as controls to prevent a potential age-related bias, especially in the infiltration of the CNS. As no differences were found (S2 Text), only uninfected mice age-matched to 7 dpi are shown in the main text. The blood samples were processed individually, but three mice were pooled to obtain adequate and robust amounts of leukocytes in the CNS samples.

First, the blood was collected from the right atrium of isoflurane-anesthetized mice and mixed with an equal volume of 10 mM EDTA in PBS on ice. Erythrocytes were lysed with

Table 1. Behavioral testing battery. The tests are listed by their temporal order.

Test	Behavior assessed	Parameters analyzed	Ref.
Elevated plus maze	anxiety; activity	time spent in the open arms; risk assessment behavior; total number of arm visits; total distance walked; looking down behavior	[107,108]
Open field	locomotor activity; anxiety	total distance walked; time spent in the center of the arena	[108–112]
Beam walking	motor coordination	time to traverse the beam; error score	[109,110,112]
Bar holding	endurance and strength of the forelimbs	tightrope hang time	[111]
Marble burying	anxiety	proportion of marbles buried to 2/3	[113]
Novelty-induced hypophagia	anxiety	amount of eaten oat flakes; number of feces; latency to first tasting	[108]
Y-maze	spatial working memory; activity	proportion of correct triads to all triads (alternation); total number of arm entrances; total distance walked	[114]
Grid test	endurance and strength of the forelimbs and hindlimbs	time to jump/fall	[112,115,116]
Tail suspension	depressive-like behavior	immobility duration	[112,117]
Forced swimming	depressive-like behavior	immobility duration	[117]
Footprint analysis	posture and gait characteristics	forelimb and hindlimb step length and step width	[116]

https://doi.org/10.1371/journal.ppat.1010302.t001

ACK buffer [29] and the remaining cells were processed for flow cytometry. Following the blood collection, the mice were transcardially perfused with PBS, and the spinal cord, the brain stem, the cerebellum, and the left hemisphere were extracted and further processed on ice. The tissues were gently mechanically homogenized, filtered through a 70 μm cell strainer, and the leukocytes were separated from myelin using 30/70% Percoll (GE Healthcare; Chicago, Illinois, USA) gradient centrifugation [118]. Specifically, the cells were carefully collected from the 30/70% Percoll interphase and processed for flow cytometry.

After cell suspensions were prepared, anti-CD16/CD32 antibody (1:100; eBioscience; San Diego, California, USA; clone 93) was added for 10 minutes, being followed by a mixture of surface marker antibodies: APC-eFluor 780 anti-CD45 (1:100; eBioscience; clone 30F11); PE-Cy7 anti-CD11b (1:120; BioLegend; San Diego, California, USA; clone M1/70); FITC anti-F4/80 (1:100; BioLegend; clone BM8); PE anti-SiglecF (1:80; BioLegend; clone S17007L); APC anti-Ly6G (1:150; BioLegend; clone 1A8). The cells were stained for 30 minutes at 4˚C in the dark, and Hoechst 33258 (1:22,500; Sigma Aldrich; St. Louis, Missouri, USA) was added 10 minutes before measurement to exclude dead cells. The samples were measured by CytoFLEX S (Beckman Coulter; Brea, California, USA; BC) using CytExpert (BC) and analyzed in FlowJo (v. 10.7.1). FMO controls were used for all markers; in the case of F4/80, isotype control was also included. The gating strategy for each tissue is shown in S2 Text. Cell populations of interest were characterized as follows: microglia: $CD45^{med}$ $CD11b^{+}$, macrophages/monocytes: $CD45^{+}$ $CD11b^{+}$ $F4/80^{+}$ $Ly6G^{-}$ $SiglecF^{med}$, eosinophils: $CD45^{+}$ $CD11b^{+}$ $F4/80^{+}$ $Ly6G^{-}$ $SiglecF^{+}$, neutrophils: $CD45^{+}$ $CD11b^{+}$ $F4/80^{+}$ $Ly6G^{+}$ $SiglecF^{low/med}$, lymphoid cells: $CD45^{+}$ $CD11b^{-}$.

Transcriptomic analysis

RNA isolation, library preparation, and sequencing. Total RNA was isolated from the whole dissected spinal cords of infected and age-matched control mice using TRIzol (Invitrogen). Four biological replicates per group were processed for each time point. Residual DNA was removed by TURBO DNA-free Kit (Invitrogen), and the quality and integrity of RNA were inspected by Bioanalyzer 2100 (Agilent; Santa Clara, California, USA). Pair-end (2x100 bp) sequencing was performed on the BGISEQ-500 platform.

Bioinformatic analysis. Raw reads were inspected for sequencing quality by FastQC (v. 0.11.5) [119], and low-quality nucleotides (Phred quality score <20) were removed using Trimmomatic (v. 0.39) [120]. Trimmed reads were mapped to transcriptome inferred from the reference genome (v. GRCm38) using RSEM (v. 1.3.3) [121], and transcripts with mapping rate >10 expected counts were considered as transcribed. Differential gene expression between the infected samples and the respective age-matched controls was calculated using DESeq2--package (v. 1.12.3) [122] in R (v. 3.5.2) at each time point. Transcripts with $\log_2$fold change ($\log_2$FC) >2 or <−2 and false discovery rate (FDR) of < = 0.05 were recorded as the differentially expressed. For a global overview of protein classes and metabolic pathways enriched at each time point, the reference transcriptome was translated using Transdecoder (v. 3.0.1) [123] and annotated by GhostKOALA (v. 2.2) [124] to KEGG database [125]. Upregulated ($\log_2$FC >2) and downregulated ($\log_2$FC <−2) transcripts with KEGG annotation were submitted to KEGG Mapper online tool to reconstruct metabolic pathways. Enriched metabolic pathways for each time point were identified by Fisher's exact test (adjusted p-value <0.05) in R (v. 3.5.2).

Laser capture microdissection and proteomic analysis

Embedding, cryosectioning, and laser microdissection. Cervical, thoracic, and lumbar spinal cord segments were extracted from mice previously perfused by heparinized (10 IU/ml)

PBS and 4% PFA. The segments were post-fixed in 4% PFA for 5 hours at room temperature (RT), washed in PBS for 3×5 min, immersed in Tissue Freezing Medium (Leica; Wetzlar, Germany) for 30 min at RT, and frozen at –80˚C. Ten-micrometer sections (CM3050 S Research Cryostat, Leica) were mounted onto membrane frame slides (MMI; Ecching, Germany) and stored at –80˚C until use.

Laser microdissection was carried out using the MMI SmartCut system (Olympus CKX41 inverted microscope; Olympus SmartCut Plus software). Areas of interest were isolated from each spinal cord segment with a final volume of 7.5×10^6 μm^3 [126]. Specifically, the area of interest was the white matter of each spinal cord segment within up to 100 μm around the schistosomula. The randomly selected white matter of appropriate segments from uninfected mice was taken as a control sample. The microdissects were stored at –80˚C until MS analysis. It was performed on either merged (cervical, thoracic, and lumbar all together, 7.5×10^6 μm^3 of each, n = 4, i.e., 22.5×10^6 μm^3 of microdissects per a replicate) or separated (n = 3, 7.5×10^6 μm^3 of microdissects per an individual segment replicate) spinal cord segments.

Additionally, the intestinal content of *T*. *regenti* schistosomula was also microdissected and analyzed. The intestinal content of schistosomula from 4 mice was pooled for one sample, and the experiment was performed in a triplicate. Due to a low yield of the microdissected material, only 1.3×10^6 μm^3 of the intestinal content was microdissected per sample.

MS analysis and data evaluation. Microdissects were processed for nanoflow liquid chromatography-MS analysis according to [126]. Briefly, proteins were denatured, reduced, and alkylated in one step using the In-StageTips method [127]. Raw data were processed and quantified with the MaxQuant software (v. 1.6.10.43) with a built-in Andromeda search engine against the protein databases of *M*. *musculus* (downloaded in June 2020 from www.uniprot.org) and *T*. *regenti* (trichobilharzia_regenti.PRJEB4662.WBPS14.protein) downloaded from the WormBase (parasite.wormbase.org) with parameter settings according to [126]. Quantification was performed using the label-free algorithm [128]. Further data analysis was done by Perseus software (v. 1.6.14.0) [129], where Student's t-tests with permutation-based FDR calculation (250 randomizations) (FDR = 0.05, S0 = 0.1) were performed. Proteins considered to be reliably identifiable were further annotated and classified into protein groups according to the KEGG database [125].

Immunohistochemistry

Ten-micrometer cryosections of spinal cords were prepared as already published [26] and stored at –80˚C before use. After tempering, they were washed with PBS, permeabilized with 0.1% (v/v) Triton X-100 in PBS, blocked with 0.1% Triton X-100 1% (w/v) bovine serum albumin (BSA) in PBS, and incubated overnight at 4˚C with primary antibodies: monoclonal rat anti-IL-4 (1:40; Abcam; Cambridge, UK; clone BVD4-1D11), monoclonal rat anti-IL-6 (1:200; Acris antibodies; Herford, Germany; clone MP5-20F3), monoclonal rat anti-MHC II (1:150; Abcam; clone NIMR-4), polyclonal rabbit anti-arginase-1 (Arg-1) (1:1000; Thermo Fisher Scientific; Waltham, Massachusetts, USA), polyclonal rabbit anti-glial fibrillary acidic protein (GFAP) (1:1000; Dako; Santa Clara, California, USA), polyclonal rabbit anti-ionized calcium-binding adaptor molecule 1 (Iba-1) (1:1000; Synaptic Systems; Göttingen, Germany). Negative rabbit serum was used as a control for Arg-1, GFAP, and Iba-1. The following day, the slides were washed with PBS, incubated with corresponding secondary antibodies (goat anti-rabbit F(ab')2 AlexaFluor 594, goat anti-rabbit F(ab')2 AlexaFluor 488, goat anti-rabbit Alexa Fluor 488 - all 1:1000; Cell Signaling Technology; Danvers, Massachusetts, USA; and goat anti-rat Alexa Fluor 568; 1:1000; Abcam) for 60 minutes at RT, washed with PBS and mounted in Fluoroshield with DAPI (Sigma Aldrich). Slides with detection of Arg-1 were captured by

NIKON TiE 2 and processed in ImageJ (v. 1.8). Other slides were captured by Olympus BX51 equipped with Olympus DP-2 camera and processed in Quick Photo Micro (v. 3.0) and Gimp (v. 2.10.22). Per each time point, 4 mice were used, and at least 3 schistosomula-positive slides per mouse per antibody combination were analyzed. The mice used for this analysis were infected independently from other experiments presented herein.

Light-sheet fluorescence microscopy

MHC II-EGFP C57BL/6J knock-in mice were perfused by ice-cold heparinized PBS and 4% PFA (pH 7.4), and their spinal cords were post-fixed in the PFA overnight at 4˚C. The tissue was cleared in CUBIC-1 solution [25% (w/v) urea, 25% (w/v) Quadrol, 15% (v/v) Triton X-100 (all Sigma-Aldrich) in dH_2O] for at least 5 days (or until the tissue was transparent) in the dark, orbital shaking at 37˚C. Afterwards, the tissue was washed [0.5% (w/v) BSA, 0.01% (w/v) sodium azide, 0.1% (v/v) Triton X-100 in PBS)] in the dark, orbital shaking at 37˚C for 5 hours. Washed samples were stained with DRAQ5 (Thermo Fisher Scientific) (1:7500) for 2 days in the dark, rocking at 4˚C. Finally, the tissue was incubated in CUBIC-2 solution [22.5% (w/v) urea, 9% (v/v) triethanolamine (Sigma-Aldrich), 45% (w/v) sucrose, 0.1% (v/v) Triton X-100 in dH_2O; refractive index = 1.47)] at least for 5 days in the dark, orbital shaking at 37˚C. The tissue clearing protocol was adapted from [130] and modified by Jaromír Novák and Jan Pačes (Department of Cell Biology, Faculty of Science, Charles University). Samples were mounted in 1% (w/v) low-melt agarose and processed on Zeiss Lightsheet Z.1 using 10× illumination and 20× detection objectives. Data were analyzed and processed in ZEN (black edition) (v. 9.2.8.54; Zeiss), Arivis (v. 3.1.3; Arivis), and DaVinci Resolve (v. 16.2.7.010; Blackmagic design). The mice used for this analysis were infected independently from other experiments presented herein.

Evaluation of the blood-brain barrier integrity

The integrity of the blood-brain barrier was evaluated by the extravasation of Evans blue into the nervous tissue [131]. The mice were subtly anesthetized (100 mg/kg ketamine, 10 mg/kg xylazine), and 200 μl of 2% (w/v) Evans blue were injected into a lateral tail vein. After 1 h, the mouse was transcardially perfused by 40 ml of heparinized (10 IU/ml) PBS and the spinal cord, brain stem, cerebellum, and hemispheres were isolated and weighed. The tissue was then mechanically homogenized in 50% of trichloroacetic acid (spinal cords, brain stems, and cerebella in 100 μl, hemispheres in 300 μl), centrifuged (20 min, 10,000×g) and the supernatant was diluted 4-fold with ethanol. The fluorescence intensity was measured at 620/680 nm and converted to the amount of Evans blue using a standard curve. The mice used for this analysis were infected independently from other experiments presented herein.

Apoptosis assays

DNA fragmentation, a hallmark of apoptotic cells, was detected on cryosections of the spinal cords (see "Immunohistochemistry" for preparation) by Click-iT Plus TUNEL Assay with Alexa Fluor 488 dye (Thermo Fisher Scientific) according to the manufacturer's instructions. Then the slides were mounted in VectaShield with DAPI to stain all nuclei and examined by a fluorescence microscope (Olympus BX51). The images were processed in ImageJ, by which the proportion of TUNEL+ nuclei around and within the schistosomula was calculated and compared to uninfected mice. Per each time point, 4 mice were used, and at least 2 schistosomula-positive slides per mouse were analyzed. The mice used for this analysis were infected independently from other experiments presented herein.

Apoptotic effects of *T. regenti* antigens were tested *in vitro* on Neuro2a cell line and primary mixed glial cultures. Neuro2a were obtained from Ondřej Honc (Department of Physiology, Faculty of Science, Charles University) and grown in Dulbecco's modified Eagle's medium supplemented by 10% (v/v) fetal bovine serum and 1% (v/v) penicillin/streptomycin (all from Lonza; Basel, Switzerland). Mixed glial cultures were prepared from newborn mouse pups and grown as already described [25]. The cells were seeded into 12-well plates and treated with a soluble fraction of schistosomula homogenate (5 and 50 μg/ml; see [25] for a detailed preparation) for 48 hours. Staurosporine (final concentration 0.1 μM) was used as a positive control. Next, the cells were washed by PBS, trypsinized, and stained by Dead Cell Apoptosis Kit with annexin V-Alexa Fluor 488 and propidium iodide (Thermo Fisher Scientific) according to the manufacturer's instructions. The samples were measured by LSR II flow cytometer using Diva (Becton Dickinson; Franklin Lakes, New Jersey, USA) and analyzed in FlowJo (v. 10.7.1).

Statistical analyses

Statistical analyses and data visualization were conducted in GraphPad Prism (v. 9) if not already stated otherwise. Particular tests applied are indicated in the figure legends, p-values <0.05 were considered significant and are indicated as follows: $^{*}p<0.05$, $^{**}p<0.01$, $^{***}p<0.001$. The exact p-value is also shown if it was 0.05–0.10. Individual data are presented within the graphs, or "n" is clearly stated if summary statistics (mean ± standard deviation) were used for better graphical representation.

Supporting information

S1 Table. Spinal cord transcriptomic data.
(XLSX)

S2 Table. Microdissection proteomic data.
(XLSX)

S1 Text. Detailed description of behavioral tests.
(DOCX)

S2 Text. Gating strategies and flow cytometry data not presented in the main text.
(DOCX)

S1 Fig. Behavioral data not presented in the main text.
(TIF)

S2 Fig. Evaluation of the blood-brain barrier integrity by Evans blue in uninfected (0 dpi) and infected (7 dpi) mice. (A) Representative images of extracted spinal cords and brains. **(B)** Quantification of Evans blue in the nervous tissue. Data were evaluated by unpaired t-test, p values are shown.
(TIF)

S1 Video. Beam walking, uninfected and infected (7 dpi) mice.
(MP4)

S2 Video. Light-sheet fluorescence microscopy, the uninfected mouse (0 dpi).
(MP4)

S3 Video. Light-sheet fluorescence microscopy, the infected mouse (7 dpi).
(MP4)

S4 Video. Light-sheet fluorescence microscopy, the infected mouse (14 dpi).
(MP4)

S5 Video. Visualization of the virtual box used for quantification of MHC II+ volume around schistosomula.
(MP4)

Acknowledgments

We would like to thank Vladimír Šteiger and Irena Parohová for their help with qPCR and apoptosis-related experiments, respectively. Our colleagues are acknowledged for sharing animals (Prof. Jan Černý), cells (Ondřej Honc), protocols (Jan Pačes, Jaromír Novák) or devices (Dr. Ivana Stružinská). We also appreciate the technical support and assistance of Dr. Zuzana Burdíková (light-sheet fluorescence microscopy), Veronika King (infection of mice), Veronika Siegelová (maintenance of *T. regenti* life cycle), Pavel Talacko (LC-MS analysis), and Dr. Jana Bulantová (animal handling).

Author Contributions

Conceptualization: Tomáš Macháček.

Data curation: Roman Leontovyč.

Formal analysis: Tomáš Macháček, Roman Leontovyč, Barbora Šmídová, Martin Majer, Oldřich Vondráček, Iveta Vojtěchová, Tomáš Petrásek.

Funding acquisition: Petr Horák.

Investigation: Tomáš Macháček, Roman Leontovyč, Barbora Šmídová, Martin Majer, Oldřich Vondráček, Iveta Vojtěchová, Tomáš Petrásek.

Methodology: Tomáš Macháček, Iveta Vojtěchová.

Project administration: Tomáš Macháček.

Resources: Iveta Vojtěchová, Tomáš Petrásek, Petr Horák.

Software: Roman Leontovyč.

Supervision: Petr Horák.

Validation: Tomáš Macháček, Roman Leontovyč, Martin Majer, Iveta Vojtěchová.

Visualization: Tomáš Macháček, Roman Leontovyč, Barbora Šmídová, Oldřich Vondráček.

Writing – original draft: Tomáš Macháček, Roman Leontovyč, Barbora Šmídová, Martin Majer, Oldřich Vondráček, Iveta Vojtěchová, Tomáš Petrásek.

Writing – review & editing: Tomáš Macháček, Roman Leontovyč, Iveta Vojtěchová, Petr Horák.

References

1. Finsterer J, Auer H. Parasitoses of the human central nervous system. J Helminthol. 2013; 87: 257–270. https://doi.org/10.1017/S0022149X12000600 PMID: 23046708
2. Carpio A, Romo ML, Parkhouse RME, Short B, Dua T. Parasitic diseases of the central nervous system: lessons for clinicians and policy makers. Expert Rev Neurother. 2016; 16: 401–414. https://doi.org/10.1586/14737175.2016.1155454 PMID: 26894629

3. Vezzani A, Fujinami RS, White HS, Preux P-M, Blümcke I, Sander JW, et al. Infections, inflammation and epilepsy. Acta Neuropathol. 2016; 131: 211–234. https://doi.org/10.1007/s00401-015-1481-5 PMID: 26423537

4. Garcia HH, Nath A, Del Brutto OH. Parasitic infections of the nervous system. Semin Neurol. 2019; 39: 358–368. https://doi.org/10.1055/s-0039-1693036 PMID: 31378871

5. Cox DM, Holland CV. Relationship between three intensity levels of *Toxocara canis* larvae in the brain and effects on exploration, anxiety, learning and memory in the murine host. J Helminthol. 2001; 75: 33–41. https://doi.org/10.1079/joh200028 PMID: 11316470

6. Adalid-Peralta L, Sáenz B, Fragoso G, Cárdenas G. Understanding host–parasite relationship: the immune central nervous system microenvironment and its effect on brain infections. Parasitology. 2018; 145: 988–999. https://doi.org/10.1017/S0031182017002189 PMID: 29231805

7. Boillat M, Hammoudi P-M, Dogga SK, Pagès S, Goubran M, Rodriguez I, et al. Neuroinflammation-associated aspecific manipulation of mouse predator fear by *Toxoplasma gondii*. Cell Rep. 2020; 30: 320–334.e6. https://doi.org/10.1016/j.celrep.2019.12.019 PMID: 31940479

8. Alvarez JI, Mishra BB, Gundra UM, Mishra PK, Teale JM. *Mesocestoides corti* intracranial infection as a murine model for neurocysticercosis. Parasitology. 2010; 137: 359–372. https://doi.org/10.1017/S0031182009991971 PMID: 20109250

9. Yang LO, Wei J, Wu Z, Zeng X, Li Y, Jia Y, et al. Differences of larval development and pathological changes in permissive and nonpermissive rodent hosts for *Angiostrongylus cantonensis* infection. Parasitol Res. 2012; 111: 1547–1557. https://doi.org/10.1007/s00436-012-2995-6 PMID: 22777701

10. Holland C V, Hamilton CM. The significance of cerebral toxocariasis: a model system for exploring the link between brain involvement, behaviour and the immune response. J Exp Biol. 2013; 216: 78–83. https://doi.org/10.1242/jeb.074120 PMID: 23225870

11. Martins YC, Tanowitz HB, Kazacos KR. Central nervous system manifestations of *Angiostrongylus cantonensis* infection. Acta Trop. 2015; 141: 46–53. https://doi.org/10.1016/j.actatropica.2014.10.002 PMID: 25312338

12. de Lange A, Mahanty S, Raimondo J V. Model systems for investigating disease processes in neurocysticercosis. Parasitology. 2019; 146: 553–562. https://doi.org/10.1017/S0031182018001932 PMID: 30430955

13. Strube C, Waindok P, Raulf M-K, Springer A. *Toxocara*-induced neural larva migrans (neurotoxocarosis) in rodent model hosts. 1st ed. In: Bowman DD, editor. Toxocara and Toxocariasis. 1st ed. 2020. pp. 189–218. https://doi.org/10.1016/bs.apar.2020.01.006

14. Silva LM, Oliveira CN de, Andrade ZA. Experimental neuroschistosomiasis: Inadequacy of the murine model. Mem Inst Oswaldo Cruz. 2002; 97: 599–600. https://doi.org/10.1590/s0074-02762002000400028 PMID: 12118299

15. Lambertucci JR, Fidelis TA, Pereira TA, Coelho PMZ, Araujo N, Souza MM de, et al. Brain schistosomiasis in mice experimentally infected with *Schistosoma mansoni*. Rev Soc Bras Med Trop. 2014; 47: 251–253. https://doi.org/10.1590/0037-8682-0083-2013 PMID: 24861305

16. Tan Z, Lei Z, Zhang Z, Zhang H, Shu K, Hu F, et al. Identification and characterization of microglia/macrophages in the granuloma microenvironment of encephalic schistosomiasis japonicum. BMC Infect Dis. 2019; 19: 1088. https://doi.org/10.1186/s12879-019-4725-5 PMID: 31888505

17. McSorley HJ, Maizels RM. Helminth infections and host immune regulation. Clin Microbiol Rev. 2012; 25: 585–608. https://doi.org/10.1128/CMR.05040-11 PMID: 23034321

18. Morris CP, Evans H, Larsen SE, Mitre E. A comprehensive, model-based review of vaccine and repeat infection trials for filariasis. Clin Microbiol Rev. 2013; 26: 381–421. https://doi.org/10.1128/CMR.00002-13 PMID: 23824365

19. Horák P, Dvořák J, Kolářová L, Trefil L. *Trichobilharzia regenti*, a pathogen of the avian and mammalian central nervous systems. Parasitology. 1999; 119: 577–581. https://doi.org/10.1017/s0031182099005132 PMID: 10633919

20. Hrádková K, Horák P. Neurotropic behaviour of *Trichobilharzia regenti* in ducks and mice. J Helminthol. 2002; 76: 137–141. https://doi.org/10.1079/JOH2002113 PMID: 12015826

21. Kouřilová P, Syrůček M, Kolářová L. The severity of mouse pathologies caused by the bird schistosome *Trichobilharzia regenti* in relation to host immune status. Parasitol Res. 2004; 93: 8–16. https://doi.org/10.1007/s00436-004-1079-7 PMID: 15034785

22. Lichtenbergová L, Lassmann H, Jones MMK, Kolářová L, Horák P. *Trichobilharzia regenti*: Host immune response in the pathogenesis of neuroinfection in mice. Exp Parasitol. 2011; 128: 328–335. https://doi.org/10.1016/j.exppara.2011.04.006 PMID: 21554878

23. Leontovyč R, Young ND, Korhonen PK, Hall RS, Bulantová J, Jeřábková V, et al. Molecular evidence for distinct modes of nutrient acquisition between visceral and neurotropic schistosomes of birds. Sci Rep. 2019; 9: 1374. https://doi.org/10.1038/s41598-018-37834-7 PMID: 30718626

24. Kolářová L, Horák P, Čada F. Histopathology of CNS and nasal infections caused by *Trichobilharzia regenti* in vertebrates. Parasitol Res. 2001; 87: 644–650. https://doi.org/10.1007/s004360100431 PMID: 11511002

25. Macháček T, Panská L, Dvořáková H, Horák P. Nitric oxide and cytokine production by glial cells exposed in vitro to neuropathogenic schistosome *Trichobilharzia regenti*. Parasit Vectors. 2016; 9: 579. https://doi.org/10.1186/s13071-016-1869-7 PMID: 27842570

26. Macháček T, Šmídová B, Pankrác J, Majer M, Bulantová J, Horák P. Nitric oxide debilitates the neuropathogenic schistosome *Trichobilharzia regenti* in mice, partly by inhibiting its vital peptidases. Parasit Vectors. 2020; 13: 426. https://doi.org/10.1186/s13071-020-04279-9 PMID: 32819437

27. Kouřilová P, Hogg KG, Kolářová L, Mountford AP. Cercarial dermatitis caused by bird schistosomes comprises both immediate and late phase cutaneous hypersensitivity reactions. J Immunol. 2004; 172: 3766–3774. https://doi.org/10.4049/jimmunol.172.6.3766 PMID: 15004181

28. Lichtenbergová L, Kolbeková P, Kouřilová P, Kašný M, Mikeš L, Haas H, et al. Antibody responses induced by *Trichobilharzia regenti* antigens in murine and human hosts exhibiting cercarial dermatitis. Parasite Immunol. 2008; 30: 585–595. https://doi.org/10.1111/j.1365-3024.2008.01059.x PMID: 19067839

29. Majer M, Macháček T, Súkeníková L, Hrdý J, Horák P. The peripheral immune response of mice infected with a neuropathogenic schistosome. Parasite Immunol. 2020; 42: e12710. https://doi.org/10.1111/pim.12710 PMID: 32145079

30. Nangaku M, Sato-Yoshitake R, Okada Y, Noda Y, Takemura R, Yamazaki H, et al. KIF1B, a novel microtubule plus end-directed monomeric motor protein for transport of mitochondria. Cell. 1994; 79: 1209–1220. https://doi.org/10.1016/0092-8674(94)90012-4 PMID: 7528108

31. Okada Y, Yamazaki H, Sekine-Aizawa Y, Hirokawa N. The neuron-specific kinesin superfamily protein KIF1A is a uniqye monomeric motor for anterograde axonal transport of synaptic vesicle precursors. Cell. 1995; 81: 769–780. https://doi.org/10.1016/0092-8674(95)90538-3 PMID: 7539720

32. Muñoz-Castañeda R, Díaz D, Peris L, Andrieux A, Bosc C, Muñoz-Castañeda JM, et al. Cytoskeleton stability is essential for the integrity of the cerebellum and its motor- and affective-related behaviors. Sci Rep. 2018; 8: 3072. https://doi.org/10.1038/s41598-018-21470-2 PMID: 29449678

33. Frisén J, Johansson CB, Török C, Risling M, Lendahl U. Rapid, widespread, and longlasting induction of nestin contributes to the generation of glial scar tissue after CNS injury. J Cell Biol. 1995; 131: 453–464. https://doi.org/10.1083/jcb.131.2.453 PMID: 7593171

34. Bradbury EJ, Burnside ER. Moving beyond the glial scar for spinal cord repair. Nat Commun. 2019; 10: 3879. https://doi.org/10.1038/s41467-019-11707-7 PMID: 31462640

35. Tatar CL, Appikatla S, Bessert DA, Paintlia AS, Singh I, Skoff RP. Increased Plp1 gene expression leads to massive microglial cell activation and inflammation throughout the brain. ASN Neuro. 2010; 2: 219–231. https://doi.org/10.1042/AN20100016 PMID: 20885931

36. Tretina K, Park E-S, Maminska A, MacMicking JD. Interferon-induced guanylate-binding proteins: Guardians of host defense in health and disease. J Exp Med. 2019; 216: 482–500. https://doi.org/10.1084/jem.20182031 PMID: 30755454

37. Ito D, Imai Y, Ohsawa K, Nakajima K, Fukuuchi Y, Kohsaka S. Microglia-specific localisation of a novel calcium binding protein, Iba1. Brain Res Mol Brain Res. 1998; 57: 1–9. https://doi.org/10.1016/s0169-328x(98)00040-0 PMID: 9630473

38. Ohsawa K, Imai Y, Sasaki Y, Kohsaka S. Microglia/macrophage-specific protein Iba1 binds to fimbrin and enhances its actin-bundling activity. J Neurochem. 2004; 88: 844–856. https://doi.org/10.1046/j.1471-4159.2003.02213.x PMID: 14756805

39. MacKinnon AC, Farnworth SL, Hodkinson PS, Henderson NC, Atkinson KM, Leffler H, et al. Regulation of alternative macrophage activation by galectin-3. J Immunol. 2008; 180: 2650–2658. https://doi.org/10.4049/jimmunol.180.4.2650 PMID: 18250477

40. Rossi C, Cusimano M, Zambito M, Finardi A, Capotondo A, Garcia-Manteiga JM, et al. Interleukin 4 modulates microglia homeostasis and attenuates the early slowly progressive phase of amyotrophic lateral sclerosis. Cell Death Dis. 2018; 9: 250. https://doi.org/10.1038/s41419-018-0288-4 PMID: 29445154

41. Bulantová J, Macháček T, Panská L, Krejčí F, Karch J, Jährling N, et al. *Trichobilharzia regenti* (Schistosomatidae): 3D imaging techniques in characterization of larval migration through the CNS of vertebrates. Micron. 2016; 83: 62–71. https://doi.org/10.1016/j.micron.2016.01.009 PMID: 26897588

42. Wolburg H, Lippoldt A. Tight junctions of the blood-brain barrier: development, composition and regulation. Vascul Pharmacol. 2002; 38: 323–37. https://doi.org/10.1016/s1537-1891(02)00200-8 PMID: 12529927

43. Escartin C, Galea E, Lakatos A, O'Callaghan JP, Petzold GC, Serrano-Pozo A, et al. Reactive astrocyte nomenclature, definitions, and future directions. Nat Neurosci. 2021; 24: 312–325. https://doi.org/10.1038/s41593-020-00783-4 PMID: 33589835

44. Okada S, Nakamura M, Mikami Y, Shimazaki T, Mihara M, Ohsugi Y, et al. Blockade of interleukin-6 receptor suppresses reactive astrogliosis and ameliorates functional recovery in experimental spinal cord injury. J Neurosci Res. 2004; 76: 265–76. https://doi.org/10.1002/jnr.20044 PMID: 15048924

45. Voskoboinik I, Whisstock JC, Trapani JA. Perforin and granzymes: function, dysfunction and human pathology. Nat Rev Immunol. 2015; 15: 388–400. https://doi.org/10.1038/nri3839 PMID: 25998963

46. Horák P, Mikeš L, Lichtenbergová L, Skála V, Soldánová M, Brant SV. Avian schistosomes and outbreaks of cercarial dermatitis. Clin Microbiol Rev. 2015; 28: 165–190. https://doi.org/10.1128/CMR.00043-14 PMID: 25567226

47. Macháček T, Turjanicová L, Bulantová J, Hrdý J, Horák P, Mikeš L. Cercarial dermatitis: a systematic follow-up study of human cases with implications for diagnostics. Parasitol Res. 2018; 117: 3881–3895. https://doi.org/10.1007/s00436-018-6095-0 PMID: 30302587

48. Katchanov J, Nawa Y. Helminthic invasion of the central nervous system: Many roads lead to Rome. Parasitol Int. 2010; 59: 491–496. https://doi.org/10.1016/j.parint.2010.08.002 PMID: 20709186

49. Jarolim KL, McCosh JK, Howard MJ, John DT. A light microscopy study of the migration of *Naegleria fowleri* from the nasal submucosa to the central nervous system during the early stage of primary amebic meningoencephalitis in mice. J Parasitol. 2000; 86: 50–55. https://doi.org/10.1645/0022-3395(2000)086[0050:ALMSOT]2.0.CO;2 PMID: 10701563

50. Jones M. A comparative review of rodent prefrontal cortex and working memory. Curr Mol Med. 2002; 2: 639–647. https://doi.org/10.2174/1566524023361989 PMID: 12420803

51. Touzani K, Puthanveettil S V., Kandel ER. Consolidation of learning strategies during spatial working memory task requires protein synthesis in the prefrontal cortex. Proc Natl Acad Sci. 2007; 104: 5632–5637. https://doi.org/10.1073/pnas.0611554104 PMID: 17369358

52. Hiraoka K, Motomura K, Yanagida S, Ohashi A, Ishisaka-Furuno N, Kanba S. Pattern of c-Fos expression induced by tail suspension test in the mouse brain. Heliyon. 2017; 3: e00316. https://doi.org/10.1016/j.heliyon.2017.e00316 PMID: 28616594

53. Cox DM, Holland CV. Influence of mouse strain, infective dose and larval burden in the brain on activity in *Toxocara*-infected mice. J Helminthol. 2001; 75: 23–32. https://doi.org/10.1079/joh200027 PMID: 11316469

54. Janecek E, Beineke A, Schnieder T, Strube C. Neurotoxocarosis: marked preference of *Toxocara canis* for the cerebrum and *T. cati* for the cerebellum in the paratenic model host mouse. Parasit Vectors. 2014; 7: 194. https://doi.org/10.1186/1756-3305-7-194 PMID: 24754900

55. Jhan K-Y, Lai G-J, Chang P-K, Tang R-Y, Cheng C-J, Chen K-Y, et al. *Angiostrongylus cantonensis* causes cognitive impairments in heavily infected BALB/c and C57BL/6 mice. Parasit Vectors. 2020; 13: 405. https://doi.org/10.1186/s13071-020-04230-y PMID: 32778140

56. Bustos J, Gonzales I, Saavedra H, Handali S, Garcia HH. Neurocysticercosis. A frequent cause of seizures, epilepsy, and other neurological morbidity in most of the world. J Neurol Sci. 2021; 427: 117527. https://doi.org/10.1016/j.jns.2021.117527 PMID: 34147957

57. Ferrari T, Gazzinelli G, Corrêa-Oliveira R. Immune response and pathogenesis of neuroschistosomiasis mansoni. Acta Trop. 2008; 108: 83–88. https://doi.org/10.1016/j.actatropica.2008.02.010 PMID: 18547533

58. Ferrari T, Moreira P, da Cunha A. Clinical characterization of neuroschistosomiasis due to *Schistosoma mansoni* and its treatment. Acta Trop. 2008; 108: 89–97. https://doi.org/10.1016/j.actatropica.2008.04.007 PMID: 18499080

59. Rauw WM. Immune response from a resource allocation perspective. Front Genet. 2012; 3: 267. https://doi.org/10.3389/fgene.2012.00267 PMID: 23413205

60. Ganeshan K, Chawla A. Metabolic regulation of immune responses. Annu Rev Immunol. 2014; 32: 609–634. https://doi.org/10.1146/annurev-immunol-032713-120236 PMID: 24655299

61. Ganeshan K, Nikkanen J, Man K, Leong YA, Sogawa Y, Maschek JA, et al. Energetic trade-offs and hypometabolic states promote disease tolerance. Cell. 2019; 177: 399–413.e12. https://doi.org/10.1016/j.cell.2019.01.050 PMID: 30853215

62. Janecek E, Waindok P, Bankstahl M, Strube C. Abnormal neurobehaviour and impaired memory function as a consequence of *Toxocara canis*- as well as *Toxocara cati*-induced neurotoxocarosis. PLoS Negl Trop Dis. 2017; 11: e0005594. https://doi.org/10.1371/journal.pntd.0005594 PMID: 28481889

63. Xiong H, Zhou Z, Wu Z, Feng Y, Xie F. BALB/c mice infected with *Angiostrongylus cantonensis*: A new model for demyelination in the brain. Anat Rec. 2021; 304: 1084–1093. https://doi.org/10.1002/ar.24538 PMID: 33068322

64. Epe C, Sabel T, Schnieder T, Stoye M. The behavior and pathogenicity of *Toxacara canis* larvae in mice of different strains. Parasitol Res. 1994; 80: 691–695. https://doi.org/10.1007/BF00932955 PMID: 7886040

65. Luo S, OuYang L, Wei J, Wu F, Wu Z, Lei W, et al. Neuronal apoptosis: Pathological basis of behavioral dysfunctions induced by *Angiostrongylus cantonensis* in rodents model. Korean J Parasitol. 2017; 55: 267–278. https://doi.org/10.3347/kjp.2017.55.3.267 PMID: 28719951

66. Janecek E, Wilk E, Schughart K, Geffers R, Strube C. Microarray gene expression analysis reveals major differences between *Toxocara canis* and *Toxocara cati* neurotoxocarosis and involvement of *T. canis* in lipid biosynthetic processes. Int J Parasitol. 2015; 45: 495–503. https://doi.org/10.1016/j.ijpara.2015.02.009 PMID: 25843806

67. Heuer L, Beyerbach M, Lühder F, Beineke A, Strube C. Neurotoxocarosis alters myelin protein gene transcription and expression. Parasitol Res. 2015; 114: 2175–2186. https://doi.org/10.1007/s00436-015-4407-1 PMID: 25773181

68. Springer A, Heuer L, Janecek-Erfurth E, Beineke A, Strube C. Histopathological characterization of *Toxocara canis*- and *T. cati*-induced neurotoxocarosis in the mouse model. Parasitol Res. 2019; 118: 2591–2600. https://doi.org/10.1007/s00436-019-06395-7 PMID: 31350619

69. Yonekawa Y, Harada A, Okada Y, Funakoshi T, Kanai Y, Takei Y, et al. Defect in synaptic vesicle precursor transport and neuronal cell death in KIF1A motor protein–deficient mice. J Cell Biol. 1998; 141: 431–441. https://doi.org/10.1083/jcb.141.2.431 PMID: 9548721

70. Zhao C, Takita J, Tanaka Y, Setou M, Nakagawa T, Takeda S, et al. Charcot-Marie-Tooth Disease type 2A caused by mutation in a microtubule motor KIF1Bβ. Cell. 2001; 105: 587–597. https://doi.org/10.1016/s0092-8674(01)00363-4 PMID: 11389829

71. Blažová K, Horák P. *Trichobilharzia regenti*: The developmental differences in natural and abnormal hosts. Parasitol Int. 2005; 54: 167–172. https://doi.org/10.1016/j.parint.2005.03.003 PMID: 15908263

72. Wei J, Wu F, He A, Zeng X, Ouyang L, Liu M, et al. Microglia activation: one of the checkpoints in the CNS inflammation caused by *Angiostrongylus cantonensis* infection in rodent model. Parasitol Res. 2015; 114: 3247–54. https://doi.org/10.1007/s00436-015-4541-9 PMID: 26002828

73. Wan S, Sun X, Wu F, Yu Z, Wang L, Lin D, et al. Chi3l3: a potential key orchestrator of eosinophil recruitment in meningitis induced by *Angiostrongylus cantonensis*. J Neuroinflammation. 2018; 15: 31. https://doi.org/10.1186/s12974-018-1071-2 PMID: 29391024

74. Strube C, Heuer L, Janecek E. *Toxocara* spp. infections in paratenic hosts. Vet Parasitol. 2013; 193: 375–389. https://doi.org/10.1016/j.vetpar.2012.12.033 PMID: 23312872

75. Pope SM, Fulkerson PC, Blanchard C, Akei HS, Nikolaidis NM, Zimmermann N, et al. Identification of a cooperative mechanism involving interleukin-13 and eotaxin-2 in experimental allergic lung inflammation. J Biol Chem. 2005; 280: 13952–13961. https://doi.org/10.1074/jbc.M406037200 PMID: 15647285

76. Owhashi M, Arita H, Hayai N. Identification of a novel eosinophil chemotactic cytokine (ECF-L) as a chitinase family protein. J Biol Chem. 2000; 275: 1279–1286. https://doi.org/10.1074/jbc.275.2.1279 PMID: 10625674

77. Klion AD, Nutman TB. The role of eosinophils in host defense against helminth parasites. J Allergy Clin Immunol. 2004; 113: 30–37. https://doi.org/10.1016/j.jaci.2003.10.050 PMID: 14713904

78. Mishra PK, Li Q, Munoz LE, Mares CA, Morris EG, Teale JM, et al. Reduced leukocyte infiltration in absence of eosinophils correlates with decreased tissue damage and disease susceptibility in ΔdblGATA mice during murine neurocysticercosis. PLoS Negl Trop Dis. 2016; 10: e0004787. https://doi.org/10.1371/journal.pntd.0004787 PMID: 27332553

79. Anwar AR, Smithers SR, Kay AB. Killing of schistosomula of *Schistosoma mansoni* coated with antibody and/or complement by human leukocytes *in vitro*: requirement for complement in preferential killing by eosinophils. J Immunol. 1979; 122: 628–637. Available: http://www.ncbi.nlm.nih.gov/pubmed/762435 PMID: 762435

80. Ehrens A, Lenz B, Neumann AL, Giarrizzo S, Reichwald JJ, Frohberger SJ, et al. Microfilariae trigger eosinophil extracellular DNA traps in a dectin-1-dependent manner. Cell Rep. 2021; 34: 108621. https://doi.org/10.1016/j.celrep.2020.108621 PMID: 33440150

81. Brown GD. Dectin-1: a signalling non-TLR pattern-recognition receptor. Nat Rev Immunol. 2006; 6: 33–43. https://doi.org/10.1038/nri1745 PMID: 16341139

82. Rock RB, Gekker G, Hu S, Sheng WS, Cheeran M, Lokensgard JR, et al. Role of microglia in central nervous system infections. Clin Microbiol Rev. 2004; 17: 942–964. https://doi.org/10.1128/CMR.17.4.942-964.2004 PMID: 15489356

83. Wei J, Wu F, Sun X, Zeng X, Liang J-Y, Zheng H-Q, et al. Differences in microglia activation between rats-derived cell and mice-derived cell after stimulating by soluble antigen of IV larva from *Angiostrongylus cantonensis in vitro*. Parasitol Res. 2013; 112: 207–14. https://doi.org/10.1007/s00436-012-3127-z PMID: 23073569

84. Olson JK, Miller SD. Microglia initiate central nervous system innate and adaptive immune responses through multiple TLRs. J Immunol. 2004; 173: 3916–3924. https://doi.org/10.4049/jimmunol.173.6.3916 PMID: 15356140

85. Gundra UM, Mishra BB, Wong K, Teale JM. Increased disease severity of parasite-infected TLR2−/− mice is correlated with decreased central nervous system inflammation and reduced numbers of cells with alternatively activated macrophage phenotypes in a murine model of neurocysticercosis. Infect Immun. 2011; 79: 2586–2596. https://doi.org/10.1128/IAI.00920-10 PMID: 21482681

86. Jurk M, Heil F, Vollmer J, Schetter C, Krieg AM, Wagner H, et al. Human TLR7 or TLR8 independently confer responsiveness to the antiviral compound R-848. Nat Immunol. 2002; 3: 499–499. https://doi.org/10.1038/ni0602-499 PMID: 12032557

87. Vázquez-Mendoza A, Carrero JC, Rodriguez-Sosa M. Parasitic infections: A role for C-type lectins receptors. Biomed Res Int. 2013; 2013: 1–11. https://doi.org/10.1155/2013/456352 PMID: 23509724

88. Gensel JC, Wang Y, Guan Z, Beckwith KA, Braun KJ, Wei P, et al. Toll-like receptors and dectin-1, a C-type lectin receptor, trigger divergent functions in CNS macrophages. J Neurosci. 2015; 35: 9966–9976. https://doi.org/10.1523/JNEUROSCI.0337-15.2015 PMID: 26156997

89. Řimnáčová J, Mikeš L, Turjanicová L, Bulantová J, Horák P. Changes in surface glycosylation and glycocalyx shedding in *Trichobilharzia regenti* (Schistosomatidae) during the transformation of cercaria to schistosomulum. PLoS One. 2017; 12: e0173217. https://doi.org/10.1371/journal.pone.0173217 PMID: 28296924

90. Raulf M-K, Lepenies B, Strube C. *Toxocara canis* and *Toxocara cati* somatic and excretory-secretory antigens are recognised by C-type lectin receptors. Pathogens. 2021; 10: 321. https://doi.org/10.3390/pathogens10030321 PMID: 33803269

91. Alvarez JJI, Rivera J, Teale JM. Differential release and phagocytosis of tegument glycoconjugates in neurocysticercosis: Implications for immune evasion strategies. PLoS Negl Trop Dis. 2008; 2: e218. https://doi.org/10.1371/journal.pntd.0000218 PMID: 18398489

92. Raes G, Van den Bergh R, De Baetselier P, Ghassabeh GH. Arginase-1 and Ym1 are markers for murine, but not human, alternatively activated myeloid cells. J Immunol. 2005; 174: 6561–6562. https://doi.org/10.4049/jimmunol.174.11.6561 PMID: 15905489

93. Ponomarev ED, Maresz K, Tan Y, Dittel BN. CNS-derived interleukin-4 is essential for the regulation of autoimmune inflammation and induces a state of alternative activation in microglial cells. J Neurosci. 2007; 27: 10714–10721. https://doi.org/10.1523/JNEUROSCI.1922-07.2007 PMID: 17913905

94. Cherry JD, Olschowka JA, O'Banion M. Neuroinflammation and M2 microglia: the good, the bad, and the inflamed. J Neuroinflammation. 2014; 11: 98. https://doi.org/10.1186/1742-2094-11-98 PMID: 24889886

95. Mishra BB, Gundra UM, Teale JM. STAT6−/− mice exhibit decreased cells with alternatively activated macrophage phenotypes and enhanced disease severity in murine neurocysticercosis. J Neuroimmunol. 2011; 232: 26–34. https://doi.org/10.1016/j.jneuroim.2010.09.029 PMID: 21051093

96. Peng H, Sun R, Zhang Q, Zhao J, Wei J, Zeng X, et al. Interleukin 33 mediates type 2 immunity and inflammation in the central nervous system of mice infected with *Angiostrongylus cantonensis*. J Infect Dis. 2013; 207: 860–869. https://doi.org/10.1093/infdis/jis682 PMID: 23148283

97. Waindok P, Strube C. Neuroinvasion of *Toxocara canis*- and *T. cati*-larvae mediates dynamic changes in brain cytokine and chemokine profile. J Neuroinflammation. 2019; 16: 147. https://doi.org/10.1186/s12974-019-1537-x PMID: 31315623

98. Alvarez JI, Teale JM. Breakdown of the blood brain barrier and blood–cerebrospinal fluid barrier is associated with differential leukocyte migration in distinct compartments of the CNS during the course of murine NCC. J Neuroimmunol. 2006; 173: 45–55. https://doi.org/10.1016/j.jneuroim.2005.11.020 PMID: 16406118

99. Chen KY, Cheng CJ, Cheng CC, Jhan KY, Chen YJ, Wang LC. The excretory/secretory products of fifth stage larval *Angiostrongylus cantonensis* induces autophagy via the sonic hedgehog pathway in mouse brain astrocytes. PLoS Negl Trop Dis. 2020; 14: 1–20. https://doi.org/10.1371/journal.pntd.0008290 PMID: 32479527

100. Kigerl KA, Gensel JC, Ankeny DP, Alexander JK, Donnelly DJ, Popovich PG. Identification of two distinct macrophage subsets with divergent effects causing either neurotoxicity or regeneration in the

injured mouse spinal cord. J Neurosci. 2009; 29: 13435–13444. https://doi.org/10.1523/JNEUROSCI.3257-09.2009 PMID: 19864556

101. Miron VE, Boyd A, Zhao J-W, Yuen TJ, Ruckh JM, Shadrach JL, et al. M2 microglia and macrophages drive oligodendrocyte differentiation during CNS remyelination. Nat Neurosci. 2013; 16: 1211–1218. https://doi.org/10.1038/nn.3469 PMID: 23872599

102. Starossom SC, Campo Garcia J, Woelfle T, Romero-Suarez S, Olah M, Watanabe F, et al. Chi3l3 induces oligodendrogenesis in an experimental model of autoimmune neuroinflammation. Nat Commun. 2019; 10: 217. https://doi.org/10.1038/s41467-018-08140-7 PMID: 30644388

103. Cai D, Deng K, Mellado W, Lee J, Ratan RR, Filbin MT. Arginase I and polyamines act downstream from cyclic AMP in overcoming inhibition of axonal growth MAG and myelin in vitro. Neuron. 2002; 35: 711–719. https://doi.org/10.1016/s0896-6273(02)00826-7 PMID: 12194870

104. Deng K, He H, Qiu J, Lorber B, Bryson JB, Filbin MT. Increased synthesis of spermidine as a result of upregulation of arginase I promotes axonal regeneration in culture and in vivo. J Neurosci. 2009; 29: 9545–9552. https://doi.org/10.1523/JNEUROSCI.1175-09.2009 PMID: 19641117

105. Frey A, Di Canzio J, Zurakowski D. A statistically defined endpoint titer determination method for immunoassays. J Immunol Methods. 1998; 221: 35–41. https://doi.org/10.1016/s0022-1759(98)00170-7 PMID: 9894896

106. Hertel J, Hamburger J, Haberl B, Haas W. Detection of bird schistosomes in lakes by PCR and filter-hybridization. Exp Parasitol. 2002; 101: 57–63. https://doi.org/10.1016/s0014-4894(02)00036-x PMID: 12243738

107. Komada M, Takao K, Miyakawa T. Elevated plus maze for mice. J Vis Exp. 2008; 1088. https://doi.org/10.3791/1088 PMID: 19229173

108. Riebe CJ, Wotjak CT. A practical guide to evaluating anxiety-related behavior in rodents. In: Szallasi A, Bíró T, editors. TRP Channels in Drug Discovery. 2012. pp. 167–185. https://doi.org/10.1007/978-1-62703-095-3_10

109. Curzon P, Zhang M, Radek RJ, Fox GB. The behavioral assessment of sensorimotor processes in the mouse: Acoustic startle, sensory gating, locomotor activity, rotarod, and beam walking. In: Buccafusco J, editor. Methods of Behavior Analysis in Neuroscience. 2009. pp. 171–176. Available: http://www.ncbi.nlm.nih.gov/pubmed/21204341

110. Hölter SM, Glasl L. High-throughput mouse phenotyping. In: Lane E, Dunnett S, editors. Animal Models of Movement Disorders. 2011. pp. 109–133. https://doi.org/10.1007/978-1-61779-298-4_7

111. Justice JN, Carter CS, Beck HJ, Gioscia-Ryan RA, McQueen M, Enoka RM, et al. Battery of behavioral tests in mice that models age-associated changes in human motor function. Age (Omaha). 2014; 36: 583–595. https://doi.org/10.1007/s11357-013-9589-9 PMID: 24122289

112. Mann A, Chesselet MF. Techniques for motor assessment in rodents. In: LeDoux M, editor. Movement Disorders. 2014. pp. 139–157. https://doi.org/10.1016/C2012-0-00370-5

113. Deacon RM. Digging and marble burying in mice: Simple methods for *in vivo* identification of biological impacts. Nat Protoc. 2006; 1: 122–124. https://doi.org/10.1038/nprot.2006.20 PMID: 17406223

114. Kraeuter A-K, Guest PC, Sarnyai Z. The Y-maze for assessment of spatial working and reference memory in mice. Pre-Clinical Models. 2019. pp. 105–111. https://doi.org/10.1007/978-1-4939-8994-2_10 PMID: 30535688

115. Deacon RM. Measuring the strength of mice. J Vis Exp. 2013; 2610. https://doi.org/10.3791/2610 PMID: 23770643

116. Sugimoto H, Kawakami K. Low-cost protocol of footprint analysis and hanging box test for mice applied the chronic restraint stress. J Vis Exp. 2019; 59027. https://doi.org/10.3791/59027 PMID: 30735178

117. Porsolt RD, Brossard G, Hautbois C, Roux S. Rodent models of depression: Forced swimming and tail suspension behavioral despair tests in rats and mice. Curr Protoc Neurosci. 2001; 14: Unit 8.10A. https://doi.org/10.1002/0471142301.ns0810as14 PMID: 18428536

118. Pino PA, Cardona AE. Isolation of brain and spinal cord mononuclear culls using Percoll gradients. J Vis Exp. 2011; 2348. https://doi.org/10.3791/2348 PMID: 21339713

119. Andrews S. FastQC: A quality control tool for high throughput sequence data. 2010 [cited 10 Aug 2021]. Available: http://www.bioinformatics.babraham.ac.uk/projects/fastqc/

120. Bolger AM, Lohse M, Usadel B. Trimmomatic: a flexible trimmer for Illumina sequence data. Bioinformatics. 2014; 30: 2114–2120. https://doi.org/10.1093/bioinformatics/btu170 PMID: 24695404

121. Li B, Dewey CN. RSEM: accurate transcript quantification from RNA-Seq data with or without a reference genome. BMC Bioinformatics. 2011; 12: 323. https://doi.org/10.1186/1471-2105-12-323 PMID: 21816040

122. Love MI, Huber W, Anders S. Moderated estimation of fold change and dispersion for RNA-seq data with DESeq2. Genome Biol. 2014; 15: 550. https://doi.org/10.1186/s13059-014-0550-8 PMID: 25516281

123. Haas BJ, Papanicolaou A, Yassour M, Grabherr M, Blood PD, Bowden J, et al. *De novo* transcript sequence reconstruction from RNA-seq using the Trinity platform for reference generation and analysis. Nat Protoc. 2013; 8: 1494–1512. https://doi.org/10.1038/nprot.2013.084 PMID: 23845962

124. Kanehisa M, Sato Y, Kawashima M, Furumichi M, Tanabe M. KEGG as a reference resource for gene and protein annotation. Nucleic Acids Res. 2016; 44: D457–D462. https://doi.org/10.1093/nar/gkv1070 PMID: 26476454

125. Kanehisa M, Goto S. KEGG: kyoto encyclopedia of genes and genomes. Nucleic Acids Res. 2000; 28: 27–30. https://doi.org/10.1093/nar/28.1.27 PMID: 10592173

126. Vondráček O, Mikeš L, Talacko P, Leontovyč R, Bulantová J, Horák P. Differential proteomic analysis of laser-microdissected penetration glands of avian schistosome cercariae with a focus on proteins involved in host invasion. Int J Parasitol. 2022. https://doi.org/10.1101/2021.08.24.457505

127. Kulak NA, Pichler G, Paron I, Nagaraj N, Mann M. Minimal, encapsulated proteomic-sample processing applied to copy-number estimation in eukaryotic cells. Nat Methods. 2014; 11: 319–324. https://doi.org/10.1038/nmeth.2834 PMID: 24487582

128. Cox J, Hein MY, Luber CA, Paron I, Nagaraj N, Mann M. Accurate proteome-wide label-free quantification by delayed normalization and maximal peptide ratio extraction, termed MaxLFQ. Mol Cell Proteomics. 2014; 13: 2513–2526. https://doi.org/10.1074/mcp.M113.031591 PMID: 24942700

129. Tyanova S, Temu T, Sinitcyn P, Carlson A, Hein MY, Geiger T, et al. The Perseus computational platform for comprehensive analysis of (prote)omics data. Nat Methods. 2016; 13: 731–740. https://doi.org/10.1038/nmeth.3901 PMID: 27348712

130. Susaki EA, Tainaka K, Perrin D, Yukinaga H, Kuno A, Ueda HR. Advanced CUBIC protocols for whole-brain and whole-body clearing and imaging. Nat Protoc. 2015; 10: 1709–1727. https://doi.org/10.1038/nprot.2015.085 PMID: 26448360

131. Goldim MP de S, Della Giustina A, Petronilho F. Using Evans blue dye to determine blood-brain barrier integrity in rodents. Curr Protoc Immunol. 2019; 126: e83. https://doi.org/10.1002/cpim.83 PMID: 31483106

Manuscript #1

Šmídová, B., Nieto Peréz, C., Ajendra, J., Macháček, T., Ehrens, A.

Eosinophils and *Trichobilharzia regenti*, the neuropathogenic schistosome, in the roles of hunters and prey.

Manuscript, 2024

Eosinophils and *Trichobilharzia regenti*, the neuropathogenic schistosome, in the roles of hunters and prey

Barbora Šmídová[1], Celia Nieto Peréz[2], Jesuthas Ajendra[2], Marc Hübner[2,3], Tomáš Macháček[1], Alexandra Ehrens[2,3]

[1] Department of Parasitology, Faculty of Science, Charles University, Prague, Czech Republic

[2] Institute for Medical Microbiology, Immunology and Parasitology, University Hospital Bonn, Bonn, Germany

[3] German Centre for Infectious Research (DZIF), partner side Cologne-Bonn, Germany

ABSTRACT

The neuropathogenic avian schistosome *Trichobilharzia regenti* is known to attract large numbers of eosinophils while being quickly eliminated from mice, its accidental hosts. Therefore, a hypothesis of eosinophils being the ones responsible for parasite clearance came to life. Eosinophils have, besides other effects, the ability to form extracellular DNA traps (during a process called ETosis) that were proven to capture and kill various pathogens. In this project, we tested the reactivity of eosinophils to *T. regenti* homogenate (TrAg) and confirmed that adding TrAg to bone marrow-derived eosinophil culture leads to apoptosis and eosinophil maturation. We have then shown that although apoptosis occurs, eosinophils also form DNA traps. This suggests that either both trap formation and apoptosis are induced or both pathways leading to DNA trap formation are stimulated. Moreover, TrAg triggered mitochondrial ROS production in eosinophils, which could indicate that TrAg induces ETosis via the well characterized calcium-dependent pathway. Together the presented data form an important first step in unraveling the interaction between eosinophils and *T. regenti*.

KEY WORDS

Eosinophil extracellular traps; EETosis; eosinophils; *Trichobilharzia regenti*

INTRODUCTION

Trichobilharzia regenti is a neuropathogenic avian schistosome usually circulating between water snails of the genus *Radix* and waterfowl. However, it can accidentally infect mice where it migrates to the central nervous system (CNS) and is eliminated within 21 days (Horák et al., 1999; Macháček et al., 2022). While the parasite itself barely damages the neural structure and functions (Macháček et al., 2022), it attracts immune cells at large. The infected CNS is predominantly infiltrated with eosinophils that are hypothesized to be the main player in parasite clearance (Macháček et al., 2022). However, the possible defensive mechanism of eosinophils during the parasite elimination has not been established yet.

Eosinophils, like neutrophils, are capable of forming extracellular DNA traps upon encountering various stimuli. These DNA traps are formed during a process called ETosis, which is a type of cell death. These traps are not only released in response to bacteria or fungi (Mukherjee et al., 2018; Muniz et al., 2018; Yousefi et al., 2012), but also against parasites such as *Haemonchus contortus* and *Strongyloides ratti larvae* (Muñoz-Caro et al., 2015; Ehrens et al., 2021b) or *Litomosomoides sigmodontis* and *Dirofilaria immitis* microfilariae (Ehrens et al., 2021a). So far, little is known about ETosis in response to schistosome. While two publications show that the eggs of *Schistosoma japonicum*, a human schistosome parasite, can induce neutrophil ETosis (Chuah et al., 2014; Liao et al., 2023), there is only little data on eosinophils ETosis in response to the adult schistosomes. Extracellular DNA with eosinophil cationic protein were also observed around *Schistosoma* sp. (Yousefi et al., 2008) but it has not been further studied yet. Even though the effect seems to be conserved in the nematode world, very little is known about other parasites.

The eosinophil extracellular DNA traps can be formed either from nuclear or mitochondrial DNA in response to different stimuli (Yousefi et al., 2012). During chronic eosinophilic diseases, rather lytic eosinophils with DNA together with nuclear histone H1 were detected (Ueki et al., 2013, 2016). This pathway can be stimulated by immunoglobulins, some cytokines or phorbol myristate acetate (PMA),

which then leads to ROS production by NADPH oxidase, nuclear DNA trap formation and ultimately to cell death (Ueki et al., 2013). This pathway is dependent on NADPH oxidase.

In contrast, when eosinophils encounter bacteria such as *Spirocheta* sp., they are likely to shoot traps formed from mitochondrial DNA, which do not necessarily decrease their viability (Mukherjee et al., 2018; Yousefi et al., 2008). The underlying mechanism has been described only in neutrophils but empirical evidence shows that the pathways are mostly similar for all granulocytes. For this much faster DNA trap formation, calcium is needed. The pathway, which can be activated for example by a calcium ionophore ionomycin, then leads to mitochondrial ROS production and is referred to as calcium-dependent ETosis pathway (Douda et al., 2015).

The origin of eosinophil DNA traps in response to nematodes has so far only been described for *L. sigmodontis* microfilariae where the stimulated eosinophils form mainly mitochondrial DNA traps (Ehrens et al., 2021a). As for the other parasites, the trap origin is yet unknown. Therefore, here we tested whether eosinophils undergo ETosis upon stimulation with T. regenti in vitro and if so, which pathway is responsible for the trap formation.

MATERIALS AND METHODS

Animal housing

C57BL/6J mice originally obtained from Janvier Labs were housed at the animal facilities of the Institute for Medical Microbiology, Immunology and Parasitology, University Hospital Bonn. Animals were kept in individually ventilated cages with food and water *ad libitum* and their wellbeing was checked daily.

Ethics statement

Animal experiments were conducted according to the Directive 2010/63/EU and animal protocols were approved by the local authorities (Landesamt für Natur, Umwelt und Verbraucherschutz Nordrhein-Westfalen register no. 84-02.04.2014.A327).

Experimental setup

Eosinophils were derived from the bone marrow of naive mice. Eosinophils were stimulated with *T. regenti* antigen and trap formation was analyzed by florescence microscopy and by DNA concentration in the supernatant. In addition, the production of mitochondrial reactive oxygen species (ROS) was measured.

Trichobilharzia regenti antigen (TrAg) preparation

The life cycle of *T. regenti* is routinely maintained at the Laboratory of Helminthology, Department of Parasitology, Faculty of Science, Charles University. To prepare the *T. regenti* schistosomula antigen, cercariae were collected, transformed to schistosomula and homogenized as described in Macháček et al., 2016. Briefly, the snails were illuminated to stimulate the cercariae emergence. Cercariae were then collected, mechanically transformed by passing through a syringe needle and kept in the schistosome culture medium (prepared according to Macháček et al. (2016)) at 37 °C with 5% CO_2 for 3 days. After that, the schistosomulum-like stages were homogenized by a sonicator and centrifuged to remove debris. In the end, protein concentration was determined. Samples were stored at -80 °C until further use.

Eosinophil culture preparation

Eosinophils were generated from the bone marrow obtained from the hind legs as described in Ehrens et al. (2021). Briefly, mice were euthanized, the hind legs were removed and bone marrow was harvested from femurs and tibias. Then, the red blood cells were lysed, the remaining cells were counted and cultured in eosinophil medium (RPMI 1640, 20% FBS, 1% penicillin/streptomycin, 0.1% gentamycin, 2.5% HEPES and 1% Glutamax) supplemented with 100 ng/ml stem cell factor (SCF, Peprotech) and 100 ng/ml FMS-like tyrosine kinase 3 ligand at first (FLT3L, Peprotech). Cell culture medium was exchanged every other day. After 4 days of culture, eosinophils medium was supplemented with 20 ng/ml IL-5 (Peprotech) instead of FLT3L and SCF. On day 13 or 14, the eosinophil purity was checked using flow cytometry. For this, the cells were stained with anti-SiglecF-PE (BD Bioscences), measured using CytoFLEX flow cytometer and analyzed in CytExpert software v2.5. The culture was used for experiments if the purity was above 92%.

Immunocytochemistry

To maximize the number of cells incubated with TrAg, polyethylenimine-coated slides were used. Both slide preparation and staining protocol were adapted from Ehrens et al., 2021 and adjusted. Round glass slides (170 ±5 µm) were incubated in a 24-well plate with 400 µl of 0.1% polyethylenimine in water for 1 hour at 37 °C, washed with dH_2O three times for 5 minutes, left to air-dry and finally sterilized under UV light for 30 min. Then, $2.5x10^5$ cells in 50 µl of Advanced RPMI 1640 medium containing 1% penicillin, 1% streptomycin (Pen/Strep, Gibco), 0.1% gentamycin (Gibco), 1% L-glutamine (Gibco), 1% GlutaMAX (Gibco), 2.5% FBS (PAN Biotech) and 20 ng/ml of murine recombinant IL-5 (Peprotech) (2.5% Eosinophil medium) were added and left to attach for 20 min at room temperature. After that, 310 µl of 2.5% Eosinophil medium was added and the cells were incubated for 30 min at 37 °C and 5% CO_2. Finally, TrAg (50 µg/ml) was added for 24 hours. Ionomycin (1 µg/ml, Merck) and phorbol-12-myristate-13-acetate (PMA, 50 ng/ml, Invivogen) were used as positive controls, PBS as a negative control.

After the incubation, the plates were centrifuged (400 g, 10 min, 4 °C), the supernatant was removed and the samples were fixed with 4% paraformaldehyde (Sigma Aldrich) in PBS for 20 min at room temperature. Then, the plates were centrifuged and washed with dH_2O. Finally, the slides were stained with 1 µm Sytox Orange (Invitrogen) in 0.3 M NaCl, 0.03 M sodium citrate (pH 7) buffer for 20 min in the dark at room temperature, washed with dH_2O and mounted using Mowiol (Carl Roth) containing ProLong Live Antifade Reagent (1/50, Invitrogen). Slides were examined and captured using the Axio Observer 7 from Zeiss. Pictures were analyzed in Fiji (ImageJ).

DNA quantification

In a 96-well plate, $1x10^5$ cells were cultured in Advanced RPMI 1640 medium containing 1% penicillin, 1% streptomycin (Pen/Strep, Gibco), 0.1% gentamycin (Gibco), 1% L-glutamine (Gibco), 1% GlutaMAX (Gibco), 5% FBS (PAN Biotech) and 20 ng/ml of murine recombinant IL-5 (Peprotech) (5% Eosinophil medium) and stimulated with TrAg (50 µg/ml), ionomycin (1 µg/ml, Merck), PMA (50 ng/ml, Invivogen) or PBS for 24 hours. The samples were then processed for DNA quantification as described in Ehrens et al. (2021). Briefly, micrococcal nuclease was added to each well to detach DNA traps from the well. After 15 min of incubation at 37°C, EDTA was added to stop the nuclease activity. The plates were centrifuged at 400g, 4°C for 10min and the supernatant containing the DNA traps was collected. The DNA in the supernatant was immediately quantified using DNA Quant-iT dsDNA Assay Kit, high

sensitivity (Invitrogen) according to the manufacturer's protocol. The absorbance was measured with the Tecan Infinite 200 Pro plate reader using excitation/emission wavelengths of 485/535 nm. DNA was quantified by generating a standard curve using the absorbance values from the standard.

Apoptosis detection

After the supernatant was taken for DNA quantification, the pellets were resuspended in 100 µl of Fc block (PBS with 1% BSA and 1/1000 diluted rat IgG (ThermoFischer)) and incubated at 4 °C for 30 min. Then, the plate was centrifuged (400 g, 10 min, 4 °C), the pellets were resuspended in 100 µl anti-SiglecF-BV421 (1:400, Biolegend) and anti-CD86-PE-Cy7 (1:400, BD Bioscience) in PBS and incubated for 30 min in the dark at 4 °C. The plate was centrifuged again, supernatant was removed and cells were stained using FITC Annexin V Apoptosis Detection Kit with PI (BioLegend) according to the manufacturer's protocol. Finally, the cells were measured at LSR Fortessa (BD Bioscience) and the data were analyzed using FlowJo v.10.1. Gating strategy is shown in Fig. S1.

MitoSOX assay

For the MitoSOX assay, $1.5x10^5$ cells in 75 µl of 5% Eosinophil medium were plated in black F-bottom plates. Cells were incubated with 75 µl of MitoSOX (1:500, Invitrogen) in 5% Eosinophil medium for 15 min at 37 °C and 5% CO_2. The cells were then washed two times by centrifugation (400 g, 10 min, 4 °C) and resuspended in 100 µl HBSS (Gibco). Finally, TrAg (50 µg/ml), ionomycin (1 µg/ml, Merck), PMA (50 ng/ml, Invivogen) or PBS were added, and the recording of the undergoing processes started immediately using the Tecan Infinite 200 Pro plate reader at 37 °C using bottom read at excitation/emission wavelengths of 510/600 nm. The signal was recorded every 10 min for 2 hours.

Statistical analysis

One-way ANOVA followed by Dunnett's test for each treated group against the unstimulated control was used and the analyses were performed in GraphPad Prism (version 10). P-values <0.05 were considered significant. The graphs show means with standard deviations or individual values with medians.

RESULTS

***T. regenti* antigen stimulates eosinophil activation and apoptosis**

Flow cytometry analysis of eosinophils revealed two distinct populations (FSC-low and FSC-high eosinophils) in the cultures (Fig. 1A). The ratio of these populations changed depending on the stimuli added. After adding the different stimuli, the relative representation shifted significantly in favor of "FSC-low" subpopulation (Fig. 1B) with TrAg showing the highest proportion of the FSC-low population. Both populations were analyzed for their relative expression of CD86, which is a marker of eosinophil activation (MacKenzie et al., 2001). While FSC-low eosinophils showed an increase in CD86 expression upon stimulation, the FSC-high subpopulation did not show any significant changes in MFI of CD86 after treatment (Fig. 1C), suggesting that the FSC-low eosinophils are more mature then the FSC-high cells. FSC-low eosinophils were mostly apoptotic after all treatments; however, significantly more cells were late apoptotic after treatment with TrAg and PMA. In the case of TrAg, this difference also led to significantly lower ratio of early apoptotic cells suggesting that TrAg is even more potent in inducing apoptosis than positive controls compared to untreated cells (Fig. 1C). Progenitors were, on the other

hand, mostly alive. However, adding TrAg to the culture induced early apoptosis in a significant number of eosinophils after stimulation with TrAg compared to untreated control (Fig. 1C).

In summary, the results show that TrAg induces eosinophil maturation and eosinophil cell death.

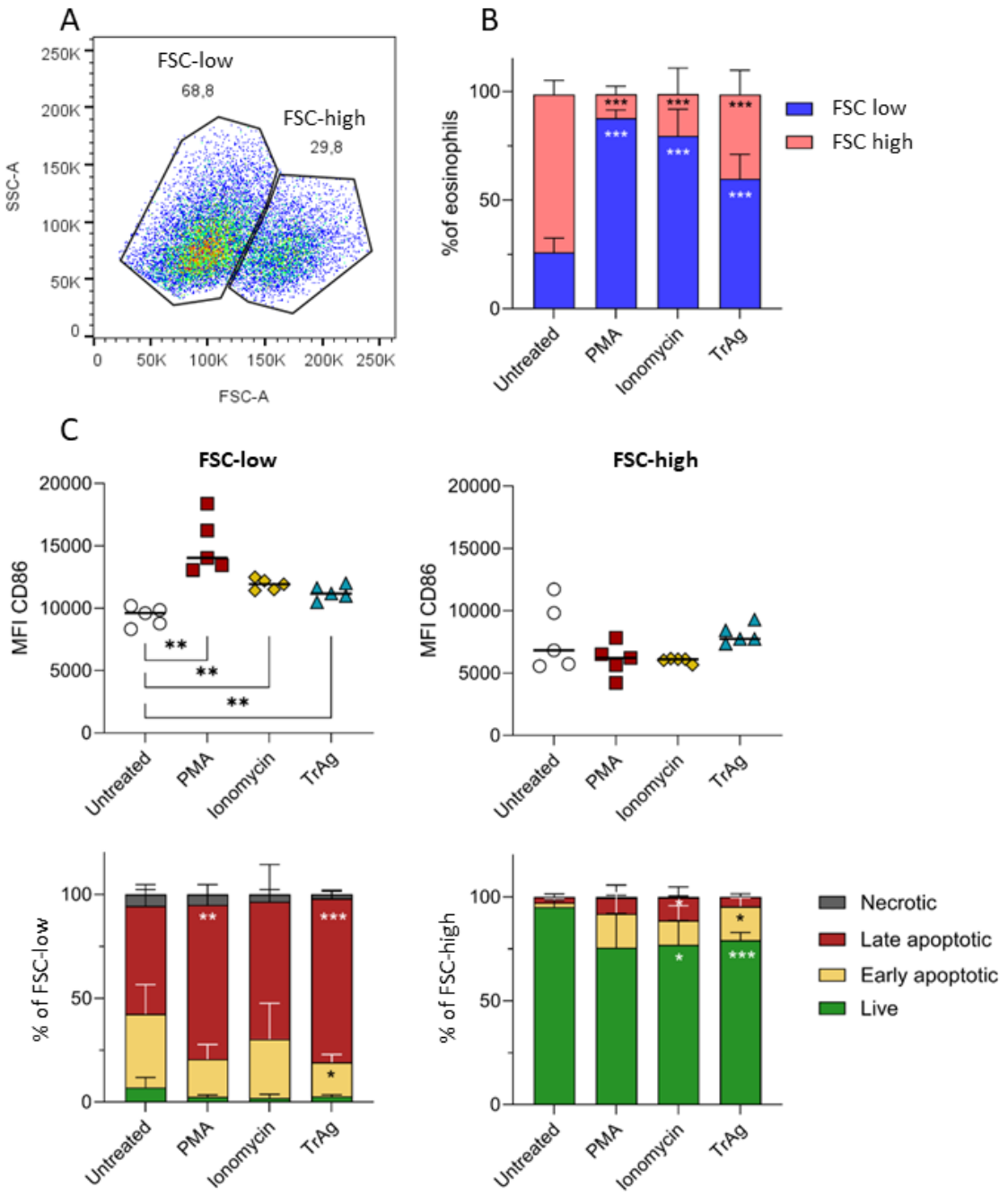

Fig. 1: A: Representative flow cytometry dotplot showing two distinct populations of eosinophils. **B:** Relative representation of FSC low and FSC high populations in eosinophil cultures after treatment with TrAg. PMA and ionomycine were used as positive controls, untreated eosinophils as a negative control. Graph shows results from 2 experiments. Statistics: separate one-way ANOVAs of mature eosinophils and progenitors (*** $P < 0.001$). **C:** Median fluorescence intensity (MFI) of CD86 and relative representation of live, early apoptotic, late apoptotic and necrotic cells in FSC low (left column) and FSC high (right column) after treatment with TrAg. PMA and ionomycine were used as positive controls, untreated eosinophils as a negative control. Graph shows results from 2 experiments. Statistics: MFI: one-way ANOVA (** $P < 0.01$), apoptosis: separate one-way ANOVAs of each cell state (* $P < 0.05$, ** $P < 0.01$, *** $P < 0.001$).

T. regenti antigen stimulates eosinophil trap formation and mitochondrial ROS production

To investigate if TrAg triggers more than apoptosis, its effect on stimulating ETosis was investigated. Using fluorescent microscopy, we observed DNA traps released by eosinophils in response to PMA and TrAg. While PMA, a positive control, induced the release of fibrous DNA traps, the traps in response to TrAg appeared to be more cloud-like. Untreated cells remained circular with DNA distributed in an eosinophil-characteristic way (Fig. 2A). To quantify the trap formation, we measured the concentration of free DNA in the culture medium after adding TrAg or the positive controls PMA and ionomycin. Consistent with the microscopy data, all treatments stimulated a significant DNA release from the eosinophils compared to the untreated cells (Fig. 2B).

Furthermore, we used a MitoSOX assay to detect mitochondrial ROS production in response to TrAg, as mitochondrial ROS is an essential step during the calcium-dependent ETosis pathway. While ionomycin is known for inducing the Ca^{2+}-dependent ETosis pathway, which involves high amounts of mitochondrial ROS (Douda et al., 2015), PMA rather triggers the NADPH-dependent pathway with minimal involvement of mitochondrial ROS formation (Ueki et al., 2016). The results show that TrAg, PMA and ionomycin induce an increase in mitochondrial ROS in eosinophils in comparison to untreated cells. In particular, ionomycin induced the highest amount with significantly higher levels of mitochondrial ROS in eosinophils after 80 min of incubation compared to untreated cells. TrAg also significantly increased MFI in the beginning and the end of the measurement compared to untreated cells and the change in MFI was smaller compared to ionomycin. Thus, TrAg may stimulate the Ca^{2+}-dependent ETosis.

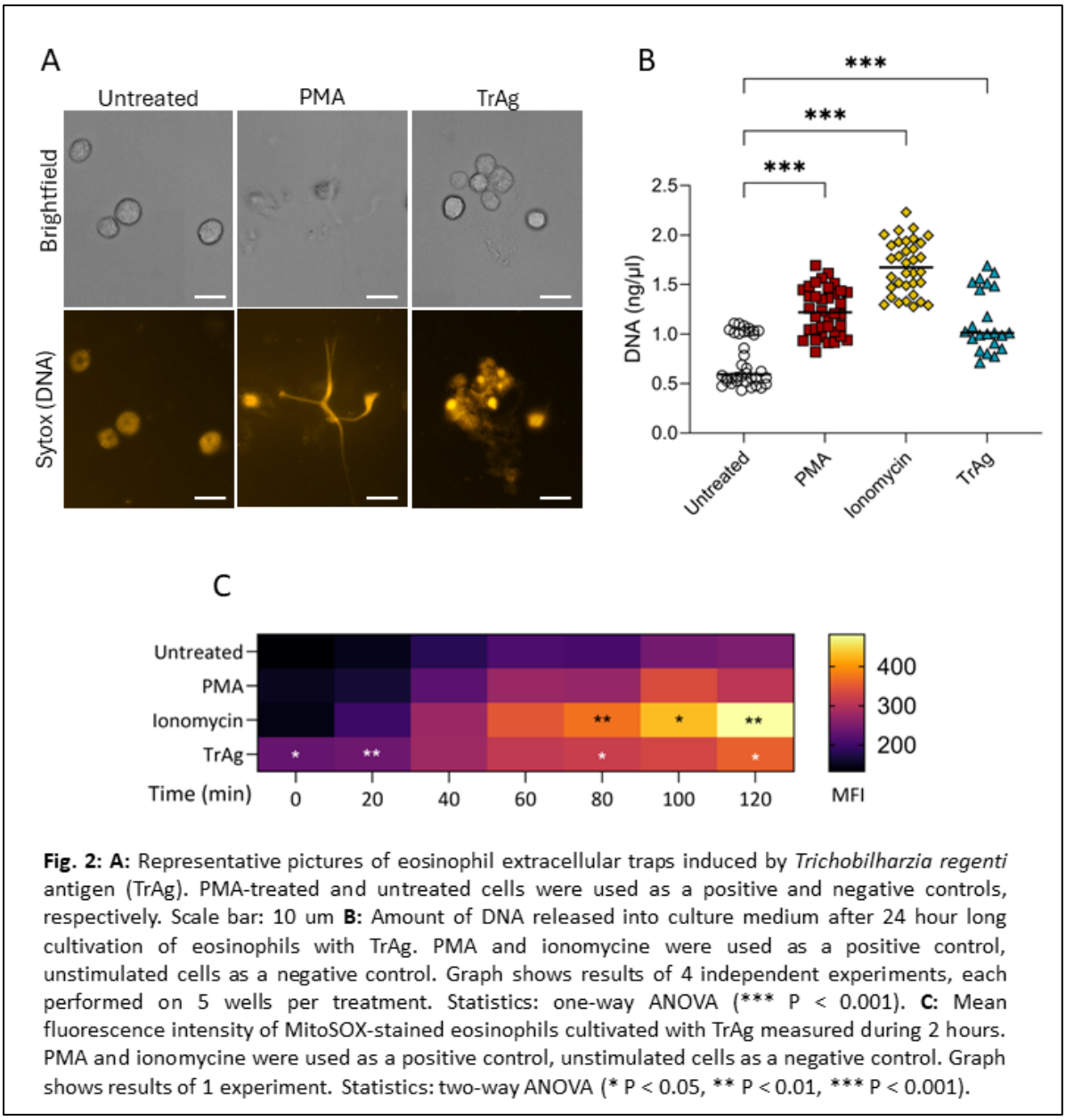

Fig. 2: A: Representative pictures of eosinophil extracellular traps induced by *Trichobilharzia regenti* antigen (TrAg). PMA-treated and untreated cells were used as a positive and negative controls, respectively. Scale bar: 10 um **B:** Amount of DNA released into culture medium after 24 hour long cultivation of eosinophils with TrAg. PMA and ionomycine were used as a positive control, unstimulated cells as a negative control. Graph shows results of 4 independent experiments, each performed on 5 wells per treatment. Statistics: one-way ANOVA (*** $P < 0.001$). **C:** Mean fluorescence intensity of MitoSOX-stained eosinophils cultivated with TrAg measured during 2 hours. PMA and ionomycine were used as a positive control, unstimulated cells as a negative control. Graph shows results of 1 experiment. Statistics: two-way ANOVA (* $P < 0.05$, ** $P < 0.01$, *** $P < 0.001$).

DISCUSSION

Although eosinophils are important in eliminating many parasitic infections (Ehrens et al., 2022; Mitre and Klion, 2021), little is known about their effector mechanisms during parasite clearance. However, after discovering that eosinophils are also capable of producing extracellular DNA traps (Yousefi et al., 2008), the research on the effect of these traps on parasites has begun. So far, the effect has been described for various nematodes (Ehrens et al., 2021b, 2021a; Muñoz-Caro et al., 2015) and once it was mentioned in case of *Schistosoma* sp. (Yousefi et al., 2008). Nevertheless, *Trichobilharzia regenti*, a schistosome attracting large numbers of eosinophils while being quickly eliminated (Macháček et al., 2022), therefore an ideal model for studying the effector mechanisms of eosinophils, has been overlooked.

In this study, we have confirmed with both fluorescent microscopy and free DNA quantification that *T. regenti* antigen (TrAg) triggers DNA trap formation in eosinophils. Given that this was already

described for nematodes (Ehrens et al., 2021b, 2021a; Muñoz-Caro et al., 2015), it suggests that the eosinophil extracellular trap formation is a conserved mechanisms. Similarly, in neutrophils, extracellular traps have been described for both uni- and multicellular parasites not only in mice and men, but also in dogs, opposums, pinnipeds and cetaceans (Ehrens et al., 2021b; Guimarães-Costa et al., 2012; Koh et al., 2023; Villagra-Blanco et al., 2019). We, however, realize that to prove the eosinophil extracellular DNA traps capture *T. regenti in vivo*, we need to perform *in vitro* experiments with *T. regenti* schistosomula and confirm them in an *in vivo* system.

Under the microscope, the stimulus for the eosinophil trap formation can be distinguished by either cloud-like appearance (ionomycine) or fiber-like structures (PMA) (Ehrens et al, unpublished data). This correlates with the different trap formation pathways after using either stimulus (Douda et al., 2015; Ueki et al., 2016). Given that TrAg triggers rather cloudy trap formation which correlates with Ca^{2+}-dependent pathway triggered by ionomycine (Douda et al., 2015), we decided to further analyze the pathway stimulated by TrAg.

As a first step in testing which trap-forming pathway is TrAg-triggered, we performed a MitoSOX assay detecting mitochondrial superoxides. TrAg, similarly to ionomycin, led to an MFI increase over time suggesting that TrAg-induced traps might be of mitochondrial origin like those induced by *L. sigmodontis* (Ehrens et al., 2021a). However, in case of *L. sigmodontis*, the DNA origin was studied as a ratio of nuclear/mitochondrial DNA markers using PCR and by histone citrullination staining (Ehrens et al., 2021a), which we believe would be necessary to perform in further experiments as well.

If TrAg-induced traps were indeed of mitochondrial origin, eosinophils should remain viable afterwards, according to literature (Douda et al., 2015; Yousefi et al., 2008). However, our data show that TrAg induces eosinophil apoptosis. There could be two explanations for this – 1) TrAg triggers apoptosis in trap-unrelated pathway as we have previously described TrAg induces apoptosis in fibroblasts and neurons (Parohová et al., unpublished data), or 2) TrAg stimulates both mitochondrial and nuclear DNA trap formation. Second explanation is supported by lesser MFI change in TrAg-stimulated eosinophils than in the cells stimulated by ionomycin-stimulated ones where the traps are of mitochondrial origin (Douda et al., 2015). Furthermore, *L. sigmodontis* was shown to also induce both DNA traps (Ehrens et al., 2021a). However, more experiment need to be conducted to determine the origin.

Taken together, this study presents a promising starting point for evaluating the role of eosinophils in eliminating *T. regenti* infection as it shows that TrAg stimulates eosinophil extracellular DNA trap formation. Further studies need to be conducted to determine the origin of the traps and to test the effect of the formed traps on the parasite itself both *in vitro* and *in vivo*.

REFERENCES

Chuah, C., Jones, M.K., Burke, M.L., Mcmanus, D.P., Owen, H.C., and Gobert, G.N. (2014). Defining a pro-inflammatory neutrophil phenotype in response to schistosome eggs. Cell. Microbiol. *16*, 1666–1677.

Douda, D.N., Khan, M.A., Grasemann, H., and Palaniyar, N. (2015). SK3 channel and mitochondrial ROS mediate NADPH oxidase-independent NETosis induced by calcium influx. Proc. Natl. Acad. Sci. U. S. A. *112*, 2817–2822.

Ehrens, A., Lenz, B., Neumann, A.L., Giarrizzo, S., Reichwald, J.J., Frohberger, S.J., Stamminger, W., Buerfent, B.C., Fercoq, F., Martin, C., et al. (2021a). Microfilariae trigger eosinophil extracellular DNA traps in a dectin-1-dependent manner. Cell Rep. *34*.

Ehrens, A., Rüdiger, N., Heepmann, L., Linnemann, L., Hartmann, W., Hübner, M.P., and Breloer, M. (2021b). Eosinophils and neutrophils eliminate migrating Strongyloides ratti larvae at the site of infection in the context of extracellular DNA trap formation. Front. Immunol. *12*, 1–17.

Ehrens, A., Hoerauf, A., and Hübner, M.P. (2022). Eosinophils in filarial infections: Inducers of protection or pathology? Front. Immunol. *13*, 1–19.

Guimarães-Costa, A.B., Nascimento, M.T.C., Wardini, A.B., Pinto-Da-Silva, L.H., and Saraiva, E.M. (2012). ETosis: A microbicidal mechanism beyond cell death. J. Parasitol. Res. *2012*.

Koh, C.C., Gollob, K.J., and Dutra, W.O. (2023). Balancing the functions of DNA extracellular traps in intracellular parasite infections: implications for host defense, disease pathology and therapy. Cell Death Dis. *14*.

Liao, Y., Zhu, Z., Liu, Y., Wu, J., Li, D., Li, Z., Xu, J., Yang, R., and Wang, L. (2023). Schistosome egg-derived extracellular vesicles deliver Sja-miR-71a inhibits host macrophage and neutrophil extracellular traps via targeting Sema4D. Cell Commun. Signal. *21*, 1–13.

Macháček, T., Panská, L., Dvořáková, H., and Horák, P. (2016). Nitric oxide and cytokine production by glial cells exposed in vitro to neuropathogenic schistosome Trichobilharzia regenti. Parasit. Vectors *9*, 579.

Macháček, T., Leontovyč, R., Šmídová, B., Majer, M., Vondráček, O., Vojtěchová, I., Petrásek, T., and Horák, P. (2022). Mechanisms of the host immune response and helminth-induced pathology during Trichobilharzia regenti (Schistosomatidae) neuroinvasion in mice. PLoS Pathog. *18*, 1–34.

Mitre, E., and Klion, A.D. (2021). Eosinophils and helminth infection: protective or pathogenic? Semin. Immunopathol. *43*, 363–381.

Mukherjee, M., Lacy, P., and Ueki, S. (2018). Eosinophil extracellular traps and inflammatory pathologies-untangling the web! Front. Immunol. *9*, 1–10.

Muniz, V.S., Silva, J.C., Braga, Y.A.V., Melo, R.C.N., Ueki, S., Takeda, M., Hebisawa, A., Asano, K., Figueiredo, R.T., and Neves, J.S. (2018). Eosinophils release extracellular DNA traps in response to Aspergillus fumigatus. J. Allergy Clin. Immunol. *141*, 571-585.e7.

Muñoz-Caro, T., Rubio R, M.C., Silva, L.M.R., Magdowski, G., Gärtner, U., McNeilly, T.N., Taubert, A., and Hermosilla, C. (2015). Leucocyte-derived extracellular trap formation significantly contributes to Haemonchus contortus larval entrapment. Parasites and Vectors *8*, 1–12.

Ueki, S., Melo, R.C.N., Ghiran, I., Spencer, L.A., Dvorak, A.M., and Weller, P.F. (2013). Eosinophil extracellular DNA trap cell death mediates lytic release of free secretion-competent eosinophil granules in humans. Blood *121*, 2074–2083.

Ueki, S., Konno, Y., Takeda, M., Moritoki, Y., Hirokawa, M., Matsuwaki, Y., Honda, K., Ohta, N., Yamamoto, S., Takagi, Y., et al. (2016). Eosinophil extracellular trap cell death-derived DNA traps: Their presence in secretions and functional attributes. J. Allergy Clin. Immunol. *137*, 258–267.

Villagra-Blanco, R., Silva, L.M.R., Conejeros, I., Taubert, A., and Hermosilla, C. (2019). Pinniped- and cetacean-derived Etosis contributes to combating emerging apicomplexan parasites (Toxoplasma gondii, neospora caninum) circulating in marine environments. Biology (Basel). *8*.

Yousefi, S., Gold, J.A., Andina, N., Lee, J.J., Kelly, A.M., Kozlowski, E., Schmid, I., Straumann, A., Reichenbach, J., Gleich, G.J., et al. (2008). Catapult-like release of mitochondrial DNA by eosinophils contributes to antibacterial defense. Nat. Med. *14*, 949–953.

Yousefi, S., Simon, D., and Simon, H.U. (2012). Eosinophil extracellular DNA traps: Molecular mechanisms and potential roles in disease. Curr. Opin. Immunol. *24*, 736–739.

Fig. S1: Gating strategy

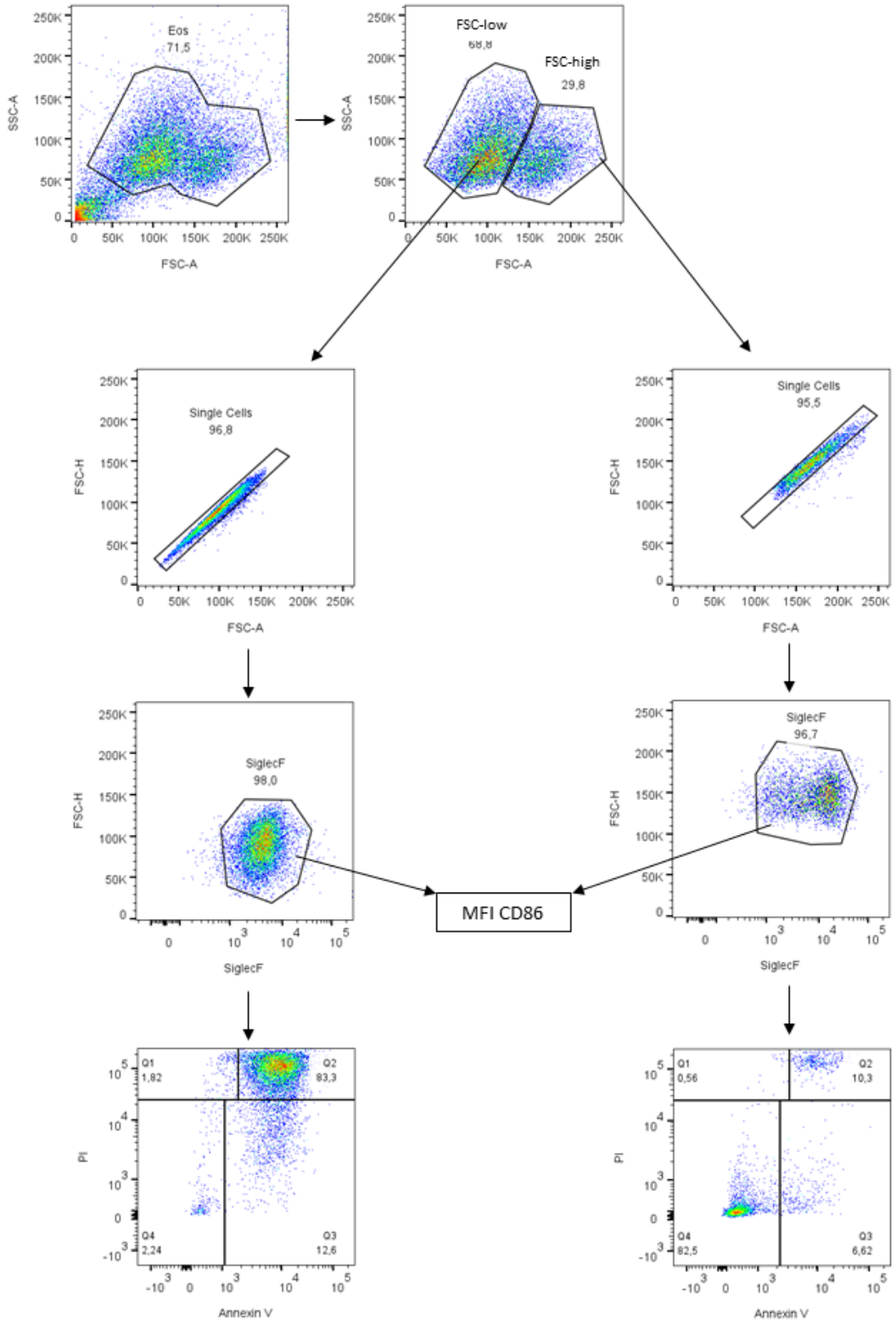

Publication #2

Šmídová, B., Majer, M., Novák, J., Revalová, A., Horák, P., and Macháček, T.

The neurotropic schistosome vs experimental autoimmune encephalomyelitis: are there any winners?

Parasitology, 2024

DOI: 10.1017/S0031182024000210

Parasitology

cambridge.org/par

The neurotropic schistosome *vs* experimental autoimmune encephalomyelitis: are there any winners?

Barbora Šmídová[1], Martin Majer[1], Jan Novák[2], Alena Revalová[1], Petr Horák[1] and Tomáš Macháček[1]

[1]Department of Parasitology, Faculty of Science, Charles University, Prague, Czechia and [2]Institute of Immunology and Microbiology, First Faculty of Medicine, Charles University and General University Hospital in Prague, Prague, Czechia

Research Article

Cite this article: Šmídová B, Majer M, Novák J, Revalová A, Horák P, Macháček T (2024). The neurotropic schistosome *vs* experimental autoimmune encephalomyelitis: are there any winners? *Parasitology* **151**, 412–420. https://doi.org/10.1017/S0031182024000210

Received: 3 January 2024
Revised: 19 February 2024
Accepted: 27 February 2024
First published online: 6 March 2024

Keywords:
demyelination; EAE; eosinophilia; experimental autoimmune encephalomyelitis; IFN-γ; neurotropic parasite; neurotropic schistosome; *Trichobilharzia regenti*

Corresponding author:
Barbora Šmídová;
Email: barbora.smid@natur.cuni.cz

Abstract

The incidences of multiple sclerosis have risen worldwide, yet neither the trigger nor efficient treatment is known. Some research is dedicated to looking for treatment by parasites, mainly by helminths. However, little is known about the effect of helminths that infect the nervous system. Therefore, we chose the neurotropic avian schistosome *Trichobilharzia regenti*, which strongly promotes M2 polarization and tissue repair in the central nervous system, and we tested its effect on the course of experimental autoimmune encephalomyelitis (EAE) in mice. Surprisingly, the symptoms of EAE tended to worsen after the infection with *T. regenti*. The infection did not stimulate tissue repair, as indicated by the similar level of demyelination. Eosinophils heavily infiltrated the infected tissue, and the microglia number increased as well. Furthermore, splenocytes from *T. regenti*-infected EAE mice produced more interferon (IFN)-γ than splenocytes from EAE mice after stimulation with myelin oligodendrocyte glycoprotein. Our research indicates that the combination of increased eosinophil numbers and production of IFN-γ tends to worsen the EAE symptoms. Moreover, the data highlight the importance of considering the direct effect of the parasite on the tissue, as the migrating parasite may further tissue damage and make tissue repair even more difficult.

Introduction

Multiple sclerosis (MS) is a lifestyle autoimmune disease of the central nervous system (CNS) with rising incidence and usual onset at the age of 30–40 years (Walton *et al.*, 2020). Neuroinflammation and neuronal damage are driven chiefly by autoreactive antibodies and cytotoxic $CD8^+$ T cells in human MS or by T helper cells (Th1 and Th17) in experimental autoimmune encephalomyelitis (EAE), the mouse model of the disease (Dendrou *et al.*, 2015; Attfield *et al.*, 2022). As the cause of MS remains to be definitely determined, the treatment is primarily symptomatic. Considering the autoimmune nature of MS, targeting the immunopathological processes seems to be a prospective way of mitigating the disease outcome (Tintore *et al.*, 2019; Hauser and Cree, 2020; Wiendl *et al.*, 2021). While searching for novel MS treatments, the importance of alternatively activated (M2) macrophages has been discovered as they may counteract neuroinflammation and promote tissue recovery (Miron *et al.*, 2013). For example, lenalidomide, one of the candidate MS drugs, directly promotes M2 polarization, which leads to reduced CNS infiltration by Th1 and Th17 and decreased tissue demyelination (Weng *et al.*, 2018). Other M2-promoting drugs also proved efficient against EAE (Che *et al.*, 2022). The beneficial effects of M2 polarization were also confirmed by the adoptive transfer of M2 macrophages (Chu *et al.*, 2021), indisputably identifying the M2 pathway as a promising treatment candidate.

To enable survival in the host and reduce tissue pathology, parasitic helminths induce anti-inflammatory (Th2/M2) or regulatory (Treg) host immune milieu (Maizels *et al.*, 2018). Hence, their interaction and possible protective effects against MS have been explored in the mouse EAE model. For example, infection of mice with *Heligmosomoides polygyrus*, *Taenia crassiceps* or *Schistosoma mansoni* mitigated the course and severity of EAE by promoting the Th2 response counteracting the neuroinflammatory processes (Dixit *et al.*, 2017; Charabati *et al.*, 2020). Moreover, Finlay *et al.* (2016) demonstrated the protective effect mediated by interleukin (IL)-5 and eosinophils in EAE mice treated with excretory–secretory products of *Fasciola hepatica*. A similar observation, supporting the role of IL-5 in alleviating EAE symptoms and inducing CNS-protective Treg cells, comes from mice infected with *Nippostrongylus brasiliensis* (Tran *et al.*, 2017). Importantly, although not strong, certain positive therapeutic effects were also reported from human MS patients infected with hookworms (Tanasescu *et al.*, 2020). These observations indicate that helminths may initiate various mechanisms that could improve the course of MS/EAE.

To explore the diversity of helminth–host interactions under the EAE conditions, we selected the neurotropic avian schistosome *Trichobilharzia regenti*. Contrary to human

schistosomes, it migrates through the CNS, being well-adapted to survive in the nervous tissue (Leontovyč *et al.*, 2016). In the incidental murine host, it causes mild, non-fatal pathology and is eliminated within 21 days post-infection (Horák *et al.*, 1999; Macháček *et al.*, 2022). In the spinal cord of experimentally infected mice, the migrating parasites induce an influx of eosinophils and trigger a short-term M1 polarization (Macháček *et al.*, 2020). The latter is, however, overwhelmed by massive upregulation of M2 markers no later than 7 days post-infection (Macháček *et al.*, 2022). Indeed, M2-canonical IL-4 and arginase are produced in the vicinity of the parasites, with arginase being the most abundant protein in the parasite-surrounding host tissue. For such M2-promoting properties, lasting at least up to 21 days post-infection (Macháček *et al.*, 2022), we chose *T. regenti* as a suitable candidate for testing its effects on the course of EAE in mice.

Materials and methods

Animal housing

Female C57BL/6JOlaHsd (ENVIGO) mice were housed in the Centre for Experimental Biomodels (Charles University, First Faculty of Medicine) under specific pathogen-free conditions according to the recommendations of the Federation of European Laboratory Animal Science Associations. Mice had unlimited access to food and water.

Experimental design

Eight-week-old mice were randomly divided into 4 groups and subjected to EAE induction and/or *T. regenti* (Tr) infection (Fig. 1). The number of mice per group was $n = 7$ for groups 'EAE Tr' and 'EAE'; $n = 3$ for groups 'Tr' and 'healthy'. The mice were weighed during the whole experiment, and the clinical score was recorded according to Hooke Laboratories (n.d.) (short version is given in Table 1). If a mouse scored '4' for 2 consecutive days, it was euthanized for ethical reasons and scored '5' for the rest of the experiment. This was necessary to perform with 2 'EAE' mice and 1 'EAE Tr' mouse in the long-term (LT) experiment with 1000 cercariae and with 2 'EAE Tr' mice and 1 EAE mouse in the persisting effect (PE) experiment. The samples were harvested on days 36, when the residuals of the parasites are still present in the spinal cord, or 49, when the spinal cord is completely cleared, to examine the LT infection or PE possibly lingering after parasite clearance, respectively.

EAE induction

EAE was induced in 'EAE' and 'EAE Tr' mice according to Novák *et al.* (2022) on day 0. Briefly, myelin oligodendrocyte glycoprotein-derived 35–55 amino acid peptide (MOG; 400 µg per mouse; APIGENEX, Prague, Czechia) was mixed with complete Freund's adjuvant containing 1 mg mL^{-1} *Mycobacterium tuberculosis* (Sigma Aldrich, St. Louis, USA) in a 1:1 ratio and injected s.c. in 2 places just above the hip joints near the spine. Pertussis toxin (500 ng per mouse; Institute of Microbiology, Czech Academy of Sciences) was injected i.p. on days 0 and 2 of the experiment.

Table 1. Scoring table of clinical symptoms of EAE

Score	Clinical observations
0.0	No obvious changes in motor function compared to non-immunized mice.
0.5	Tip of the tail is limp.
1.0	Limp tail.
1.5	Limp tail and hind leg inhibition.
2.0	Limp tail and weakness of hind legs.
2.5	Limp tail and dragging of hind legs.
3.0	Limp tail and complete paralysis of hind legs.
3.5	Limp tail and complete paralysis of hind legs. Mouse is moving around the cage, but when placed on its side, is unable to right itself.
4.0	Limp tail, complete hind leg and partial front leg paralysis.
4.5	Complete hind and partial front leg paralysis, no movement around the cage.
5.0	Death.

Adapted from Hooke Laboratories (n.d.).

Trichobilharzia regenti *infection*

With the first symptoms of EAE on day 15, 'Tr' and 'EAE Tr' mice were infected with *T. regenti* according to a protocol routinely used in our laboratory (Macháček *et al.*, 2022). Briefly, cercariae shedding from *Radix* sp. snails were collected and counted, and mice were exposed to either 400 or 1000 cercariae in 50 mL of water in the dark for 1 h.

Flow cytometry of the CNS

Mice were anaesthetized with Isoflurin (Vetpharma Animal Health, Barcelona, Spain) and transcardially perfused with phosphate-buffered saline (PBS). Cell suspension from the entire CNS was prepared according to Macháček *et al.* (2022). Briefly, the tissue was extracted, gently mechanically homogenized and filtered through a 70 µm cell strainer. Myelin was separated from the cells using 30/70% Percoll (GE Healthcare, Chicago, USA) gradient centrifugation and the cells were collected from the 30/70% interphase. They were washed with PBS, treated

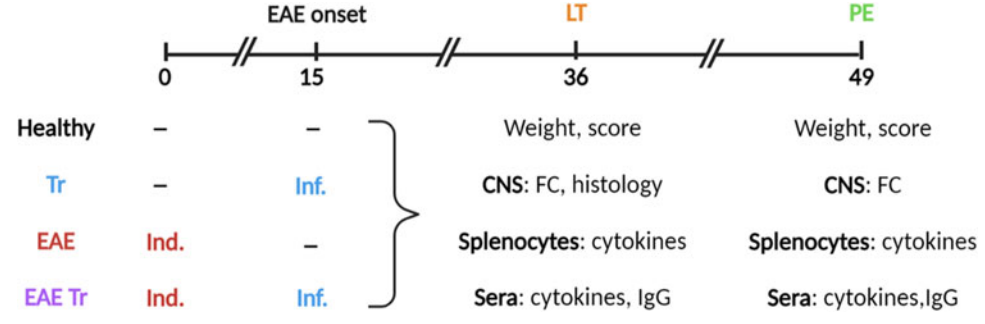

Figure 1. Experimental design. LT, long-term effect; PE, persisting effect; Tr, *Trichobilharzia regenti*; Inf., infection; Ind., induction; FC, flow cytometry.

https://doi.org/10.1017/S0031182024000210 Published online by Cambridge University Press

with anti-CD16/32 antibody for 10 min, transferred to 96-well U-bottom plates and incubated with a mixture of antibodies against surface markers (CD4, CD11b, F4/80, Ly6G, SiglecF, CD45) at 4°C in the dark for 30 min. The cells were washed with PBS, fixed with a True-Nuclear Transcription Factor Buffer Set (BioLegend, San Diego, USA) and incubated with a mixture of anti-transcription factor antibodies (T-bet, RORγT, FoxP3) for 30 min in the dark. Redundant antibodies were washed with PBS and the cells were acquired with BC CytoFLEX (Beckman Coulter, Brea, USA). Data were analysed in FlowJo (v10.8.1, BD Biosciences, San Jose, USA). Fluorescence minus one controls were used for CD11b, T-bet and RORγT. The gating strategy is presented in Fig. S1. Clones and dilutions of the used antibodies are shown in Table S1.

Histological staining

Mice were anaesthetized with Isoflurin and transcardially perfused with heparinized PBS (10 IU mL^{-1}) and ice-cold 4% formaldehyde. The spinal cord was isolated, post-fixed in 4% formaldehyde, dehydrated and embedded in paraffin. Five micrometre slices were prepared and stained with haematoxylin–eosin and Luxol fast blue as follows. First, slides were hydrated with xylene and decreasing alcohol series (100, 96, 75%) and kept for 2 h in 0.1% Luxol fast blue (Solvent Blue 38, Sigma Aldrich) in 96% ethanol with 0.5% glacial acetic acid warmed to 50°C. After cooling, slides were washed with distilled water, differentiated in 0.05% lithium carbonate in distilled water and washed again with distilled water. Then they were stained with Ehrlich's haematoxylin, washed with water, differentiated in acid alcohol (0.2% hydrochloric acid in 70% ethanol) and kept in eosin Y. Finally, slides were washed with water, hydrated in increasing alcohol series (75, 96, 100%) and xylene and mounted with Canada balsam (Sigma Aldrich). Slides were then scanned using Zeiss Axioscan Z1 and analysed in QuPath 0.4.4. Pixel classification was used to determine the dyes, while object classification was used to detect nuclei in the white matter. Both tools were trained specifically for this dataset. Slides used for analysis were then observed and captured using an Olympus BX51 with a camera Olympus DP-2 and processed in GIMP 2.10.36.

Splenocyte cultivation and cytokine measurement

Mice were anaesthetized with Isoflurin and transcardially perfused with PBS. Spleen was dissected, and splenocyte suspension was prepared according to Majer *et al.* (2020). Briefly, the spleen was homogenized, filtered through a 70 µm cell strainer and got rid of red blood cells with an ACK lysis buffer. Splenocytes were counted using the Countess Automated Cell Counter (ThermoFisher Scientific, Waltham, USA). Two million splenocytes per well (2 million cells mL^{-1}) were cultivated in RPMI 1640 supplemented as described in Majer *et al.* (2020) in 12-well plates and stimulated with either MOG (10 or 50 µg mL^{-1}), concanavalin A (1.25 µg mL^{-1}) or left untreated for 72 h. Concentrations of interferon (IFN)-γ, IL-17, IL-1β, IL-4, IL-5 and IL-10 were measured in the culture supernatants using ELISA MAX Standard kits (BioLegend) according to the manufacturer's protocol. The concentration of transforming growth factor (TGF)-β was measured in the culture media using Mouse TGF-beta 1 DuoSet ELISA (R&D Systems, Minneapolis, USA) according to the manufacturer's protocol.

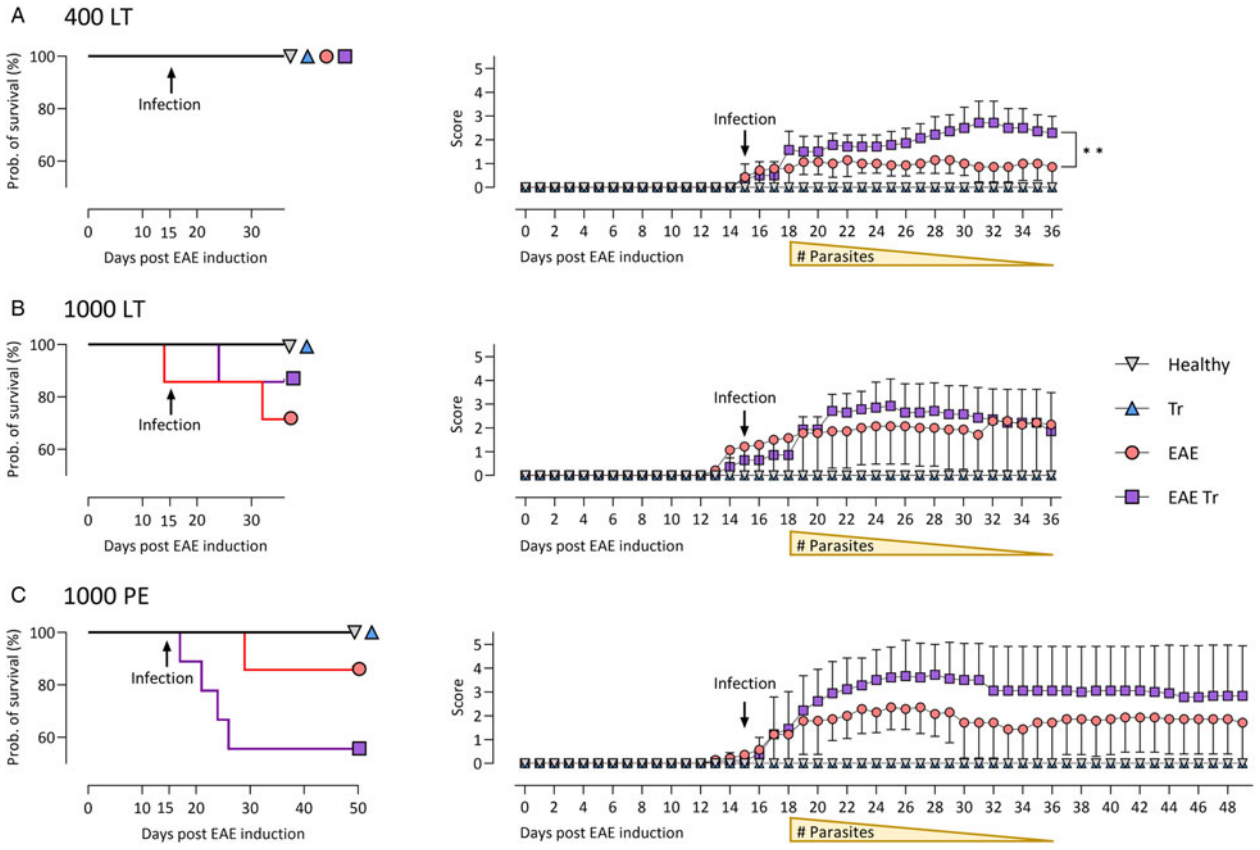

Figure 2. Probability of survival (left column) and clinical score (right column) of experimental mice during long-term infection with either 400 ('400 LT', A) or 1000 *T. regenti* cercariae ('1000 LT', B) or during persisting effect of the infection with 1000 *T. regenti* cercariae ('1000 PE', C). Yellow triangles indicate when and how many migrating parasites can be found in the spinal cord. EAE was induced on day 0 in groups EAE Tr ($n = 7$) and EAE ($n = 7$); EAE Tr and Tr ($n = 3$) mice were infected with *T. regenti* on day 15 (indicated by arrows). Healthy mice ($n = 3$) were used as a control. All mice were scored daily. If a mouse was withdrawn from the experiment for scoring '4' for 2 consecutive days, it was scored 5 for the rest of the experiment. Statistics: Kaplan–Meier survival analysis (left column), mixed effects model of 2-way ANOVA (right column) (**$P < 0.01$).

https://doi.org/10.1017/S0031182024000210 Published online by Cambridge University Press

Serum analyses

Sera were prepared from blood obtained after anaesthesia with Isoflurin (prior perfusion) and used for cytokine measurement and detection of anti-MOG immunoglobulin G (IgG).

Cytokines IL-4, IL-5, IL-10, IL-17 and IFN-γ were measured by Cytokine Bead Array (BD Biosciences) according to the manufacturer's protocol using BD LSR II (BD Biosciences) and analysed in FlowJo (v10.8.1, BD Biosciences).

Anti-MOG IgG levels were detected using an Anti-MOG (35–55) IgG ELISA Kit (Creative Diagnostics, New York City, USA) according to the manufacturer's protocol.

Statistical analysis

According to the number of factors analysed, either 1- or 2-way analysis of variance (ANOVA) followed by Dunnett's or Šidák's test was used; when the data did not have normal distribution, the Kruskal–Wallis test was used. The survival rate was calculated *via* Kaplan–Meier survival analysis. The analyses were performed in GraphPad Prism (versions 9 and 10), and P values <0.05 were considered significant. Data are shown as means with standard deviations or individual values with medians. If not stated otherwise, only significance between the EAE and EAE Tr groups are shown in the graphs.

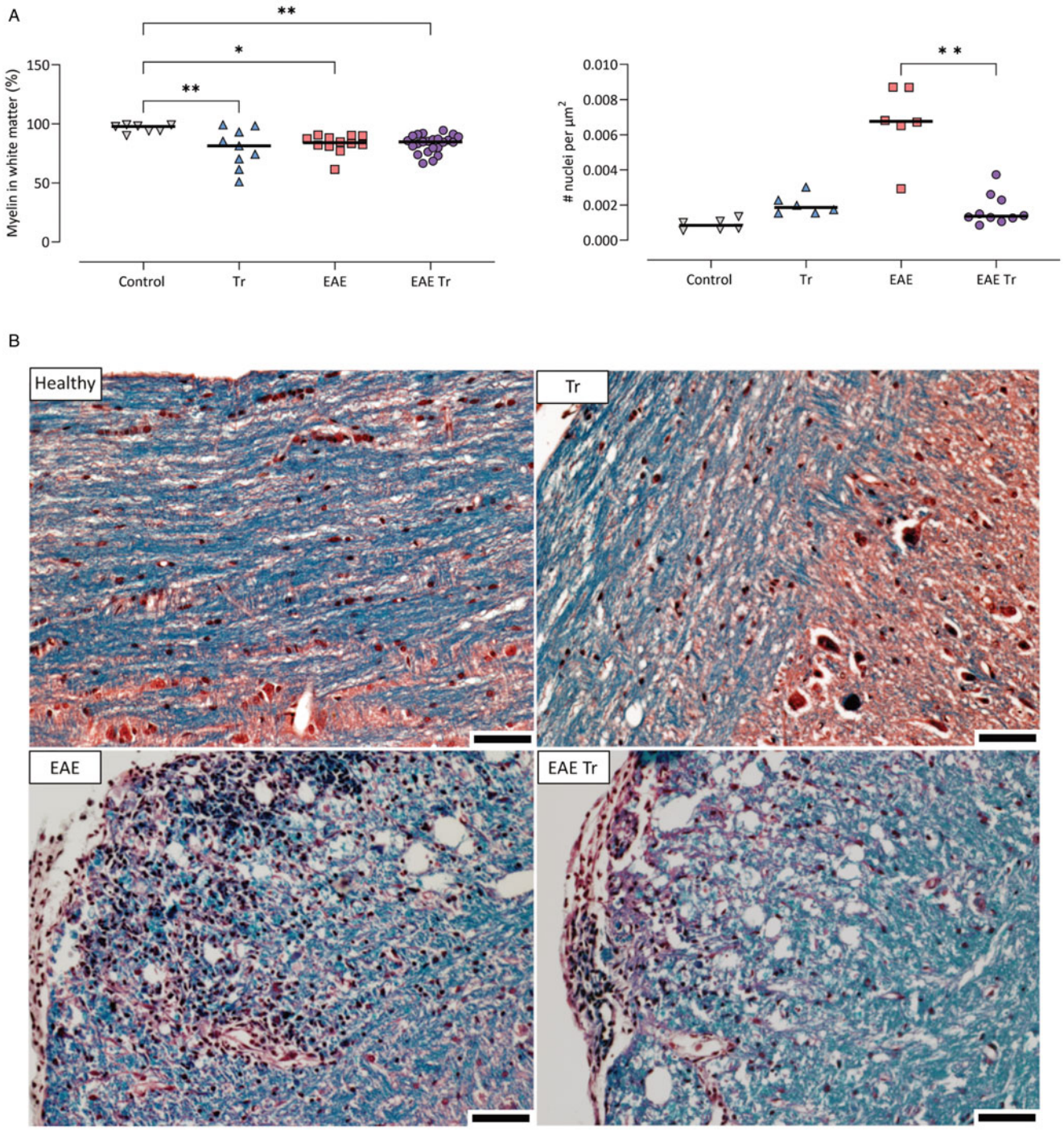

Figure 3. (A) Demyelination and number of nuclei per µm^2 of white matter in the spinal cord of 1000 LT mice. Pixel and object classification was performed on images of spinal cord sections stained with haematoxylin–eosin and Luxol fast blue. EAE was induced in EAE Tr and EAE mice, groups EAE Tr and Tr were infected with *T. regenti*. 1000 LT, long-term infection with 1000 cercariae. Statistics: 1-way ANOVA (*P < 0.05, **P < 0.01). All significant comparisons are shown for myelin coverage (left graph). (B) Representative photos of the stained sections used for the analysis. Myelin is stained blue. Scale bars: 50 µm. EAE was induced in EAE Tr and EAE mice, groups EAE Tr and Tr were infected with *T. regenti*.

https://doi.org/10.1017/S0031182024000210 Published online by Cambridge University Press

Results

Infection with T. regenti *tended to worsen the symptoms of EAE in mice*

Infecting EAE mice with *T. regenti* (EAE Tr) significantly worsened the clinical score of mice in long-term infections with 400 cercariae (400 LT) compared to EAE mice (Fig. 2A). The trend was similar when using 1000 cercariae (1000 LT) (Fig. 2B) and the effect persisted for up to 5 weeks post-infection (Fig. 2C). EAE Tr mice also tended to have a lower probability of survival than EAE mice studied for persisting effect of the infection (1000 PE). On a systemic degree, levels of anti-MOG IgG in sera were slightly elevated only in the EAE group in 1000 PE (Fig. S2). The relative weight of EAE Tr *vs* EAE mice did not change in any experiment (data not shown), and neither did the weight ratio of CNS:body nor spleen:body (Fig. S3).

Given that *T. regenti* is found mostly in the white matter up to 21 days post-infection (Macháček *et al.*, 2020, 2022), we quantified its myelination and cell infiltration in 1000 LT mice as possible factors contributing to pathology. Representative photos of the spinal cord sections are shown in Fig. 3. A similar level of demyelination was observed in Tr mice as well as in both EAE and EAE Tr mice. However, nuclei density in the white matter was significantly higher in the EAE group compared to the EAE Tr group (Fig. 3), suggesting that the cellular infiltration is stronger in the white matter of the EAE group than in the same tissue of the EAE Tr group.

Trichobilharzia regenti *infection increased microglia and eosinophil numbers in the CNS and eosinophil-related IL-5 levels in the serum of EAE Tr mice*

To further describe the infiltrating immune cells, we performed flow cytometry analysis of the CNS. In timepoints when *T. regenti* is still present in the CNS (Macháček *et al.*, 2022), i.e. in 400 LT and 1000 LT experiments, the numbers of total leucocytes and microglia, the resident immune cells, were significantly higher in EAE Tr mice (Fig. 4). However, the relative representation of microglia was decreased in both EAE and EAE Tr mice in all experiments, mainly in favour of T cells or eosinophils

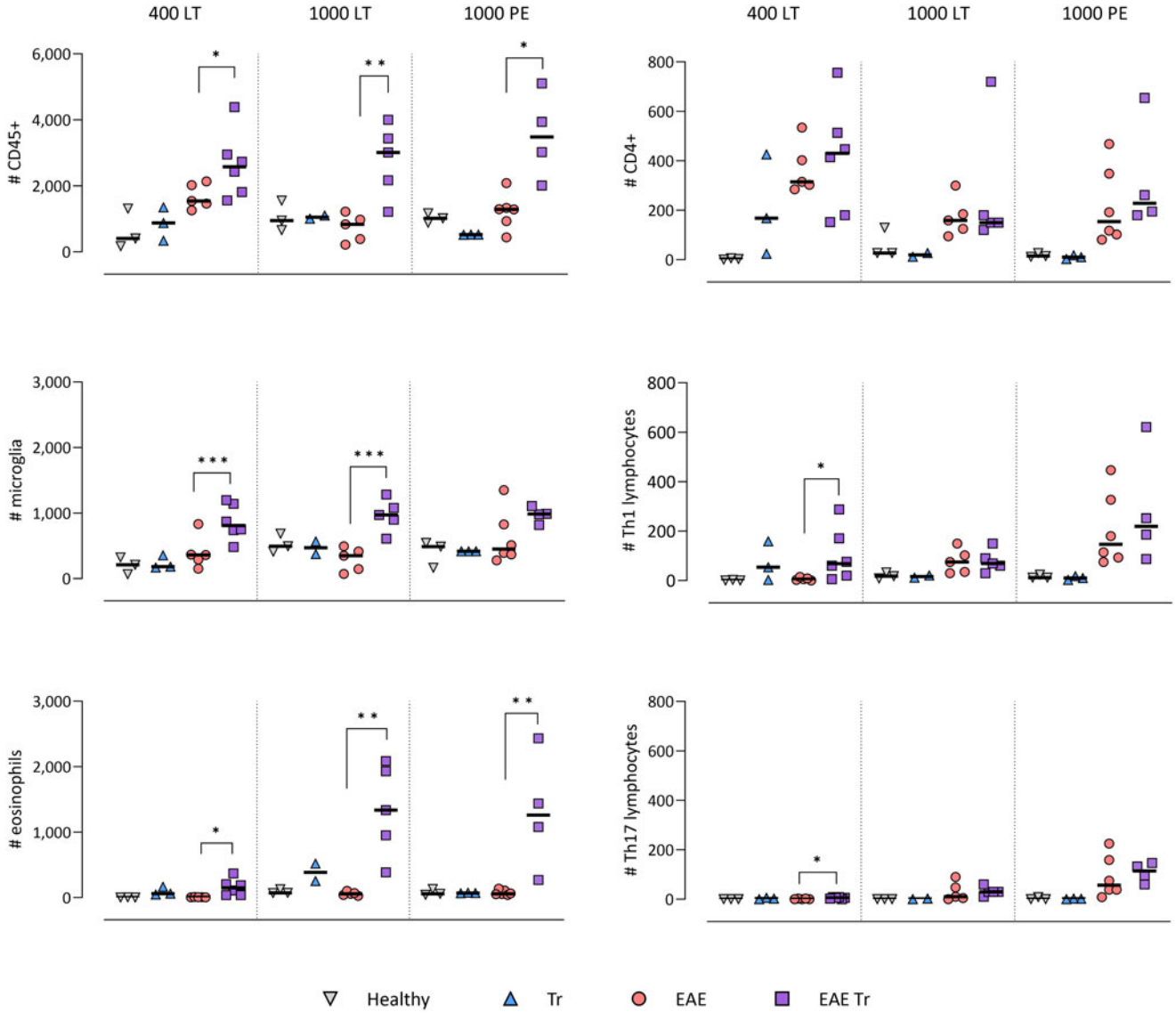

Figure 4. Flow cytometry analysis of overall number of CD45$^+$ cells in the CNS (top-left corner), further focused on myeloid cells (left column) and T-lymphocytes (right column). EAE was induced in EAE Tr and EAE mice, groups EAE Tr and Tr were infected with *T. regenti*. Microglia were described as CD45med CD11b$^+$; monocytes/macrophages as CD45$^+$ CD11b$^+$ F4/80$^+$; eosinophils as CD45$^+$ CD11b$^+$ SiglecF$^+$; CD4$^+$ as CD45$^+$ CD4$^+$; Th1 lymphocytes as CD45$^+$ CD4$^+$ Tbet$^+$ and Th17 lymphocytes as CD45$^+$ CD4$^+$ RORγT$^+$. 400 LT, long-term infection with 400 cercariae; 1000 LT, long-term infection with 1000 cercariae; 1000 PE, persisting effect of infection with 1000 cercariae. Statistics: 1-way ANOVA (*$P < 0.05$, **$P < 0.01$, ***$P < 0.001$).

https://doi.org/10.1017/S0031182024000210 Published online by Cambridge University Press

(Fig. S4). Eosinophils were the non-resident myeloid cells that most infiltrated the EAE Tr CNS compared to EAE CNS. Their numbers were rather dependent on the initial infection dose than the duration of the infection/EAE, as revealed by the comparison of 1000 LT and 1000 PE groups (Fig. 4). The eosinophil influx in EAE Tr mice was accompanied by an increase in serum IL-5, the cytokine important for eosinophil activation, during long-term infections (Fig. 5). Moreover, splenocytes obtained from EAE Tr mice produced more IL-5 after stimulation with MOG when compared with splenocytes from EAE mice (Fig. 6). Taken together, the data pointed to the importance of eosinophils infiltrating the CNS in EAE Tr mice.

CD4$^+$ cells infiltrating the CNS of EAE Tr mice were mostly Th1 and Th17

Given that T lymphocytes cause the pathology of EAE, we focused on their numbers and phenotype in the CNS, and we also monitored the systemic cytokine profile represented by MOG-stimulated splenocytes. Flow cytometry analysis of the CNS revealed a slightly higher influx of CD4$^+$ T cells into the CNS of EAE Tr mice in the 400 LT and 1000 PE groups when compared to EAE mice. Most of them were either Th1 (Tbet$^+$) or Th17 (RORγT$^+$). A significant difference in Th1 lymphocytes between EAE Tr and EAE was observed in 400 LT (Fig. 4), and at the same time, the serum levels of Th1-related cytokines, namely IFN-γ and TNF, were significantly higher in EAE Tr than in EAE (Fig. 5). Furthermore, EAE Tr splenocytes produced significantly more IFN-γ than EAE splenocytes when stimulated with MOG in all experiments (Fig. 6).

As for Th17 cells, they infiltrated the EAE Tr CNS significantly more than the EAE CNS in 400 LT, but the trend was similar in other experiments as well (Fig. 4). Serum levels of IL-17, the prominent Th17-related cytokine, were not significantly different (data not shown). However, in the 1000 PE experiment, EAE Tr splenocytes produced significantly more IL-17 than EAE splenocytes after MOG stimulation (Fig. 6).

Treg cells were also detected *via* flow cytometry of the CNS, but their numbers were similar in all groups in all experiments (data not shown). However, we detected a decrease in serum IL-10 in EAE Tr when compared to EAE in 1000 LT (Fig. 5). Moreover, TGF-β, another Treg-related cytokine, was produced less by EAE Tr splenocytes than EAE after MOG stimulation in 1000 PE (Fig. 6). Together the data suggest an important role of IFN-γ and propose slight downregulation of Treg response during the infection of EAE mice.

Discussion

As MS is a disease without an effective definitive cure, the research broadened into studying the possibilities of helminthotherapy. However, most studied helminths do not directly contact the inflamed CNS. Furthermore, in most cases the parasite is introduced before or together with EAE meaning only their prophylactic effect is tested (Dixit *et al.*, 2017). Therefore, we focused on the therapeutic effect of *T. regenti*, the neuropathogenic schistosome capable of inducing a strong M2 response and tissue regenerating process in the CNS (Macháček *et al.*, 2022). Although the data overall did not reveal a positive impact of the *T. regenti* infection on the course of the disease, we managed to uncover *T. regenti*-specific relationships between the parasite and the disease.

The general status of EAE mice (mainly the probability of survival) tended to worsen with the infection and the length of the experiment. However, statistical significance was recorded only in EAE mice infected with a lower infection dose, suggesting a dose-dependent effect. Presumably, the low number of parasites reaching the CNS induced only the early-phase inflammation

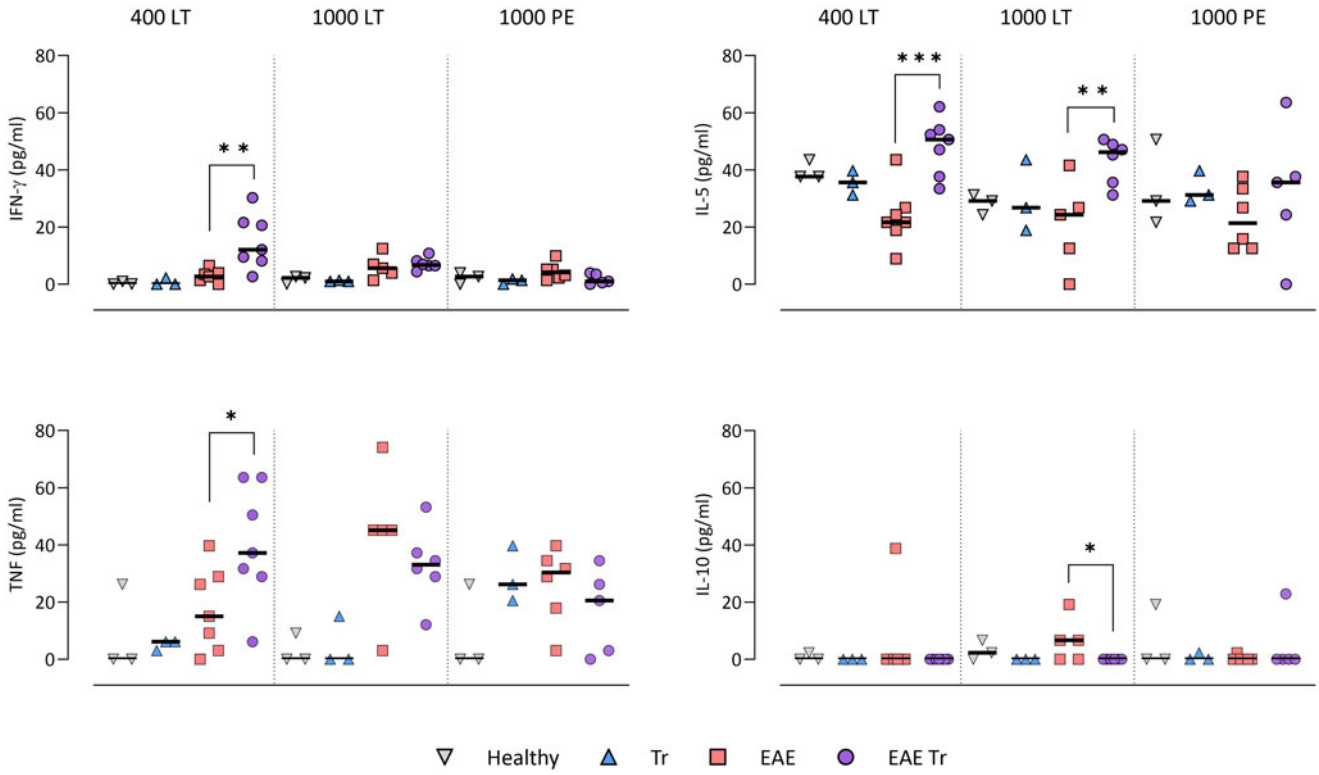

Figure. 5. Cytokines measured in sera using cytokine bead assay for flow cytometry. EAE was induced in EAE Tr and EAE mice, groups EAE Tr and Tr were infected with *T. regenti*. 400 LT, long-term infection with 400 cercariae; 1000 LT, long-term infection with 1000 cercariae; 1000 PE, persisting effect of infection with 1000 cercariae. Statistics: 1-way ANOVA (*$P < 0.05$, **$P < 0.01$, ***$P < 0.001$).

https://doi.org/10.1017/S0031182024000210 Published online by Cambridge University Press

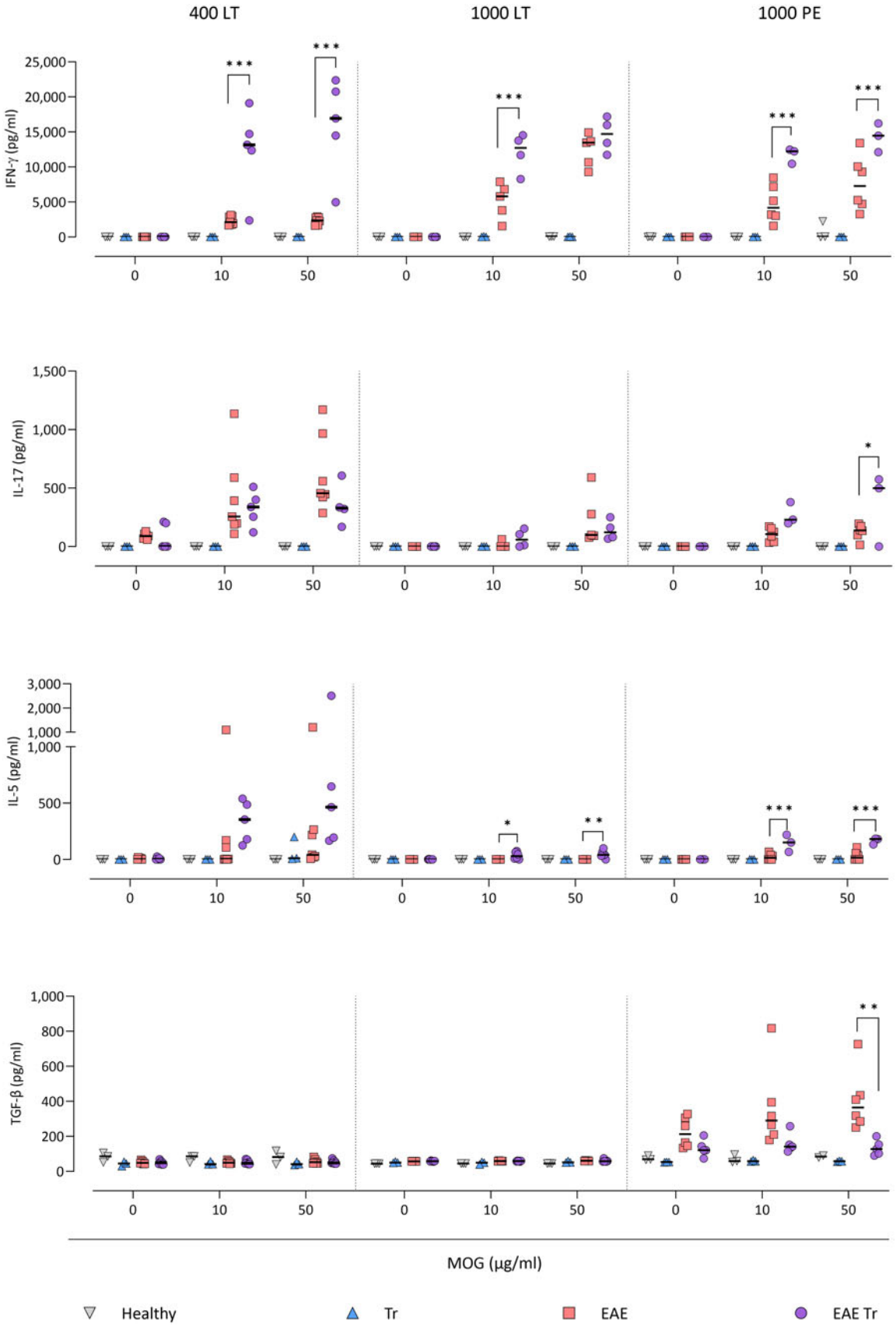

Figure 6. Cytokines measured using ELISA in splenocyte culture media after 72 h stimulation with MOG. EAE was induced in EAE Tr and EAE mice, groups EAE Tr and Tr were infected with *T. regenti*. 400 LT, long-term infection with 400 cercariae; 1000 LT, long-term infection with 1000 cercariae; 1000 PE, persisting effect of infection with 1000 cercariae. Statistics: 1-way ANOVA (*$P < 0.05$, **$P < 0.01$, ***$P < 0.001$).

(further described in Macháček *et al.*, 2020) but only a few larvae remained in the nervous tissue later in the infection when they induce M2 switch (Macháček *et al.*, 2022). On the contrary, a higher infection dose would lead to more larvae and the stimulation of the M2 polarization would be sufficient for counteracting the inflammatory processes. In general, the dose effect is known,

https://doi.org/10.1017/S0031182024000210 Published online by Cambridge University Press

e.g. for *F. hepatica* excretory–secretory products (Finlay *et al.*, 2016, Lund *et al.*, 2016), *T. crassiceps* larvae (Reyes *et al.*, 2011) and *Trichuris muris* which triggers Th1 in low-dose infections, but Th2 in high-dose infections (Hayes and Grencis, 2021).

Another explanation of the observed mild worsening of the symptoms might be provided by IFN-γ, a cytokine generally associated with inflammation, which was produced in large quantities by splenocytes incubated with MOG peptide. This cytokine supports EAE development (Arellano *et al.*, 2015) and can reduce microglial activation under the EAE conditions (Tichauer *et al.*, 2023). On the contrary, during the later symptomatic phase of EAE, IFN-γ mitigates the disease manifestations (Arellano *et al.*, 2015) by supporting TGF-β production by microglia (Tichauer *et al.*, 2023) and depriving the inflammatory response to further promote Treg function (Furlan *et al.*, 2001). Therefore, during the longer-term experiments (such as those presented here), the presence of IFN-γ could even be beneficial for the host as it could prevent chronic EAE exacerbation. Further experiments using IFN-γ-depleted mice would be necessary to test this hypothesis.

However, the nervous tissue was also infiltrated by many eosinophils which polarize to 'type 1' cells when stimulated by IFN-γ (Dolitzky *et al.*, 2021, 2022). These cells have markers similar to those of M1 macrophages, such as *Cd86*, *Cd53* and *Cd36* (Dolitzky *et al.*, 2021). Type 1 eosinophils can produce other inflammatory cytokines (Sakkal *et al.*, 2016; Dolitzky *et al.*, 2021), and their ability to repair the tissue and stimulate M2 polarization is allayed (Dolitzky *et al.*, 2021, 2022). Furthermore, eosinophils can forge even more IFN-γ (Lucarini *et al.*, 2017) and create a stimulatory loop and inflammatory milieu.

Surprisingly, when the parasite products incite the influx of eosinophils but not the rise of the IFN-γ levels, the symptoms of EAE are milder, especially in short-term settings. This effect was observed in EAE mice treated with *F. hepatica* excretory–secretory products (Finlay *et al.*, 2016). This brings up 2 questions: (1) Why do eosinophils and IFN-γ relieve the EAE symptoms separately but not together, which needs to be further addressed experimentally, and (2) why does *T. regenti*, but not *F. hepatica*, instigate IFN-γ production?

To answer the second question, we should consider the tissue damage caused by the parasite migration. For example, the nematode *Toxocara canis*, like *T. regenti*, migrates through the nervous tissue and otherwise has protective immunomodulatory effects (Maizels, 2013), but when combined with EAE, it leads to high levels of IFN-γ in the sera and significantly worse symptoms (Novák *et al.*, 2022). Indeed, there were also other similarities between these 2 neuropathogens – they both increased the amount of $CD4^+$ cells in the CNS, albeit *T. regenti*-triggered increase was not significant. However, in the case of neurotropic unicellular protists (not causing significant tissue damage), such as *Toxoplasma gondii*, the results are opposing. *Toxoplasma gondii* ameliorates the disease symptoms and decreases the levels of inflammatory cytokines (Ham *et al.*, 2021), similarly to *F. hepatica* and other non-CNS-resident parasites (Dixit *et al.*, 2017). Therefore, we might hypothesize that for experimental EAE helminthotherapy, rather remote immunomodulatory effects associated with non-neurotropic helminths would be beneficial as the neurotropic helminths further damage the nervous tissue and promote inflammation.

To summarize, the data described above lead us to the following hypothesis: when *T. regenti* enters the spinal cord in the symptomatic EAE mice, the early pro-inflammatory response to the parasite (further described in Macháček *et al.*, 2020) combines with the ongoing EAE-related neuroinflammation. This is further supported by IFN-γ and tissue-infiltrating eosinophils, and the parasite-induced immunomodulatory M2-stimulating properties are not strong enough to overcome this, especially in shorter and low-dose infections. Furthermore, our research highlights the necessity of considering the effect of the migrating parasite itself, especially in a tissue as delicate as the CNS, and supports the strategy of utilizing the immunomodulatory properties of the parasite rather on a systemic level.

Supplementary material. The supplementary material for this article can be found at https://doi.org/10.1017/S0031182024000210

Data availability statement. All data are presented within the article or Supplementary materials.

Acknowledgements. The authors thank Prof. Peter Šebo for providing the pertussis toxin, Veronika King for technical help and Vojtěch Vajs for illustrations for the graphical abstract.

Author's contribution. B. Š. and T. M. conceived and designed the study. B. Š. and M. M. performed the experiments. A. R. performed the cytokine bead assay. J. N. taught B. Š. EAE induction, performed anti-MOG IgG ELISA and critically discussed and interpreted the results. B. Š. performed statistical analyses. B. Š. drafted the manuscript. P. H. and T. M. provided financial support and comments on the final manuscript.

Financial support. This study was supported by Czech Science Foundation (18-11140S), Ministry of Education, Youth and Sports of the Czech Republic (CZ.02.1.01/0.0/0.0/16_019/ 0000759: Centre for Research of Pathogenicity and Virulence of Parasites), Charles University Grant Agency (580120), Charles University institutional funding (PROGRES Q43 and Cooperatio Biology, UNCE/SCI/012-204072/2018, UNCE24/SCI/011, SVV 260432/2018 and SVV 260563/2020).

Competing interests. None.

Ethical standards. The experimental procedures including animals were reviewed by the Animal Welfare Committee of Charles University, Faculty of Science and approved by the Czech Ministry of Education, Youth and Sports (ref. no. MSMT-31963/2020-5). All experiments were performed by authorized persons in accordance with the European Directive 2010/63/EU and Czech Laws for Biomedical Research (246/1992 and 359/2012).

References

Arellano G, Ottum PA, Reyes LI, Burgos PI and Naves R (2015) Stage-specific role of interferon-γ in experimental autoimmune encephalomyelitis and multiple sclerosis. *Frontiers in Immunology* **6**, 1–9.

Attfield KE, Jensen LT, Kaufmann M, Friese MA and Fugger L (2022) The immunology of multiple sclerosis. *Nature Reviews Immunology* **22**, 734–750.

Charabati M, Donkers SJ, Kirkland MC and Osborne LC (2020) A critical analysis of helminth immunotherapy in multiple sclerosis. *Multiple Sclerosis Journal* **26**, 1448–1458.

Che J, Li D, Hong W, Wang L, Guo Y, Wu M, Lu J, Tong L, Weng Q, Wang J and Dong X (2022) Discovery of new macrophage M2 polarization modulators as multiple sclerosis treatment agents that enable the inflammation microenvironment remodeling. *European Journal of Medicinal Chemistry* **243**, 1–19.

Chu F, Shi M, Lang Y, Chao Z, Jin T, Cui L and Zhu J (2021) Adoptive transfer of immunomodulatory M2 macrophages suppresses experimental autoimmune encephalomyelitis in C57BL/6 mice *via* blockading NF-κB pathway. *Clinical and Experimental Immunology* **204**, 199–211.

Dendrou CA, Fugger L and Friese MA (2015) Immunopathology of multiple sclerosis. *Nature Reviews Immunology* **15**, 545–558.

Dixit A, Tanaka A, Greer JM and Donnelly S (2017) Novel therapeutics for multiple sclerosis designed by parasitic worms. *International Journal of Molecular Sciences* **18**, 1–17.

Dolitzky A, Shapira G, Grisaru-Tal S, Hazut I, Avlas S, Gordon Y, Itan M, Shomron N and Munitz A (2021) Transcriptional profiling of mouse eosinophils identifies distinct gene signatures following cellular activation. *Frontiers in Immunology* **12**, 1–15.

Dolitzky A, Hazut I, Avlas S, Grisaru-Tal S, Itan M, Zaffran I, Levi-Schaffer F, Gerlic M and Munitz A (2022) Differential regulation of type 1 and type

2 mouse eosinophil activation by apoptotic cells. *Frontiers in Immunology* **13**, 1–16.

Finlay CM, Stefanska AM, Walsh KP, Kelly PJ, Boon L, Lavelle EC, Walsh PT and Mills KHG (2016) Helminth products protect against autoimmunity *via* innate type 2 cytokines IL-5 and IL-33, which promote eosinophilia. *The Journal of Immunology* **196**, 703–714.

Furlan R, Brambilla E, Ruffini F, Poliani PL, Bergami A, Marconi PC, Franciotta DM, Penna G, Comi G, Adorini L and Martino G (2001) Intrathecal delivery of IFN-γ protects C57BL/6 mice from chronic-progressive experimental autoimmune encephalomyelitis by increasing apoptosis of central nervous system-infiltrating lymphocytes. *Journal of Immunology* **167**, 1821–1829.

Ham DW, Kim SG, Seo SH, Shin JH, Lee SH and Shin EH (2021) Chronic *Toxoplasma gondii* infection alleviates experimental autoimmune encephalomyelitis by the immune regulation inducing reduction in IL-17A/Th17 *via* upregulation of SOCS3. *Neurotherapeutics: The Journal of the American Society for Experimental NeuroTherapeutics* **18**, 430–447.

Hauser SL and Cree BAC (2020) Treatment of multiple sclerosis: a review. *The American Journal of Medicine* **133**, 1380–1390.e2.

Hayes KS and Grencis RK (2021) *Trichuris muris* and comorbidities – within a mouse model context. *Parasitology* **148**, 1774–1782.

Hooke Laboratories (n.d.) Mouse EAE Scoring. Retrieved from Hooke Laboratories website: https://hookelabs.com/services/cro/eae/MouseEAEscoring.html (accessed 2 February 2024).

Horák P, Dvořák J, Kolářová L and Trefil L (1999) *Trichobilharzia regenti*, a pathogen of the avian and mammalian central nervous systems. *Parasitology* **119**, 577–581.

Leontovyč R, Young ND, Korhonen PK, Hall RS, Tan P, Mikeš L, Kašný M, Horák P and Gasser RB (2016) Comparative transcriptomic exploration reveals unique molecular adaptations of neuropathogenic *Trichobilharzia* to invade and parasitize its avian definitive host. *PLoS Neglected Tropical Diseases* **10**, 1–24.

Lucarini V, Zicchedda G, Macchia I, La Sorsa V, Peschiaroli F, Buccione C, Sistigu A, Sanchez M, Andreone S, D'Urso MT, Spada M, Macchia D, Afferni C, Mattei F and Schiavoni G (2017) IL-33 restricts tumor growth and inhibits pulmonary metastasis in melanoma-bearing mice through eosinophils. *OncoImmunology* **6**, e1317420.

Lund ME, Greer J, Dixit A, Alvarado R, McCauley-Winter P, To J, Tanaka A, Hutchinson AT, Robinson MW, Simpson AM, O'Brien BA, Dalton JP and Donnelly S (2016) A parasite-derived 68-mer peptide ameliorates autoimmune disease in murine models of Type 1 diabetes and multiple sclerosis. *Scientific Reports* **6**, 1–11.

Macháček T, Šmídová B, Pankrác J, Majer M, Bulantová J and Horák P (2020) Nitric oxide debilitates the neuropathogenic schistosome *Trichobilharzia regenti* in mice, partly by inhibiting its vital peptidases. *Parasites & Vectors* **13**, 1–14.

Macháček T, Leontovyč R, Šmídová B, Majer M, Vondráček O, Vojtěchová I, Petrásek T and Horák P (2022) Mechanisms of the host immune response and helminth-induced pathology during *Trichobilharzia regenti* (Schistosomatidae) neuroinvasion in mice. *PLoS Pathogens* **18**, 1–34.

Maizels RM (2013) *Toxocara canis*: molecular basis of immune recognition and evasion. *Veterinary Parasitology* **193**, 365–374.

Maizels RM, Smits HH and McSorley HJ (2018) Modulation of host immunity by helminths: the expanding repertoire of parasite effector molecules. *Immunity* **49**, 801–818.

Majer M, Macháček T, Súkeníková L, Hrdý J and Horák P (2020) The peripheral immune response of mice infected with a neuropathogenic schistosome. *Parasite Immunology* **42**, 1–11.

Miron VE, Boyd A, Zhao J-W, Yuen TJ, Ruckh JM, Shadrach JL, van Wijngaarden P, Wagers AJ, Williams A and Franklin RJM and ffrench-Constant C. (2013) M2 microglia and macrophages drive oligodendrocyte differentiation during CNS remyelination. *Nature Neuroscience* **16**, 1211–1218.

Novák J, Macháček T, Majer M, Kostelanská M, Skulinová K, Černý V, Kolářová L, Hrdý J and Horák P (2022) *Toxocara canis* infection worsens the course of experimental autoimmune encephalomyelitis in mice. *Parasitology* **149**, 1720–1728.

Reyes J, Espinoza-Jiménez A, González M, Verdin L and Terrazas LI (2011) *Taenia crassiceps* infection abrogates experimental autoimmune encephalomyelitis. *Cellular Immunology* **267**, 77–87.

Sakkal S, Miller S, Apostolopoulos V and Nurgali K (2016) Eosinophils in cancer: favourable or unfavourable? *Current Medicinal Chemistry* **23**, 650–666.

Tanasescu R, Tench CR, Constantinescu CS, Telford G, Singh S, Frakich N, Onion D, Auer DP, Gran B, Evangelou N, Falah Y, Ranshaw C, Cantacessi C, Jenkins TP and Pritchard DI (2020) Hookworm treatment for relapsing multiple sclerosis: a randomized double-blinded placebo-controlled trial. *JAMA Neurology* **77**, 1089–1098.

Tichauer JE, Arellano G, Acuña E, González LF, Kannaiyan NR, Murgas P, Panadero-Medianero C, Ibañez-Vega J, Burgos PI, Loda E, Miller SD, Rossner MJ, Gebicke-Haerter PJ and Naves R (2023) Interferon-gamma ameliorates experimental autoimmune encephalomyelitis by inducing homeostatic adaptation of microglia. *Frontiers in Immunology* **14**, 1–22.

Tintore M, Vidal-Jordana A and Sastre-Garriga J (2019) Treatment of multiple sclerosis – success from bench to bedside. *Nature Reviews Neurology* **15**, 53–58.

Tran GT, Wilcox PL, Dent LA, Robinson CM, Carter N, Verma ND, Hall BM and Hodgkinson SJ (2017) Interleukin-5 mediates parasite-induced protection against experimental autoimmune encephalomyelitis: association with induction of antigen-specific $CD4^{+}CD25^{+}$ T regulatory cells. *Frontiers in Immunology* **8**, 1–13.

Walton C, King R, Rechtman L, Kaye W, Leray E, Marrie RA, Robertson N, La Rocca N, Uitdehaag B, Van der Mei I, Wallin M, Helme A, Angood Napier C, Rijke N and Baneke P (2020) Rising prevalence of multiple sclerosis worldwide: insights from the Atlas of MS, third edition. *Multiple Sclerosis Journal* **26**, 1816–1821.

Weng Q, Wang J, Wang J, Wang J, Sattar F, Zhang Z, Zheng J, Xu Z, Zhao M, Liu X, Yang L, Hao G, Fang L, Lu QR, Yang B and He Q (2018) Lenalidomide regulates CNS autoimmunity by promoting M2 macrophages polarization. *Cell Death & Disease* **9**, 1–13.

Wiendl H, Gold R, Berger T, Derfuss T, Linker R, Mäurer M, Aktas O, Baum K, Berghoff M, Bittner S, Chan A, Czaplinski A, Deisenhammer F, Di Pauli F, Du Pasquier R, Enzinger C, Fertl E, Gass A, Gehring K, Gobbi C, Goebels N, Guger M, Haghikia A, Hartung HP, Heidenreich F, Hoffmann O, Kallmann B, Kleinschnitz C, Klotz L, Leussink VI, Leutmezer F, Limmroth V, Lünemann JD, Lutterotti A, Meuth SG, Meyding-Lamadé U, Platten M, Rieckmann P, Schmidt S, Tumani H, Weber F, Weber MS, Zettl UK, Ziemssen T and Zipp F (2021) Multiple Sclerosis Therapy Consensus Group (MSTCG): position statement on disease-modifying therapies for multiple sclerosis (white paper). *Therapeutic Advances in Neurological Disorders* **14**, 1–39.

https://doi.org/10.1017/S0031182024000210 Published online by Cambridge University Press

4. Discussion

Although *T. regenti* is known and studied for over 30 years, the mechanism of parasite clearance in the spinal cord of mice has not been fully unraveled yet despite the parasite being a good candidate for parasite neuropathology model. In his dissertation thesis, Majer (2023) presented the findings mainly on lymphoid cells, almost omitting the myeloid cells. Therefore, this thesis is aimed at describing the role of selected myeloid cells in the elimination of *T. regenti* schistosomula and tissue repair mechanisms afterwards. It even takes the topic one step further – it explores the effect of the *T. regenti* stimulated cells on the course of multiple sclerosis, an inflammatory disease of the nervous tissue. The results are presented in 2 publications and 1 manuscript, me being the first author of the manuscript and one publication. This chapter brings the results together and concludes the findings.

Eosinophils, the parasite killers

The description of the immune response to *T. regenti* in the spinal cord of mice has so far been scarce and sometimes contradictory (see Introduction). Yet, they have one thing in common – all studies (Kolářová et al., 2001; Kouřilová et al., 2004; Lichtenbergová et al., 2011) describing the composition of the immune cell infiltrate in the spinal cord speak of eosinophils. In these studies, eosinophils were histologically observed between 9 and 14 dpi. In this respect, our complex study (Macháček et al., 2022 = Publication #1) not only quantitatively confirms this data but points to a much bigger importance of these cells. Following the example of the previous studies, we have performed histological staining of spinal cord sections containing the migrating parasite. We were able to further describe the process of eosinophil infiltration of the infected spinal cord. At 7 dpi, the eosinophils were slowly getting to the tissue. Already at 14 dpi, the cells were reaching and encapsulating schistosomula. The encapsulated schistosomula were damaged and as the infection went on, at 21 dpi only the remnants of the parasite were found and the immune cell infiltrate was already fading, being gone by 28 dpi.

To characterize the immune response in all segments of the CNS more specifically, we performed flow cytometry analysis of the tissue. The results were in accordance with histological pictures but provided further insight. They showed that the eosinophils are not only around the parasite but the whole CNS is heavily infiltrated by eosinophils. Comparing the ratio of eosinophils to other immune cells revealed that after the infection, eosinophils can form more than 50% of the overall immune cell population in the CNS (Macháček et al., 2022).

The importance of eosinophils in defending the host against a helminthic infection has been shown over and over again. Sometimes the eosinophils have a necessary supporting role in parasite clearance (Gazzinelli-Guimaraes et al., 2019; Masure et al., 2013; O'Connell et al., 2011; Svensson et al., 2011),

in many nematode infection the eosinophils themselves are the killers (Cadman et al., 2014; Ehrens et al., 2021b, 2021a; Frohberger et al., 2019; Muñoz-Caro et al., 2015; Yasuda et al., 2012).

Eosinophils are mostly known for releasing granules containing various proteins, cytokines and chemokines. In context of helminthoses, it is important to note that the granule contents can damage the parasite, induce M2 polarization in macrophages, smooth muscle contraction or mucus production all of which are a useful host defense (Inclan-Rico and Siracusa, 2018). Granule release occurs in three ways – piecemeal degranulation, which is usually connected with cytokine release; exocytosis and eosinophil extracellular trap formation (EETosis), where protein components are more important (Fettrelet et al., 2021; Inclan-Rico and Siracusa, 2018). Usually, when eosinophil importance is established for fighting helminths, the specific way of defense is unknown.

However, for *H. contortus*, *L. sigmodontis*, *D. immitis* and *S. ratti* it was proven that the EETosis is the effector mechanism (Ehrens et al., 2021b, 2021a; Muñoz-Caro et al., 2015). Yousefi et al. (2008) have observed the protein connected to eosinophil trap formation around *Schistosoma* spp. as well but it has not been further studied. The flukes are generally ommited in the research of EETosis even though two major model flukes, *Schistosoma* spp. and *F. hepatica*, attract eosinophils at large and can be damaged by them (Escamilla et al., 2016; Frigerio et al., 2020; Malta et al., 2022; Moqbel et al., 1983; de Oliveira et al., 2022). Therefore, we decided to test whether the EETosis could be the eosinophil effector pathway of defense against *T. regenti* schistosomula, a fluke quickly entrapped by a large number of eosinophils (Macháček et al., 2022).

In *in vitro* settings, the bone marrow-derived eosinophils produced extracellular traps upon stimulation with *T. regenti* schistosomula homogenate (TrAg) (Šmídová et al., unpublished = Manuscript #1) suggesting the traps could indeed capture and damage the parasite in the CNS. Unfortunately, to confirm this and compare the results with the published data, we would need experiments with live schistosomula followed by *in vivo* experiments.

Furthermore, stimulating eosinophils with TrAg triggered their apoptosis. TrAg-induced apoptosis was already described in fibroblasts and neurons (Parohová, 2020) but it has not been described why it happened. For eosinophil apoptosis, two explanations are possible. Either it is the result of a nuclear DNA trap formation as was described in *L. sigmodontis* (Ehrens et al., 2021a) or it is an active immune evasion mechanism of *T. regenti* similarly to *F. hepatica* (Escamilla et al., 2016). As our preliminary data point to a mitochondrial, but not nuclear, DNA trap formation and apoptosis of antigen presenting cells and T lymphocytes was described for closely related *S. mansoni* (Chen et al., 2002; Cook et al., 2011; Prendergast et al., 2015), apoptosis as a *T. regenti* immune evasion is more plausible. After all, neuron apoptosis, which might be induced by *T. regenti* (Macháček et al., 2022), can diminish the immune response as well as neurons are an important player in innate immunity induction (Deng et

al., 2024; Saraiva-Santos et al., 2024). Nevertheless, more experiments studying *T. regenti*-induced eosinophil apoptosis are necessary to decide the reason for it.

Taken together, we have shown that eosinophils are the main cells infiltrating the CNS after *T. regenti* infection, they form the largest part of the inflammatory loci around the schistosomula and that their appearance in the vicinity of the migrating schistosomula correlate with parasite damage (Macháček et al., 2022 = Publication #1). Therefore, eosinophils likely take on the protective role which was previously assigned to microglia (Lichtenbergová et al., 2011). Next, we took the first steps in exploring the possibility of eosinophil extracellular traps being responsible for parasite elimination by proving TrAg stimulates trap formation in bone marrow-derived eosinophils (Šmídová et al., 2024, unpublished = Manuscript #1). Although the trap part still leaves a lot to explore, it provides a promising preliminary data pointing to a possible *T. regenti*-clearing mechanism.

Trichobilharzia regenti as a treatment for multiple sclerosis

Multiple sclerosis, an inflammatory disease of the CNS with rising incidence worldwide, greatly worsens the quality of life of patients with this diagnosis (WHO). Although there are treatment regimes available, they are not suitable for all patients and influence the immune system as a whole allowing a variety of side effects (Miyazaki and Niino, 2022). Therefore, the immunology of the disease is heavily studied using experimental immune encephalomyelitis (EAE), a laboratory model of multiple sclerosis (Robinson et al., 2014).

According to recent studies, M2-polarized macrophages are very potent in diminishing the neuroinflammation and symptoms of EAE (Che et al., 2022; Chu et al., 2021; Mazzon et al., 2016; Sun et al., 2023). There are already several compounds inducing M2 polarization tested for EAE treatment with promising results (Che et al., 2022; Wang et al., 2022; Weng et al., 2018). The improvement is likely due to two effects of M2 macrophages: production of Th2-related cytokines and their tissue remodeling capacities (Shapouri-Moghaddam et al., 2018). M2 macrophages/microglia produce two molecules that are very important for regenerating the nervous tissue. Arg-1, a molecule associated with M2 response the most, induces axon regeneration (Zhang et al., 2020), while Ym1 supports oligodendrogenesis resulting in the remyelination of the neurons (Starossom et al., 2019). M2-driven oligodendrogenesis is even provenly the mechanism behind the symptom relief in EAE (Miron et al., 2013).

In our study presented here as Publication #1, we have shown that *Trichobilharzia regenti* induces a strong M2 response in the CNS of mice from 7 dpi onwards. This was first observed on a transcriptomic level where we detected an upregulation in genes like *Arg-1*, *Chil3l3*, *Il-4* or *Tgfb*. The expression of *Arg-1* and *Chil3l3*, the tissue repairing molecules, peaked at 14 dpi when most of the schistosomula

are damaged or dead (Kouřilová et al., 2004b; Lichtenbergová et al., 2011) and the regeneration processes can start (Macháček et al., 2022).

The production of Arg-1 and IL-4 was also confirmed immunohistochemically directly in the infected tissue. Both molecules were detected in close vicinity of the parasite and collocalized with microglia/macrophage signal. Eventually, all proteins were detected where there once was a schistosomulum. Moreover, according to proteomics, Arg-1 was the most abundant protein in the tissue surrounding the *T. regenti* schistosomulum. Taken together, these data suggest that *T. regenti* migrating through the spinal cord supports the M2 polarization and associated tissue regeneration (Macháček et al., 2022).

Although *T. regenti* is rarely found in other CNS parts than the spinal cord (see Introduction), the flow cytometry analysis of the CNS revealed that the immune cell infiltration is similar in all of the segments (Macháček et al., 2022) suggesting the tissue-repairing molecules are spread through the whole CNS as well. Taken together, the facts that *T. regenti* eagerly migrates through the CNS but does not cause significant damage, quite the opposite, and promotes M2 response efficient in relieving EAE symptoms and repairing the damage caused by neuroinflammation, made T. regenti a promising candidate for improving the symptoms of EAE mice via immunomodulation.

Usually, when testing the effect of helminths on the course of EAE, the infection occurs before or simultaneously with EAE induction (see Introduction). However, MS is rarely diagnosed before the symptom onset. Therefore, we infected mice with *T. regenti* on the first day of EAE symptoms to better simulate patient conditions. Furthermore, to the best of our knowledge, we were only the second team (the first being Novák et al., 2022) testing the immunomodulatory potential of a neurotropic helminth which can influence the immune response directly at the site of the disease (Šmídová et al., 2024 = Publication #2).

Contrary to our hypothesis, *T. regenti* did not decrease the symptom score in EAE mice. Infection with lower dose of 400 cercariae even significantly worsened the score (Šmídová et al., 2024). Similar effect, only statistically significant in all settings, was also observed in experiments testing the effect of *T. canis* on the course of EAE (Novák et al., 2022) but never after the infection with any other tested helminth residing in the organs of the peritoneum (Donskow-Łysoniewska et al., 2012; Finlay et al., 2016; La Flamme et al., 2003; Wilson et al., 2010). Further experiments are necessary to establish whether the negative effect is caused only by *T. canis* and *T. regenti* or if the infection with neurotropic helminths is unsuitable for EAE treatment in general.

Nevertheless, tissue analyses provided a valuable insight into the underlying mechanisms. Flow cytometry analysis of the CNS revealed a significant influx of eosinophil and multiplication of microglia

after the *T. regenti* infection of EAE mice. Eosinophilia correlated with IL-5 levels in the sera and in the culture media of splenocytes stimulated with MOG, the EAE-causing antigen (Šmídová et al., 2024). This was comparable with the effect of *F. hepatica* infection on the course of EAE where, contrary to our results, it correlated with milder symptoms after the infection (Finlay et al., 2016).

Similarly, we observed an increase in IFN-γ levels in the splenocyte cultures in EAE mice infected with *T. regenti* (Šmídová et al., 2024) where *F. hepatica* did not have such effect (Finlay et al., 2016. IFN-γ is a hallmark cytokine of M1 response and in context of eosinophils, it can cause a stimulatory loop resulting in eosinophils producing IFN-γ (Lucarini et al., 2017) and other pro-inflammatory cytokines (Dolitzky et al., 2022; Sakkal et al., 2016). Furthermore, due to the high IFN-γ levels but almost no difference in M2 cytokines between only EAE mice and EAE mice infected with *T. regenti*, the high numbers of microglia were most likely M1-polarized. These then in turn cannot produce neuroregenerative moleculers Arg-1 and Chil3l3. Lack of these molecules was also supported by demyelination score which showed no differences between EAE mice and EAE-*T. regenti* mice. Taken together, the results suggest that the immunomodulatory properties of *T. regenti* were not strong enough to overcome the EAE-related inflammation but accidentally supported the inflammation by attracting eosinophils and increasing the levels of IFN-γ.

To summarize, we have shown a strong M2 response to *T. regenti* migrating through the spinal cord from 7 dpi onward. The highlight of this was Arg-1 which was the most differentially expressed gene from those M2 related while being the most abundant in the proteomic analysis of the tissue surrounding the schistosomulum. Immunohistochemistry then provided collocalization of Arg-1 with microglia/macrophages and their invasion of the space occupied by the parasite pointing to a possible neuroregenerative role of M2 microglia/macrophages (Macháček et al., 2022 = Publication #1). This hypothesis was then put to test in the setting of a chronic neuroinflammatory disease in mice and was unfortunately disproven. Nevertheless, the project testing the effect of *T. regenti* infection on the course of EAE still provided an important insight into the immune response to the interwined disease and helminth infection (Šmídová et al., 2024 = Publication #2).

5. Summary

This thesis uncovers the role of myeloid cells in the spinal cord phase of *T. regenti* infection in mice while adding more evidence to the importance of eosinophils during neurohelminthoses, in this case to fight the migrating schistosomula. It also broadens the spectrum of parasites inducing EETosis and suggests it as a mechanism leading to *T. regenti* clearance from the CNS of mice. Furthermore, it proves that M2-polarized microglia/macrophages have crucial role in repairing a damaged nervous tissue. Finally, the thesis suggests a neurodamaging interplay of IFN-γ and eosinophils, and a possible dual role of eosinophils in the CNS depending on the cytokine milieu.

Specifically, the most important findings of this thesis are:

- Microglia/macrophages in the spinal cord of mice infected with *T. regenti* are M2 polarized, therefore the former hypothesis of their involvement in parasite clearance is invalid. Instead, they seem to play a big part in the tissue regeneration process by producing molecules like arginase 1 or chitinase 3-like protein which induce neuron regeneration and oligodendrogenesis, respectively.
- Eosinophils form the biggest part of the immune cell infiltrate in the CNS of mice infected with *T. regenti*. Their numbers peak at 14 days post infection when the damaged schistosomula are usually observed suggesting their involvement in the parasite clearance.
- Eosinophils respond to *T. regenti* schistosomula homogenate by forming extracellular traps which are provenly efficient in damaging various nematodes. However, whether this mechanism is effective against *T. regenti* as well, remains to be tested.
- *T. regenti* schistosomula homogenate also induce eosinophil apoptosis which could be their form of immune evasion. Unfortunately, this hypothesis also remains to be examined.
- Mouse infection with *T. regenti* does not improve the symptoms of experimental autoimmune encephalomyelitis, the laboratory model of multiple sclerosis. However, the results suggest an important interplay between eosinophils and IFN-γ and point to the importance of considering the tissue damage caused by the migrating parasite when looking for a parasite capable of reversing the chronic inflammatory diseases.

References

Abou-El-Naga, I.F., and Mogahed, N.M.F.H. (2023). Potential roles of *Toxocara canis* larval excretory secretory molecules in immunomodulation and immune evasion. Acta Trop. *238*, 106784.

Al-Jubury, A., Duan, Y., Kania, P.W., Tracz, E.S., Bygum, A., Jørgensen, L.V.G., Horák, P., and Buchmann, K. (2021). Avian schistosome species in Danish freshwater lakes: relation to biotic and abiotic factors. J. Helminthol. *95*.

Alicata, J.E. (1991). The discovery of *Angiostrongylus cantonensis* as a cause of human eosinophilic meningitis. Parasitol. Today *7*, 151–153.

Alonso-Trujillo, J., Rivera-Montoya, I., Rodríguez-Sosa, M., and Terrazas, L.I. (2007). Nitric oxide contributes to host resistance against experimental *Taenia crassiceps* cysticercosis. Parasitol. Res. *100*, 1341–1350.

Annibali, V., Mechelli, R., Romano, S., Buscarinu, M.C., Fornasiero, A., Umeton, R., Ricigliano, V.A.G., Orzi, F., Coccia, E.M., Salvetti, M., et al. (2015). IFN-β and multiple sclerosis: From etiology to therapy and back. Cytokine Growth Factor Rev. *26*, 221–228.

Arai, T., and Lopes, F. (2022). Potential of human helminth therapy for resolution of inflammatory bowel disease: The future ahead. Exp. Parasitol. *232*, 108189.

Aranami, T., and Yamamura, T. (2008). Th17 cells and autoimmune encephalomyelitis (EAE/MS). Allergol. Int. *57*, 115–120.

Becher, B., Durell, B.G., and Noelle, R.J. (2003). IL-23 produced by CNS-resident cells controls T cell encephalitogenicity during the effector phase of experimental autoimmune encephalomyelitis. J. Clin. Invest. *112*, 1186–1191.

Berkowitz, A.L., Raibagkar, P., Pritt, B.S., and Mateen, F.J. (2015). Neurologic manifestations of the neglected tropical diseases. J. Neurol. Sci. *349*, 20–32.

Bispo, M.T., Calado, M., Maurício, I.L., Ferreira, P.M., and Belo, S. (2024). Zoonotic threats: The (re)emergence of cercarial dermatitis, its dynamics, and impact in Europe. Pathogens *13*.

Bjornevik, K., Cortese, M., Healy, B.C., Kuhle, J., Mina, M.J., Leng, Y., Elledge, S.J., Niebuhr, D.W., Scher, A.I., Munger, K.L., et al. (2022). Longitudinal analysis reveals high prevalence of Epstein-Barr virus associated with multiple sclerosis. Science (80-.). *375*, 296–301.

Bogdan, C. (2001). Nitric oxide and the immune response. Nat. Immunol. *2*, 907–916.

Bulantová, J., Macháček, T., Panská, L., Krejčí, F., Karch, J., Jährling, N., Saghafi, S., Dodt, H.U., and

Horák, P. (2016). *Trichobilharzia regenti* (Schistosomatidae): 3D imaging techniques in characterization of larval migration through the CNS of vertebrates. Micron *83*, 62–71.

Cadman, E.T., Thysse, K.A., Bearder, S., Cheung, A.Y.N., Johnston, A.C., Lee, J.J., and Lawrence, R.A. (2014). Eosinophils are important for protection, immunoregulation and pathology during infection with nematode microfilariae. PLoS Pathog. *10*.

Chauhan, A., Quenum, F.Z., Abbas, A., Bradley, D.S., Nechaev, S., Singh, B.B., Sharma, J., and Mishra, B.B. (2015). Epigenetic modulation of microglial inflammatory gene loci in helminth-induced immune suppression: Implications for immune regulation in neurocysticercosis. ASN Neuro *7*, 1–12.

Chavarría, A., Roger, B., Fragoso, G., Tapia, G., Fleury, A., Dumas, M., Dessein, A., Larralde, C., and Sciutto, E. (2003). Th2 profile in asymptomatic *Taenia solium* human neurocysticercosis. Microbes Infect. *5*, 1109–1115.

Che, J., Li, D., Hong, W., Wang, L., Guo, Y., Wu, M., Lu, J., Tong, L., Weng, Q., Wang, J., et al. (2022). Discovery of new macrophage M2 polarization modulators as multiple sclerosis treatment agents that enable the inflammation microenvironment remodeling. Eur. J. Med. Chem. *243*, 1–19.

Chen, L., Rao, K.V.N., He, Y.X., and Ramaswamy, K. (2002). Skin-stage schistosomula of *Schistosoma mansoni* produce an apoptosis-inducing factor that can cause apoptosis of T cells. J. Biol. Chem. *277*, 34329–34335.

Chu, F., Shi, M., Lang, Y., Chao, Z., Jin, T., Cui, L., and Zhu, J. (2021). Adoptive transfer of immunomodulatory M2 macrophages suppresses experimental autoimmune encephalomyelitis in C57BL/6 mice via blockading NF-κB pathway. Clin. Exp. Immunol. *204*, 199–211.

Chuang, C.C., Su, K.E., Chen, C.W., Fan, C.K., Lin, F.K., Chen, Y.S., and Du, W.Y. (2010). Anti-CCR3 monoclonal antibody inhibits eosinophil infiltration in *Angiostrongylus cantonensis*-infected ICR mice. Acta Trop. *113*, 209–213.

Chuang, C.C., Chen, C.W., Huang, Y.T., and Du, W.Y. (2014). Anti-ST2 monoclonal antibody inhibits eosinophil infiltration in *Angiostrongylus cantonensis*-infected mice. J. Microbiol. Immunol. Infect. *49*, 91–96.

Comi, G., Bar-Or, A., Lassmann, H., Uccelli, A., Hartung, H.P., Montalban, X., Sørensen, P.S., Hohlfeld, R., and Hauser, S.L. (2021). Role of B cells in multiple sclerosis and related disorders. Ann. Neurol. *89*, 13–23.

Compston, A., and Coles, A. (2008). Multiple sclerosis. Lancet *372*, 1502–1517.

Cook, P.C., Aynsley, S.A., Turner, J.D., Jenkins, G.R., van Rooijen, N., Leeto, M., Brombacher, F., and

Mountford, A.P. (2011). Multiple helminth infection of the skin causes lymphocyte hypo-responsiveness mediated by Th2 conditioning of dermal myeloid cells. PLoS Pathog. *7*.

Cowie, R.H. (2017). Angiostrongylus cantonensis: Agent of a sometimes fatal globally emerging infectious disease (rat lungworm disease). ACS Chem. Neurosci. *8*, 2102–2104.

Cox, D.M., and Holland, C. V (2001). Influence of mouse strain, infective dose and larval burden in the brain on activity in Toxocara-infected mice. J. Helminthol. *75*, 23–32.

Coyle, C.M., and Tanowitz, H.B. (2009). Diagnosis and treatment of neurocysticercosis. Interdiscip. Perspect. Infect. Dis. *2009*, 1–9.

Dastoli, P.A., da Costa, M.D.S., Nicácio, J.M., Pinho, R.S., Ferrarini, M.A.G., and Cavalheiro, S. (2023). Mansonic neuroschistosomiasis in the childhood: an undiagnosed pathology? Child's Nerv. Syst. *39*, 481–489.

Dendrou, C.A., Fugger, L., and Friese, M.A. (2015). Immunopathology of multiple sclerosis. Nat. Rev. Immunol. *15*, 545–558.

Deng, L., Gillis, J.E., Chiu, I.M., and Kaplan, D.H. (2024). Sensory neurons: An integrated component of innate immunity. Immunity *57*, 815–831.

Dixit, A., Tanaka, A., Greer, J.M., and Donnelly, S. (2017). Novel therapeutics for multiple sclerosis designed by parasitic worms. Int. J. Mol. Sci. *18*, 1–17.

Dolitzky, A., Hazut, I., Avlas, S., Grisaru-Tal, S., Itan, M., Zaffran, I., Levi-Schaffer, F., Gerlic, M., and Munitz, A. (2022). Differential regulation of Type 1 and Type 2 mouse eosinophil activation by apoptotic cells. Front. Immunol. *13*, 1–16.

Donskow-Łysoniewska, K., Krawczak, K., and Doligalska, M. (2012). *Heligmosomoides polygyrus*: EAE remission is correlated with different systemic cytokine profiles provoked by L4 and adult nematodes. Exp. Parasitol. *132*, 243–248.

Eamsobhana, P. (2014). Eosinophilic meningitis caused by *Angiostrongylus cantonensis*: a neglected disease with escalating importance. Trop. Biomed. *31*, 569–578.

Eberhardt, O., Bialek, R., Nägele, T., and Dichgans, J. (2005). Eosinophilic meningomyelitis in toxocariasis: Case report and review of the literature. Clin. Neurol. Neurosurg. *107*, 432–438.

Ehrens, A., Lenz, B., Neumann, A.L., Giarrizzo, S., Reichwald, J.J., Frohberger, S.J., Stamminger, W., Buerfent, B.C., Fercoq, F., Martin, C., et al. (2021a). Microfilariae trigger eosinophil extracellular DNA traps in a dectin-1-dependent manner. Cell Rep. *34*.

Ehrens, A., Rüdiger, N., Heepmann, L., Linnemann, L., Hartmann, W., Hübner, M.P., and Breloer, M. (2021b). Eosinophils and neutrophils eliminate migrating *Strongyloides ratti* larvae at the site of infection in the context of extracellular DNA trap formation. Front. Immunol. *12*, 1–17.

Escamilla, A., Bautista, M.J., Zafra, R., Pacheco, I.L., Ruiz, M.T., Martínez-Cruz, S., Méndez, A., Martínez-Moreno, A., Molina-Hernández, V., and Pérez, J. (2016). *Fasciola hepatica* induces eosinophil apoptosis in the migratory and biliary stages of infection in sheep. Vet. Parasitol. *216*, 84–88.

Fan, C.K., Holland, C. V., Loxton, K., and Barghouth, U. (2015). Cerebral toxocariasis: Silent progression to neurodegenerative disorders? Clin. Microbiol. Rev. *28*, 663–686.

Ferrari, T.C.A., and Moreira, P.R.R. (2011). Neuroschistosomiasis: Clinical symptoms and pathogenesis. Lancet Neurol. *10*, 853–864.

Ferrari, T.C.A., Moreira, P.R.R., Sampaio, M.J., da Cunha, A.S., de Oliveira, J.T., Gazzinelli, G., and Correa-Oliveira, R. (2006). Intrathecal cytokines in spinal cord schistosomiasis. J. Neuroimmunol. *177*, 136–141.

Ferrari, T.C.A., Moreira, P.R.R., and Cunha, A.S. (2008). Clinical characterization of neuroschistosomiasis due to *Schistosoma mansoni* and its treatment. Acta Trop. *108*, 89–97.

Fettrelet, T., Gigon, L., Karaulov, A., Yousefi, S., and Simon, H.U. (2021). The enigma of eosinophil degranulation. Int. J. Mol. Sci. *22*, 1–19.

Finlay, C.M., Stefanska, A.M., Walsh, K.P., Kelly, P.J., Boon, L., Lavelle, E.C., Walsh, P.T., and Mills, K.H.G. (2016). Helminth products protect against autoimmunity via innate type 2 cytokines IL-5 and IL-33, which promote eosinophilia. J. Immunol. *196*, 703–714.

Finsterer, J., and Auer, H. (2013). Parasitoses of the human central nervous system. J. Helminthol. *87*, 257–270.

La Flamme, A.C., Ruddenklau, K., and Bäckström, B.T. (2003). Schistosomiasis decreases central nervous system inflammation and alters the progression of experimental autoimmune encephalomyelitis. Infect. Immun. *71*, 4996–5004.

Fleury, A., Cardenas, G., Adalid-Peralta, L., Fragoso, G., and Sciutto, E. (2016). Immunopathology in *Taenia solium* neurocysticercosis. Parasite Immunol. *38*, 147–157.

Frigerio, S., da Costa, V., Costa, M., Festari, M.F., Landeira, M., Rodríguez-Zraquia, S.A., Härtel, S., Toledo, J., and Freire, T. (2020). Eosinophils control liver damage by modulating immune responses against *Fasciola hepatica*. Front. Immunol. *11*, 1–15.

Frischer, J.M., Bramow, S., Dal-Bianco, A., Lucchinetti, C.F., Rauschka, H., Schmidbauer, M., Laursen, H., Sorensen, P.S., and Lassmann, H. (2009). The relation between inflammation and neurodegeneration in multiple sclerosis brains. Brain *132*, 1175–1189.

Frohberger, S.J., Ajendra, J., Surendar, J., Stamminger, W., Ehrens, A., Buerfent, B.C., Gentil, K., Hoerauf, A., and Hübner, M.P. (2019). Susceptibility to *L. sigmodontis* infection is highest in animals lacking IL-4R/IL-5 compared to single knockouts of IL-4R, IL-5 or eosinophils. Parasites and Vectors *12*, 1–16.

Garcia, H.H., Rodriguez, S., and Friedland, J.S. (2014). Immunology of *Taenia solium* taeniasis and human cysticercosis. Parasite Immunol. *36*, 388–396.

Garcia, H.H., Gonzalez, A.E., and Gilman, R.H. (2020). *Taenia solium* cysticercosis and its impact in neurological disease. Clin. Microbiol. Rev. *33*.

Gazzinelli-Guimaraes, P.H., De Queiroz Prado, R., Ricciardi, A., Bonne-Année, S., Sciurba, J., Karmele, E.P., Fujiwara, R.T., and Nutman, T.B. (2019). Allergen presensitization drives an eosinophil-dependent arrest in lung-specific helminth development. J. Clin. Invest. *129*, 3686–3701.

Gohardehi, S., Fakhar, M., and Madjidaei, M. (2013). Avian schistosomes and human cercarial dermatitis in a wildlife refuge in Mazandaran Province, Northern Iran. Zoonoses Public Health *60*, 442–447.

Gosnell, W.L., and Kramer, K.J. (2013). The role of eosinophils in angiostrongyliasis: multiple roles for a versatile cell? Hawaii. J. Med. Public Health *72*, 49–51.

Greenfield, A.L., and Hauser, S.L. (2018). B-cell therapy for multiple sclerosis: Entering an era. Ann. Neurol. *83*, 13–26.

Gundra, U.M., Mishra, B.B., Wong, K., and Teale, J.M. (2011). Increased disease severity of parasite-infected TLR2-/- mice is correlated with decreased central nervous system inflammation and reduced numbers of cells with alternatively activated macrophage phenotypes in a murine model of neurocysticercosis. Infect. Immun. *79*, 2586–2596.

Handel, A.E., Williamson, A.J., Disanto, G., Handunnetthi, L., Giovannoni, G., and Ramagopalan, S. V. (2010). An updated meta-analysis of risk of multiple sclerosis following infectious mononucleosis. PLoS One *5*, 1–5.

Hart, B.A.T. (2019). Experimental autoimmune encephalomyelitis in the common marmoset: A translationally relevant model for the cause and course of multiple sclerosis. Primate Biol. *6*, 17–58.

Hauser, S.L., Bar-Or, A., Comi, G., Giovannoni, G., Hartung, H.-P., Hemmer, B., Lublin, F., Montalban,

X., Rammohan, K.W., Selmaj, K., et al. (2017). Ocrelizumab versus interferon beta-1a in relapsing multiple sclerosis. N. Engl. J. Med. *376*, 221–234.

Helmby, H. (2015). Human helminth therapy to treat inflammatory disorders - where do we stand? BMC Immunol. *16*.

Horák, P., Kolářová, L., and Dvořák, J. (1998). *Trichobilharzia regenti* n. sp. (Schistosomatidae, Bilharziellinae), a new nasal schistosome from Europe. Parasite *5*, 349–357.

Horák, P., Dvořák, J., Kolářová, L., and Trefil, L. (1999). *Trichobilharzia regenti*, a pathogen of the avian and mammalian central nervous systems. Parasitology *119*, 577–581.

Horák, P., Mikeš, L., Lichtenbergová, L., Skála, V., Soldánová, M., and Brant, S.V. (2015). Avian schistosomes and outbreaks of cercarial dermatitis. Clin. Microbiol. Rev. *28*, 165–190.

Horák, P., Bulantová, J., and Mikeš, L. (2024). Other Schistosomatoidea and Diplostomoidea. In Digenetic Trematodes, R. Toledo, and B. Fried, eds. (Cham: Springer International Publishing), pp. 107–155.

Hrádková, K., and Horák, P. (2002). Neurotropic behaviour of *Trichobilharzia regenti* in ducks and mice. J. Helminthol. *76*, 137–142.

Inclan-Rico, J.M., and Siracusa, M.C. (2018). First responders: Innate immunity to helminths. Trends Parasitol. *34*, 861–880.

Janecek, E., Beineke, A., Schnieder, T., and Strube, C. (2014). Neurotoxocarosis: Marked preference of *Toxocara canis* for the cerebrum and *T. cati* for the cerebellum in the paratenic model host mouse. Parasites and Vectors *7*.

Johnston, C.J.C., Smyth, D.J., Kodali, R.B., White, M.P.J., Harcus, Y., Filbey, K.J., Hewitson, J.P., Hinck, C.S., Ivens, A., Kemter, A.M., et al. (2017). A structurally distinct TGF-β mimic from an intestinal helminth parasite potently induces regulatory T cells. Nat. Commun. *8*.

Katchanov, J., and Nawa, Y. (2010). Helminthic invasion of the central nervous system: Many roads lead to Rome. Parasitol. Int. *59*, 491–496.

Kerr, O., Juhász, A., Jones, S., and Stothard, J.R. (2024). Human cercarial dermatitis (HCD) in the UK: an overlooked and under-reported nuisance? Parasites and Vectors *17*, 1–6.

Khan, A.R., and Fallon, P.G. (2013). Helminth therapies: Translating the unknown unknowns to known knowns. Int. J. Parasitol. *43*, 293–299.

Kolářová, L. (2007). Schistosomes causing cercarial dermatitis: A mini-review of current trends in

systematics and of host specificity and pathogenicity. Folia Parasitol. (Praha). *54*, 81–87.

Kolářová, L., Horák, P., and Čada, F. (2001). Histopathology of CNS and nasal infections caused by *Trichobilharzia regenti* in vertebrates. Parasitol. Res. *87*, 644–650.

Kolářová, L., Horák, P., Skírnisson, K., Marečková, H., and Doenhoff, M. (2013). Cercarial dermatitis, a neglected allergic disease. Clin. Rev. Allergy Immunol. *45*, 63–74.

Kouřilová, P., Hogg, K.G., Kolářová, L., and Mountford, A.P. (2004a). Cercarial dermatitis caused by bird schistosomes comprises both immediate and late phase cutaneous hypersensitivity reactions. J. Immunol. *172*, 3766–3774.

Kouřilová, P., Syrůček, M., and Kolářová, L. (2004b). The severity of mouse pathologies caused by the bird schistosome *Trichobilharzia regenti* in relation to host immune status. Parasitol. Res. *93*, 8–16.

Kwon, H.S., and Koh, S.H. (2020). Neuroinflammation in neurodegenerative disorders: the roles of microglia and astrocytes. Transl. Neurodegener. *9*, 1–12.

Lam, H.Y.P., Chen, T.T.-W., Chen, C.-C., Yang, T.-H., Cheng, P.-C., and Peng, S.Y. (2020). *Angiostrongylus cantonensis* activates inflammasomes in meningoencephalitic BALB/c mice. Parasitol. Int. *77*, 102119.

Larochelle, C., Wasser, B., Jamann, H., Löffel, J.T., Cui, Q.L., Tastet, O., Schillner, M., Luchtman, D., Birkenstock, J., Stroh, A., et al. (2021). Pro-inflammatory T helper 17 directly harms oligodendrocytes in neuroinflammation. Proc. Natl. Acad. Sci. U. S. A. *118*, 1–12.

Lashaki, E.K., Teshnizi, S.H., Gholami, S., Fakhar, M., Brant, S. V., and Dodangeh, S. (2020). Global prevalence status of avian schistosomes: A systematic review with meta-analysis. Parasite Epidemiol. Control *9*, e00142.

Lassmann, H. (2013). Pathology and disease mechanisms in different stages of multiple sclerosis. J. Neurol. Sci. *333*, 1–4.

Lassmann, H., and Bradl, M. (2017). Multiple sclerosis: experimental models and reality. Acta Neuropathol. *133*, 223–244.

Leontovyč, R., Young, N.D., Korhonen, P.K., Hall, R.S., Tan, P., Mikeš, L., Kašný, M., Horák, P., and Gasser, R.B. (2016). Comparative transcriptomic exploration reveals unique molecular adaptations of neuropathogenic Trichobilharzia to invade and parasitize its avian definitive host. PLoS Negl. Trop. Dis. *10*, 1–24.

Li, J.J., Zhang, R.L., Fu, Y.C., Wu, W. ping, Chen, M.X., Geng, Y.J., Huang, D.N., Ai, L., Yang, F., and Hu, Z. (2012). Monoclonal antibody 12D5 inhibits eosinophil infiltration in the brain of Angiostrongylus

cantonensis-infected BALB/c mice. Acta Trop. *121*, 118–124.

Lichtenbergová, L., and Horák, P. (2012). Pathogenicity of *Trichobilharzia* spp. for vertebrates. J. Parasitol. Res. *2012*.

Lichtenbergová, L., Lassmann, H., Jones, M.K., Kolářová, L., and Horák, P. (2011). *Trichobilharzia regenti*: host immune response in the pathogenesis of neuroinfection in mice. Exp. Parasitol. *128*, 328–335.

Linington, C., Bradl, M., Lassmann, H., Brunner, C., and Vass, K. (1988). Augmentation of demyelination in rat acute allergic encephalomyelitis by circulating mouse monoclonal antibodies directed against a myelin/oligodendrocyte glycoprotein. Am. J. Pathol. *130*, 443–454.

Liu, R., Du, S., Zhao, L., Jain, S., Sahay, K., Rizvanov, A., Lezhnyova, V., Khaibullin, T., Martynova, E., Khaiboullina, S., et al. (2022). Autoreactive lymphocytes in multiple sclerosis: Pathogenesis and treatment target. Front. Immunol. *13*, 1–23.

Loker, E.S., Dejong, R.J., and Brant, S. V. (2022). Scratching the Itch: Updated Perspectives on the Schistosomes Responsible for Swimmer's Itch around the World. Pathogens *11*, 1–27.

Lucarini, V., Ziccheddu, G., Macchia, I., La Sorsa, V., Peschiaroli, F., Buccione, C., Sistigu, A., Sanchez, M., Andreone, S., D'Urso, M.T., et al. (2017). IL-33 restricts tumor growth and inhibits pulmonary metastasis in melanoma-bearing mice through eosinophils. Oncoimmunology *6*.

Luna, G., Alping, P., Burman, J., Fink, K., Fogdell-Hahn, A., Gunnarsson, M., Hillert, J., Langer-Gould, A., Lycke, J., Nilsson, P., et al. (2020). Infection risks among patients with multiple sclerosis treated with fingolimod, natalizumab, rituximab, and injectable therapies. JAMA Neurol. *77*, 184–191.

Lund, M.E., Greer, J., Dixit, A., Alvarado, R., McCauley-Winter, P., To, J., Tanaka, A., Hutchinson, A.T., Robinson, M.W., Simpson, A.M., et al. (2016). A parasite-derived 68-mer peptide ameliorates autoimmune disease in murine models of Type 1 diabetes and multiple sclerosis. Sci. Rep. *6*, 1–11.

Lv, S., Zhang, Y., Steinmann, P., Zhou, X.N., and Utzinger, J. (2010). Helminth infections of the central nervous system occurring in Southeast Asia and the Far East. Adv. Parasitol. *72*, 351–408.

Macháček, T., Panská, L., Dvořáková, H., and Horák, P. (2016). Nitric oxide and cytokine production by glial cells exposed in vitro to neuropathogenic schistosome *Trichobilharzia regenti*. Parasit. Vectors *9*, 579.

Macháček, T., Turjanicová, L., Bulantová, J., Hrdý, J., Horák, P., and Mikeš, L. (2018). Cercarial dermatitis: a systematic follow-up study of human cases with implications for diagnostics. Parasitol. Res. *117*, 3881–3895.

Macháček, T., Šmídová, B., Pankrác, J., Majer, M., Bulantová, J., and Horák, P. (2020). Nitric oxide debilitates the neuropathogenic schistosome Trichobilharzia regenti in mice, partly by inhibiting its vital peptidases. Parasites and Vectors *13*, 1–14.

Macháček, T., Leontovyč, R., Šmídová, B., Majer, M., Vondráček, O., Vojtěchová, I., Petrásek, T., and Horák, P. (2022). Mechanisms of the host immune response and helminth-induced pathology during *Trichobilharzia regenti* (Schistosomatidae) neuroinvasion in mice. PLoS Pathog. *18*, 1–34.

Maizels, R.M. (2013). Toxocara canis: Molecular basis of immune recognition and evasion. Vet. Parasitol. *193*, 365–374.

Maizels, R.M., Smits, H.H., and McSorley, H.J. (2018). Modulation of host immunity by helminths: The expanding repertoire of parasite effector molecules. Immunity *49*, 801–818.

Malta, K.K., Palazzi, C., Neves, V.H., Aguiar, Y., Silva, T.P., and Melo, R.C.N. (2022). Schistosomiasis mansoni-recruited eosinophils: An overview in the granuloma context. Microorganisms *10*.

Martins, Y.C., Tanowitz, H.B., and Kazacos, K.R. (2015). Central nervous system manifestations of Angiostrongylus cantonensis infection. Acta Trop. *141*, 46–53.

Masure, D., Wang, T., Vlaminck, J., Claerhoudt, S., Chiers, K., Van den Broeck, W., Saunders, J., Vercruysse, J., and Geldhof, P. (2013). The intestinal expulsion of the roundworm *Ascaris suum* is associated with eosinophils, intra-epithelial T cells and decreased intestinal transit time. PLoS Negl. Trop. Dis. *7*, 1–9.

Mazzon, C., Zanotti, L., Wang, L., Del Prete, A., Fontana, E., Salvi, V., Poliani, P.L., and Sozzani, S. (2016). CCRL2 regulates M1/M2 polarization during EAE recovery phase. J. Leukoc. Biol. *99*, 1027–1033.

McGinley, A.M., Edwards, S.C., Raverdeau, M., and Mills, K.H.G. (2018). Th17 cells, γδ T cells and their interplay in EAE and multiple sclerosis. J. Autoimmun. *87*, 97–108.

Miron, V.E., and Franklin, R.J.M. (2014). Macrophages and CNS remyelination. J. Neurochem. *130*, 165–171.

Miron, V.E., Boyd, A., Zhao, J.-W., Yuen, T.J., Ruckh, J.M., Shadrach, J.L., van Wijngaarden, P., Wagers, A.J., Williams, A., Franklin, R.J.M., et al. (2013). M2 microglia and macrophages drive oligodendrocyte differentiation during CNS remyelination. Nat. Neurosci. *16*, 1211–1218.

Mishra, B.B., Gundra, U.M., Wong, K., and Teale, J.M. (2009). MyD88-deficient mice exhibit decreased parasite-induced immune responses but reduced disease severity in a murine model of neurocysticercosis. Infect. Immun. *77*, 5369–5379.

Miyazaki, Y., and Niino, M. (2022). B-cell depletion therapy for multiple sclerosis. Immunol. Med. *45*, 54–62.

Mohammad, Z., Zahra, S., Najmeh, M., and Saeed, B. (2019). Human toxocara infection: Allergy and immune responses. Antiinflamm. Antiallergy. Agents Med. Chem. *18*, 82–90.

Moqbel, R., Sass Kuhn, S.P., Goetzl, E.J., and Kay, A.B. (1983). Enhancement of neutrophil- and eosinophil-mediated complement-dependent killing of schistosomula of *Schistosoma mansoni* in vitro by leukotriene B4. Clin. Exp. Immunol. *52*, 519–527.

Müller, V., and Kimmig, P. (1994). *Trichobilharzia franki* n. sp.- the cause of swimmer's dermatitis in southwest German dredged lakes. Appl. Parasitol. *35*, 12–31.

Muñoz-Caro, T., Rubio R, M.C., Silva, L.M.R., Magdowski, G., Gärtner, U., McNeilly, T.N., Taubert, A., and Hermosilla, C. (2015). Leucocyte-derived extracellular trap formation significantly contributes to *Haemonchus contortus* larval entrapment. Parasites and Vectors *8*, 1–12.

Neuhaus, W. (1952). Biology and development of *Trichobilharzia szidati* n. sp. (Trematoda, Schistosomatidae), a parasite causing dermatitis in man. Z. Parasitenkd. *15*, 203–266.

Nicoletti, A. (2016). Neurotoxocariais: A rare or neglected disease? J. Neuroinfectious Dis. *07*, 18–19.

Novák, J., Macháček, T., Majer, M., Kostelanská, M., Skulinová, K., Černý, V., Kolářová, L., Hrdý, J., and Horák, P. (2022). *Toxocara canis* infection worsens the course of experimental autoimmune encephalomyelitis in mice. Parasitology *149*, 1720–1728.

O'Connell, A.E., Hess, J.A., Santiago, G.A., Nolan, T.J., Lok, J.B., Lee, J.J., and Abraham, D. (2011). Major basic protein from eosinophils and myeloperoxidase from neutrophils are required for protective immunity to *Strongyloides stercoralis* in mice. Infect. Immun. *79*, 2770–2778.

Okano, M., Satoskar, A.R., Nishizaki, K., Abe, M., and Harn, D.A.J. (1999). Induction of Th2 responses and IgE is largely due to carbohydrates functioning as adjuvants on *Schistosoma mansoni* egg antigens. J. Immunol. *163*, 6712–6717.

de Oliveira, V.G., Rodrigues, V.F., Moreira, J.M.P., Rodrigues, J.L., Maggi, L., Resende, S.D., and Negrão-Corrêa, D. (2022). Eosinophils participate in modulation of liver immune response and tissue damage induced by *Schistosoma mansoni* infection in mice. Cytokine *149*.

Parohová, I. (2020). Parasite-induced apoptosis in mice infected with the neuropathogenic schistosome *Trichobilharzia regenti*. Diplpma thesis.

Peng, H., Sun, R., Zhang, Q., Zhao, J., Wei, J., Zeng, X., Zheng, H., and Wu, Z. (2013). Interleukin 33

mediates type 2 immunity and inflammation in the central nervous system of mice infected with *Angiostrongylus cantonensis*. J. Infect. Dis. *207*, 860–869.

Pittella, J.E.H. (1997). Neuroschistosomiasis. Brain Pathol. *7*, 649–662.

Pokrupová, Z. (2021). Avian schistosomes and cercarial dermatitis in Czech Republic: distribution, diversity and factors influencing their occurrence. Diploma thesis.

Prabhakaran, V., Jayaraman, T., Rajshekhar, V., and Oommen, A. (2010). Neurocysticercosis, IgG immunoglobulins, and nitric oxide. Parasitol. Res. *106*, 1287–1291.

Prendergast, C.T., Sanin, D.E., Cook, P.C., and Mountford, A.P. (2015). CD4+ T cell hyporesponsiveness after repeated exposure to *Schistosoma mansoni* larvae is dependent upon interleukin-10. Infect. Immun. *83*, 1418–1430.

Qi, B., Ge, P., Yang, H., Bi, C., and Li, Y. (2011). Spinal intramedullary cysticercosis: A case report and literature review. Int. J. Med. Sci. *8*, 420–423.

Quenum Zangbede, F.O., Chauhan, A., Sharma, J., and Mishra, B.B. (2018). Galectin-3 in M2 macrophages plays a protective role in resolution of neuropathology in brain parasitic infection by regulating neutrophil turnover. J. Neurosci. *38*, 6737–6750.

Quinn, S.M., Raverdeau, M., McGinley, A.M., and Mills, K.H.G. (2019). Helminths products directly modulate T cells that mediate experimental autoimmune encephalomyelitis. Eur. J. Immunol. *49*, 1291–1294.

Resende, N.M., Gazzinelli-Guimarães, P.H., Barbosa, F.S., Oliveira, L.M., Nogueira, D.S., Gazzinelli-Guimarães, A.C., Gonçalves, M.T.P., Amorim, C.C.O., Oliveira, F.M.S., Caliari, M. V., et al. (2015). New insights into the immunopathology of early *Toxocara canis* infection in mice. Parasites and Vectors *8*, 1–11.

Robinson, A.P., Harp, C.T., Noronha, A., and Miller, S.D. (2014). The experimental autoimmune encephalomyelitis (EAE) model of MS: utility for understanding disease pathophysiology and treatment. (Elsevier B.V.).

Robinson, M.W., Donnelly, S., Hutchinson, A.T., To, J., Taylor, N.L., Norton, R.S., Perugini, M.A., and Dalton, J.P. (2011). A family of helminth molecules that modulate innate cell responses via molecular mimicry of host antimicrobial peptides. PLoS Pathog. *7*.

Rock, R.B., Gekker, G., Hu, S., Sheng, W.S., Cheeran, M., Lokensgard, J.R., and Peterson, P.K. (2004). Role of microglia in central nervous system infections. Clin. Microbiol. Rev. *17*, 942–964.

Rodríguez-Sosa, M., Satoskar, A.R., Calderón, R., Gomez-Garcia, L., Saavedra, R., Bojalil, R., and Terrazas, L.I. (2002). Chronic helminth infection induces alternatively activated macrophages expressing high levels of CCR5 with low interleukin-12 production and Th2-biasing ability. Infect. Immun. *70*, 3656–3664.

Rostami, A., Ma, G., Wang, T., Koehler, A. V., Hofmann, A., Chang, B.C.H., Macpherson, C.N., and Gasser, R.B. (2019). Human toxocariasis – a look at a neglected disease through an epidemiological 'prism.' Infect. Genet. Evol. *74*, 104002.

Sakkal, S., Miller, S., Apostolopoulos, V., and Nurgali, K. (2016). Eosinophils in cancer: Favourable or unfavourable? Curr. Med. Chem. *23*, 650–666.

Saraiva-Santos, T., Zaninelli, T.H., and Pinho-Ribeiro, F.A. (2024). Modulation of host immunity by sensory neurons. Trends Immunol. *45*, 381–396.

Sewell, D., Qing, Z., Reinke, E., Elliot, D., Weinstock, J., Sandor, M., and Fabry, Z. (2003). Immunomodulation of experimental autoimmune encephalomyelitis by helminth ova immunization. Int. Immunol. *15*, 59–69.

Shapouri-Moghaddam, A., Mohammadian, S., Vazini, H., Taghadosi, M., Esmaeili, S.A., Mardani, F., Seifi, B., Mohammadi, A., Afshari, J.T., and Sahebkar, A. (2018). Macrophage plasticity, polarization, and function in health and disease. J. Cell. Physiol. *233*, 6425–6440.

Shen, J., Lai, D.-H., Wilson, R.A., Chen, Y.-F., Wang, L.-F., Yu, Z.-L., Li, M.-Y., He, P., Hide, G., Sun, X., et al. (2017). Nitric oxide blocks the development of the human parasite *Schistosoma japonicum*. Proc. Natl. Acad. Sci. 201708578.

Skirnisson, K., Aldhoun, J.A., and Kolarov, L. (2009). A review on swimmer's itch and the occurrence of bird schistosomes in Iceland. J. Helminthol. *83*, 165–171.

Šmídová, B., Majer, M., Novák, J., Revalová, A., Horák, P., and Macháček, T. (2024). The neurotropic schistosome vs experimental autoimmune encephalomyelitis: are there any winners? Parasitology *151*, 412–420.

Soldánová, M., Selbach, C., Kalbe, M., Kostadinova, A., and Sures, B. (2013). Swimmer's itch: Etiology, impact, and risk factors in Europe. Trends Parasitol. *29*, 65–74.

Sousa-Pereira, S.R., Teixeira, A.L., Silva, L.C.S., Souza, A.L.S., Antunes, C.M., Teixeira, M.M., and Lambertucci, J.R. (2006). Serum and cerebral spinal fluid levels of chemokines and Th2 cytokines in *Schistosoma mansoni* myeloradiculopathy. Parasite Immunol. *28*, 473–478.

Springer, A., Heuer, L., Janecek-erfurth, E., Beineke, A., and Strube, C. (2019). Histopathological

characterization of *Toxocara canis*- and *T . cati*-induced neurotoxocarosis in the mouse model.

Starossom, S.C., Campo Garcia, J., Woelfle, T., Romero-Suarez, S., Olah, M., Watanabe, F., Cao, L., Yeste, A., Tukker, J.J., Quintana, F.J., et al. (2019). Chi3l3 induces oligodendrogenesis in an experimental model of autoimmune neuroinflammation. Nat. Commun. *10*.

Strube, C., Heuer, L., and Janecek, E. (2013). *Toxocara* spp. infections in paratenic hosts. Vet. Parasitol. *193*, 375–389.

Sugaya, H., Aoki, M., Yoshida, T., Takatsu, K., and Yoshimura, K. (1997). Eosinophilia and intracranial worm recovery in interleukin-5 transgenic and interleukin-5 receptor α chain-knockout mice infected with *Angiostrongylus cantonensis*. Parasitol. Res. *83*, 583–590.

Sun, W., Wang, Q., Zhang, R., and Zhang, N. (2023). Ketogenic diet attenuates neuroinflammation and induces conversion of M1 microglia to M2 in an EAE model of multiple sclerosis by regulating the NF-κB/NLRP3 pathway and inhibiting HDAC3 and P2X7R activation. Food Funct. *14*, 7247–7269.

Sun, Y., Chauhan, A., Sukumaran, P., Sharma, J., Singh, B.B., and Mishra, B.B. (2014). Inhibition of store-operated calcium entry in microglia by helminth factors: Implications for immune suppression in neurocysticercosis. J. Neuroinflammation *11*, 1–12.

Svensson, M., Bell, L., Little, M.C., Deschoolmeester, M., Locksley, R.M., and Else, K.J. (2011). Accumulation of eosinophils in intestine-draining mesenteric lymph nodes occurs after *Trichuris muris* infection. Parasite Immunol. *33*, 1–11.

Tharmalingam, J., Prabhakar, A.T., Gangadaran, P., Dorny, P., Vercruysse, J., Geldhof, P., Rajshekhar, V., Alexander, M., and Oommen, A. (2016). Host Th1/Th2 immune response to *Taenia solium* cyst antigens in relation to cyst burden of neurocysticercosis. Parasite Immunol. *38*, 628–634.

Tian, L., Ma, L., Kaarela, T., and Li, Z. (2012). Neuroimmune crosstalk in the central nervous system and its significance for neurological diseases. J. Neuroinflammation *9*, 1–10.

Toenjes, S.A., and Kuhn, R.E. (2003). The initial immune response during experimental cysticercosis is of the mixed Th1/Th2 type. Parasitol. Res. *89*, 407–413.

Tracy, S.I., Kakalacheva, K., Lünemann, J.D., Luzuriaga, K., Middeldorp, J., and Thorley-Lawson, D.A. (2012). Persistence of Epstein-Barr Virus in Self-Reactive Memory B Cells. J. Virol. *86*, 12330–12340.

Trinchieri, G. (2003). Interleukin-12 and the regulation of innate resistance and adaptive immunity. Nat. Rev. Immunol. *3*, 133–146.

Trujillo-Vargas, C.M., Werner-Klein, M., Wohlleben, G., Polte, T., Hansen, G., Ehlers, S., and Erb, K.J.

(2007). Helminth-derived products inhibit the development of allergic responses in mice. Am. J. Respir. Crit. Care Med. *175*, 336–344.

Turjanicova, L., Mikes, L., Peckova, M., and Horak, P. (2015). Antibody response of definitive hosts against antigens of two life stages of the neuropathogenic schistosome *Trichobilharzia regenti*. Parasit. Vectors *8*, 400.

Vale, T.C., de Sousa-Pereira, S.R., Ribas, J.G.R., and Lambertucci, J.R. (2012). Neuroschistosomiasis mansoni: Literature review and guidelines. Neurologist *18*.

Valero, M.A., and Bargues, M.D. (2008). Effects of climate change on animal and zoonotic helminthiases and helminth development. Oceania *27*, 443–452.

Vietzen, H., Berger, S.M., Kühner, L.M., Furlano, P.L., Bsteh, G., Berger, T., Rommer, P., and Puchhammer-Stöckl, E. (2023). Ineffective control of Epstein-Barr-virus-induced autoimmunity increases the risk for multiple sclerosis. Cell *186*, 5705-5718.e13.

Waindok, P., and Strube, C. (2019). Neuroinvasion of *Toxocara canis*- and *T. cati*-larvae mediates dynamic changes in brain cytokine and chemokine profile. J. Neuroinflammation *16*, 1–12.

Walsh, K.P., Brady, M.T., Finlay, C.M., Boon, L., and Mills, K.H.G. (2009). Infection with a helminth parasite attenuates autoimmunity through TGF-β-mediated suppression of Th17 and Th1 responses. J. Immunol. *183*, 1577–1586.

Walton, C., King, R., Rechtman, L., Kaye, W., Leray, E., Marrie, R.A., Robertson, N., La Rocca, N., Uitdehaag, B., van der Mei, I., et al. (2020). Rising prevalence of multiple sclerosis worldwide: Insights from the Atlas of MS, third edition. Mult. Scler. J. *26*, 1816–1821.

Wang, C., Zhou, W., Su, G., Hu, J., and Yang, P. (2022). Progranulin suppressed autoimmune uveitis and autoimmune neuroinflammation by inhibiting Th1/Th17 cells and promoting Treg cells and M2 macrophages. Neurol. Neuroimmunol. NeuroInflammation *9*, 1–11.

Wang, Q.P., Wu, Z.D., Wei, J., Owen, R.L., and Lun, Z.R. (2012). Human *Angiostrongylus cantonensis*: An update. Eur. J. Clin. Microbiol. Infect. Dis. *31*, 389–395.

Wei, J., Wu, F., He, A., Zeng, X., Ouyang, L. si, Liu, M. she, Zheng, H. qin, Lei, W. long, Wu, Z. dao, and Lv, Z. yue (2015). Microglia activation: one of the checkpoints in the CNS inflammation caused by *Angiostrongylus cantonensis* infection in rodent model. Parasitol. Res. *114*, 3247–3254.

Weng, Q., Wang, J., Wang, J., Wang, J., Sattar, F., Zhang, Z., Zheng, J., Xu, Z., Zhao, M., Liu, X., et al. (2018). Lenalidomide regulates CNS autoimmunity by promoting M2 macrophages polarization. Cell Death Dis. *9*, 1–13.

White, M.P.J., Johnston, C.J.C., Grainger, J.R., Konkel, J.E., O'Connor, R.A., Anderton, S.M., and Maizels, R.M. (2020). The helminth parasite *Heligmosomoides polygyrus* attenuates EAE in an IL-4Rα-dependent manner. Front. Immunol. *11*.

Wilson, M.S., Taylor, M.D., O'Gorman, M.T., Balic, A., Barr, T.A., Filbey, K., Anderton, S.M., and Maizels, R.M. (2010). Helminth-induced CD19+ CD23hi B cells modulate experimental allergic and autoimmune inflammation. Eur. J. Immunol. *40*, 1682–1696.

Yasuda, K., Muto, T., Kawagoe, T., Matsumoto, M., Sasaki, Y., Matsushita, K., Taki, Y., Futatsugi-Yumikura, S., Tsutsui, H., Ishii, K.J., et al. (2012). Contribution of IL-33-activated type II innate lymphoid cells to pulmonary eosinophilia in intestinal nematode-infected mice. Proc. Natl. Acad. Sci. U. S. A. *109*, 3451–3456.

Yousefi, S., Gold, J.A., Andina, N., Lee, J.J., Kelly, A.M., Kozlowski, E., Schmid, I., Straumann, A., Reichenbach, J., Gleich, G.J., et al. (2008). Catapult-like release of mitochondrial DNA by eosinophils contributes to antibacterial defense. Nat. Med. *14*, 949–953.

Zhang, J., Li, Y., Duan, Z., Kang, J., Chen, K., Li, G., Weng, C., Zhang, D., Zhang, L., Wang, J., et al. (2020). The effects of the M2a macrophage-induced axonal regeneration of neurons by arginase 1. Biosci. Rep. *40*, 1–11.

Zhao, J., Lv, Z., Wang, F., Wei, J., Zhang, Q., Li, S., Yang, F., Zeng, X., Wu, X., and Wu, Z. (2013). Ym1, an eosinophilic chemotactic factor, participates in the brain inflammation induced by Angiostrongylus cantonensis in mice. Parasitol. Res. *112*, 2689–2695.

Zheng, X., Hu, X., Zhou, G., Lu, Z., Qiu, W., Bao, J., and Dai, Y. (2008). Soluble egg antigen from *Schistosoma japonicum* modulates the progression of chronic progressive experimental autoimmune encephalomyelitis via Th2-shift response. J. Neuroimmunol. *194*, 107–114.

Online sources

WHO (2024). Schistosomiasis. Retrieved from website: https://www.who.int/news-room/fact-sheets/detail/schistosomiasis (accessed 29 July 2024).

WHO (2024). Taeniasis/cysticercosis. Retrieved from website: https://www.who.int/news-room/fact-sheets/detail/taeniasis-cysticercosis (accessed 29 July 2024).